

Electronic Supplementary Information

Photoelectrochemical Cross-Dehydrogenative Coupling of Benzothiazoles with Strong Aliphatic C–H Bonds

Luca Capaldo,[†] Lorenzo Lafayette Quadri,[†] Daniele Merli, Davide Ravelli*

Department of Chemistry, University of Pavia, viale Taramelli 12, 27100 Pavia, Italy

Fax: +39 0382 987323; Tel: +39 0382 987316. E-mail: davide.ravelli@unipv.it

[†] These Authors contributed equally to this work.

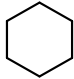
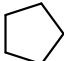
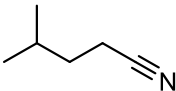
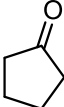
CONTENT (69 pages)

1.	Data cited in the main text	S2
1.1	Preparative experiments with Glassy Carbon (GC) anode	S2
1.2	Kinetic analysis	S3
1.3	Reactivity of intermediate 2-cyclohexylbenzothiazoline (3')	S7
1.4	Laser Flash Photolysis	S9
1.5	Electrochemical data	S16
2.	Experimental section	S20
2.1	General information	S20
2.2	General procedure for the synthesis of substituted benzothiazoles	S20
2.3	General procedure for the photoelectrochemical cross-dehydrogenative coupling	S21
2.4	Characterization of benzothiazoles	S26
2.5	Synthesis and characterization of intermediate 2-cyclohexylbenzothiazoline (3')	S29
2.6	Characterization of products 3-16	S30
2.7	Crude 700 MHz ¹ H-NMR for the reaction with norbornane	S37
3	References	S38
4	¹ H, ¹⁹ F and ¹³ C NMR spectra	S39

1. Data cited in the main text

1.1 Preparative experiments with Glassy Carbon (GC) anode

Table S1. Comparison of the isolated reaction yields when using a Pt or a Glassy Carbon (GC) anode on selected entries: in most cases, the yields are comparable.

<i>H-donor</i>		Pt as the anode (see Table 2 in the main text)	Glassy Carbon (GC) as the anode
 <i>1a</i>	5 equiv	78%	79%
 <i>1b</i>	5 equiv	49% (>99% brsm)	32% (74% brsm)
	10 equiv	62% (88% brsm)	61% (91% brsm)
	20 equiv	73%	47% (67% brsm)
 <i>1e</i>	10 equiv	88%	72%
 <i>1f</i>	10 equiv	81%	80%

1.2 Kinetic analysis

The reaction mechanism was studied by monitoring the progress of the reaction between **1a** and **2a** over time (Figure S1a). In particular, we subjected aliquots of the reaction mixture to ^1H -NMR analysis at regular time intervals and found that the redox-neutral adduct 2-cyclohexylbenzothiazoline (**3'**) was formed at short reaction times, along with the desired product **3**. However, while the latter kept accumulating in solution, the concentration of **3'** reached a maximum (at *ca.* 1 h) and then started to decrease, being completely consumed at the end of the reaction (20 h). By contrast, the current flowing through the cell peaked at *ca.* 5.5 mA within the first ten minutes from the beginning of the reaction, then settled to a 3 mA plateau from 1 to 7 h (see gray line shown in the background).

We also assessed the faradaic efficiency (FE) throughout the reaction course (see Figure S1b) by comparing the chemical yield of **3** (the only net-oxidation product formed, blue line referred to left axis) with the amount of charge flowing through the cell (red line referred to right axis). Upon adjusting the scale of the two axes by considering that two moles of electrons are required in an ideal scenario per mole of **3** formed, it is noteworthy that the two traces are almost superimposable ($\text{FE} \approx 100\%$) until *ca.* 10 h. After this time, the blue line flattens out while the red one keeps increasing, with FE decreasing to a *ca.* 80% final value.

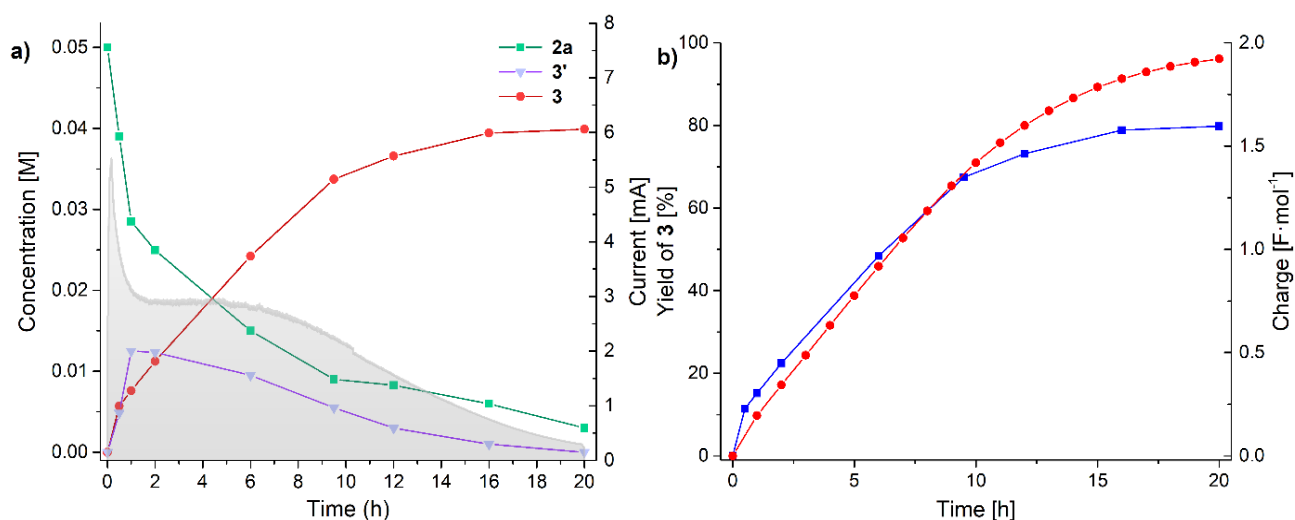


Figure S1. a) Kinetic study of the model reaction between cyclohexane **1a** and benzothiazole **2a**. b) Comparison of the chemical yield of **3** and the amount of charge passed through the cell.

Furthermore, we demonstrated the direct connection between the photocatalytic system and the current flowing through the cell by switching the light on and off at regular time intervals (5 min., Figure S2). We found that the current intensity increases steadily during the irradiation periods, while starts decreasing immediately after turning the light off. Notably, this behavior is replicable for multiple cycles with minimal changes.

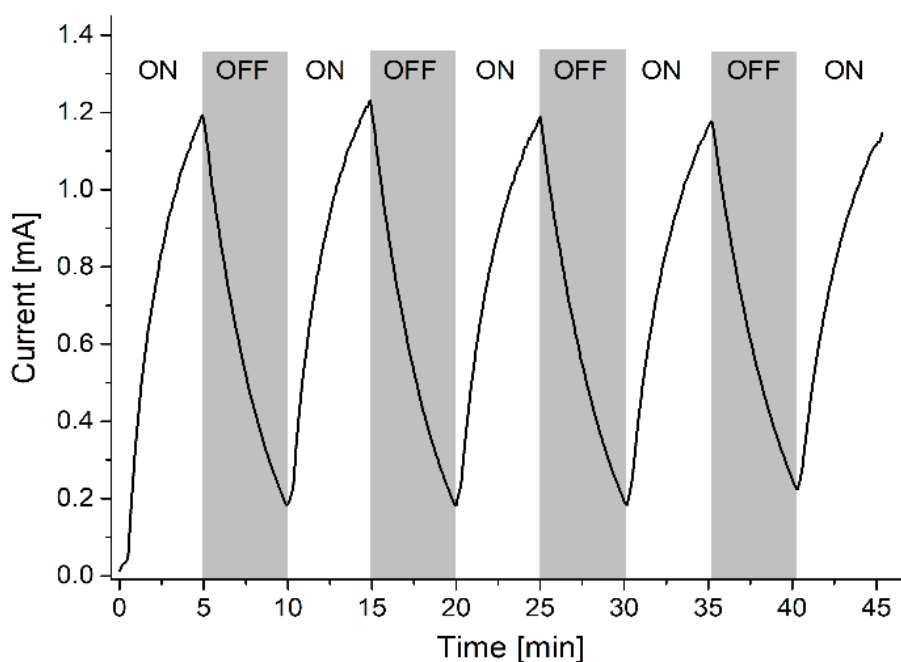


Figure S2. Light ON-OFF experiment.

Considering Scheme 2 in the main text, we may speculate about the relative importance of paths *a* vs *b*, in other words: is the formation of **3'** a prerequisite on the route to **3**? To this end, we compared the data gathered in Figure S1a with an ideal kinetic model for two consecutive reactions (Figure S3). While an overall good agreement among experimental and simulated data was found, the consecutive reactions model implies a certain induction period for the formation of product **3**, which is not observed in the experiment. Accordingly, we can confirm that the direct formation of **3** from **1a** + **2a** occurs, especially in the initial period of the process, when most of the employed catalyst is present in solution in its oxidized form (W), thus behaving as electrocatalyst and favoring path *b* over path *a*.

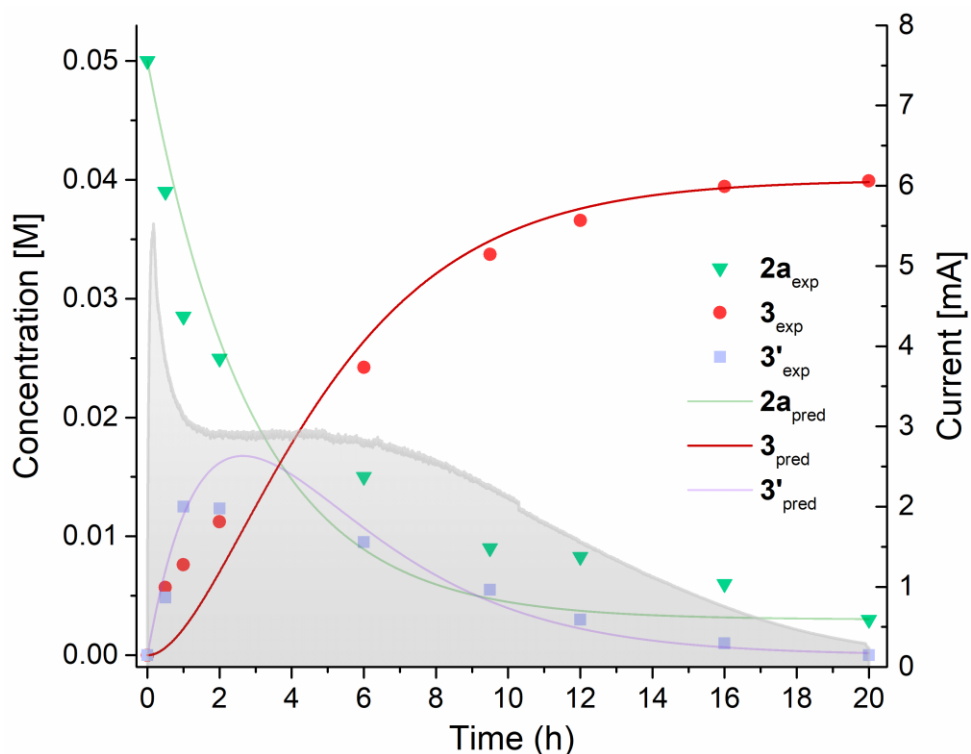


Figure S3. Kinetic profile of the reaction between **1a** and **2a**: the scatter plots represent the experimental concentrations of **2a** (green triangles), **3'** (violet squares) and **3** (red circles) at different reaction times, while line plots are predicted curves according to the kinetic model.

For the kinetic analysis of the model reaction (**1a**+**2a**), we adopted the kinetic model for consecutive reactions in which **2a** is converted into **3'** and, afterwards, **3'** is transformed into **3**. In the case of first-order kinetics with comparable constants ($k_1 \approx k_2$), the kinetic laws for **2a**, **3'** and **3** are the following:

$$\text{for } \mathbf{2a}, [A]_t = [A]_0 \cdot e^{-k_1 t} \quad (\text{eq. S1})$$

$$\text{for } \mathbf{3'}, \frac{k_1}{(k_2 - k_1)} * (e^{-k_1 t} - e^{-k_2 t}) \cdot [A]_0 \quad (\text{eq. S2})$$

$$\text{for } \mathbf{3}, [A]_0 \cdot \left[1 + \frac{(k_2 e^{-k_1 t} - k_1 e^{-k_2 t})}{(k_1 - k_2)} \right] \quad (\text{eq. S3})$$

We applied suitable correction factors to equations (eq. S1) and (eq. S3) to account for the observed remaining starting material and yield, respectively. As for equation (eq. S2), an average correction factor was applied. Accordingly, the corrected laws for **2a**, **3'** and **3** are the following:

$$\text{for } \mathbf{2a}, [A]_t = [A]_0 \cdot (0.06 + \mathbf{0.94} \cdot e^{-k_1 t}) \quad (\text{eq. S1}_c)$$

$$\text{for } \mathbf{3'}, [I]_t = \mathbf{0.87} \cdot [A]_0 \cdot \frac{k_1}{(k_2 - k_1)} * (e^{-k_1 t} - e^{-k_2 t}) \quad (\text{eq. S2}_c)$$

$$\text{for } \mathbf{3}, [P]_t = \mathbf{0.80} \cdot [A]_0 \cdot \left[1 + \frac{(k_2 e^{-k_1 t} - k_1 e^{-k_2 t})}{(k_1 - k_2)} \right] \quad (\text{eq. S3}_c)$$

We used equations S1-3_c to fit the experimental data and found that:

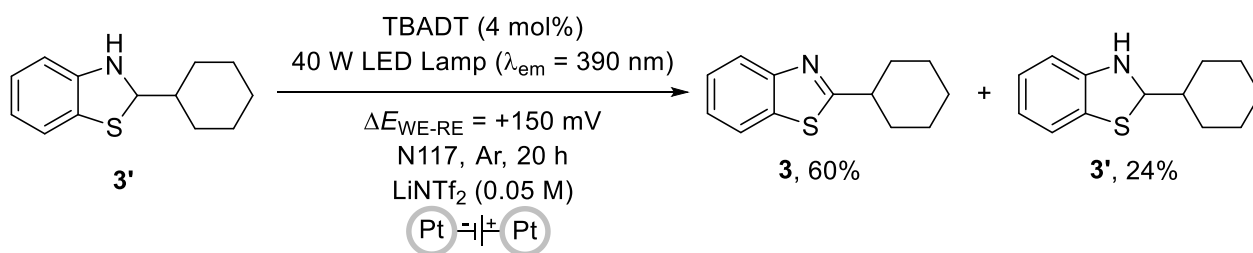
$$k_1 = 0.34 \text{ h}^{-1}$$

$$k_2 = 0.41 \text{ h}^{-1}$$

1.3 Reactivity of intermediate 2-cyclohexylbenzothiazoline (3')

1.3.1 Reactivity of 3' under optimized photoelectrochemical conditions

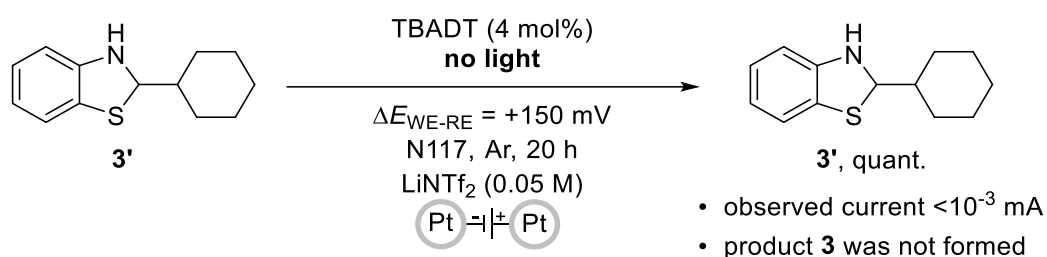
Compound **3'** was subjected to optimized photoelectrochemical conditions, according to the general procedure reported above. Thus, apart from the electrolyte and the photocatalyst (TBADT, 4 mol%), only compound **3'** (0.05 M) was placed in the anolyte. This experiment was intended to verify whether product **3** could be formed from **3'** via the described photoelectrochemical approach. The reaction was stopped after 20 h, then usual work up and purification of the crude mixture allowed to obtain product **3** in 60% yield, along with 24% of unreacted starting material **3'** (**Scheme S1**).



Scheme S1. Reactivity of compound **3'** under optimized photoelectrochemical conditions.

1.2.2 Reactivity of **3'** under purely electrochemical conditions (control experiment in the dark)

Next, we subjected compound **3'** to purely electrochemical conditions, *viz.* adopting the same reaction setup described above in the general procedure, while omitting irradiation (reaction performed in the dark). Thus, a constant voltage of +150 mV was set between WE and RE through the potentiostat. After 1 h electrolysis, product **3** was not observed (**Scheme S2**), with very low current values observed throughout the entire experiment ($< 10^{-3}$ mA).



Scheme S2. Reactivity of compound **3'** under purely electrochemical conditions.

1.4 Laser Flash Photolysis

Laser flash photolysis (LFP) experiments were performed to study the decay of the reactive excited state of decatungstate (tagged **wO**), which can be monitored at 780 nm.^{S1-S3} Thus, after verifying that LiNTf₂ does not act as a quencher of **wO**, we measured the quenching constants for **1a** and **3'** under the present reaction conditions. As for the former, a bimolecular rate constant $k_Q(\mathbf{1a}) = 3.3 \times 10^8 \text{ M}^{-1} \cdot \text{s}^{-1}$ was determined, a value significantly higher than that found in neat MeCN ($2.3 \times 10^7 \text{ M}^{-1} \cdot \text{s}^{-1}$), in accordance with that previously reported in the literature, namely $k_Q(\mathbf{1a}, \text{MeCN}) = 4.0 \times 10^7 \text{ M}^{-1} \cdot \text{s}^{-1}$.^{S4} On the other hand, **3'** quenched **wO** with a nearly diffusion-controlled bimolecular rate constant, $k_Q(\mathbf{3}') > 10^9 \text{ M}^{-1} \cdot \text{s}^{-1}$. Furthermore, upon careful inspection of the shape of the recorded spectral traces, we ascertained that the activation of **1a** and **3'** occurs via HAT and SET, respectively.^{S3}

Experimental Laser flash photolysis studies were performed by adopting the third harmonic of a Q-switched Nd:YAG laser ($\lambda_{\text{exc}} = 355 \text{ nm}$). $1.0 \times 10^{-4} \text{ M}$ starting solutions of TBADT ($n\text{Bu}_4\text{N}$)₄[W₁₀O₃₂] were employed, with an absorbance value of ~ 0.5 at 355 nm. The sample solution was placed in a 1×1 cm quartz cell and excited with single pulses (10 mJ, 1 Hz) delivered from the laser and analyzed with a pulsed Xe arc lamp. Lifetimes of the reactive transient **wO** were obtained by fitting the first order decay profiles recorded at 780 nm (band width: 2 nm) by using the following equation:

$$y = y_0 + A \cdot e^{-\frac{x}{\tau}}$$

As already demonstrated by Texier *et al.*, the excited state of TBADT (**wO**) can be quenched via two distinct mechanisms, namely Hydrogen Atom Transfer (HAT, **Figure S4** left) or Single-Electron Transfer (SET, **Figure S4** right).^{S3}

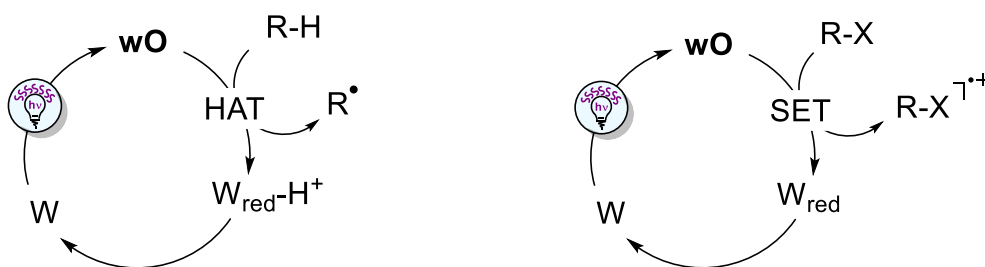


Figure S4. Modes of quenching of **wO**: HAT (left) and SET (right).

Upon quenching of **wO**, the (protonated) reduced photocatalyst ($W_{\text{red}}(\text{H}^+) \equiv \text{H}^+[\text{W}_{10}\text{O}_{32}]^{5-}$) is generated. Note that both **wO** and ($W_{\text{red}}(\text{H}^+)$) absorb at 780 nm.^{S3}

The transient absorption spectroscopy (TAS) of TBADT offers different outcomes, depending on the actual mechanism of quenching, namely HAT or SET. In other words, the decay profile can be used as a “footprint” to ascertain the activation mechanism. In fact, the HAT mechanism leads to the accumulation of an appreciable amount of the reduced photocatalyst ($W_{\text{red}}(\text{H}^+)$), which results in a persistent signal at 780 nm observed even at long times after the laser pulse (>400 ns). On the contrary, if SET operates, this signal is not present and the pre-pulse situation is rapidly restored, no persistent signal being observed. This difference can be appreciated by looking at the simulated profiles reported in **Figure S5**.

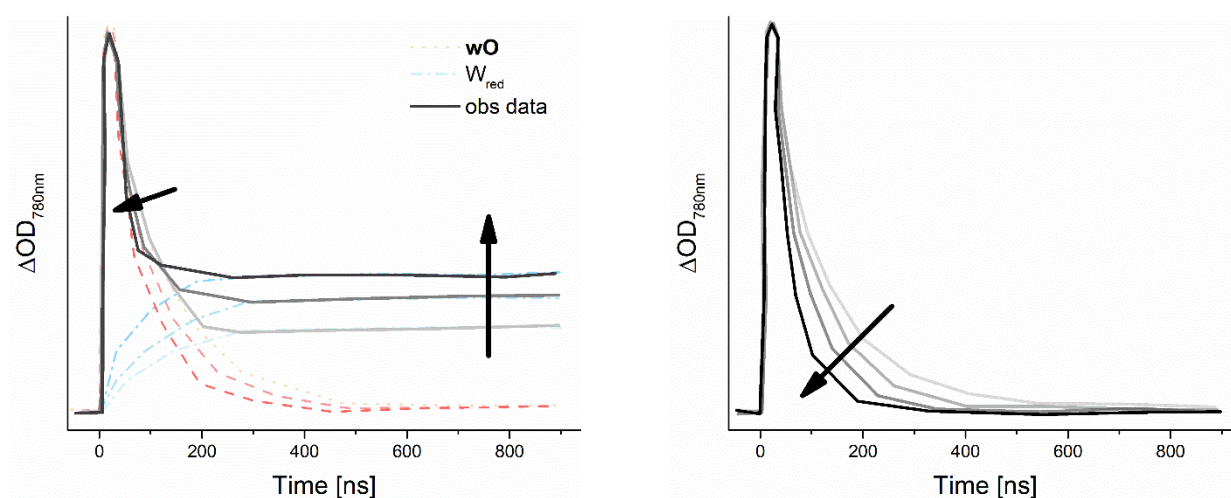


Figure S5. Simulated decay profiles of **wO** at increasing concentrations of the quencher followed at 780 nm in the case of a quenching occurring via HAT (left) or SET (right).

Summing up, when the profile reported in **Figure S5**, left, is observed in the presence of increasing amounts of the quencher, the quencher is activated by TBADT via a HAT mechanism. This profile is typically observed for cycloalkanes or aliphatic alcohols, for example. Conversely, when the profile reported in **Figure S5**, right, is observed, the quenching is occurring via SET, as previously demonstrated for arylamines.^{S3}

Coming to the present work, we postulated that **1a** and **3'** might quench **wO** via HAT and SET, respectively (**Figure S6**).

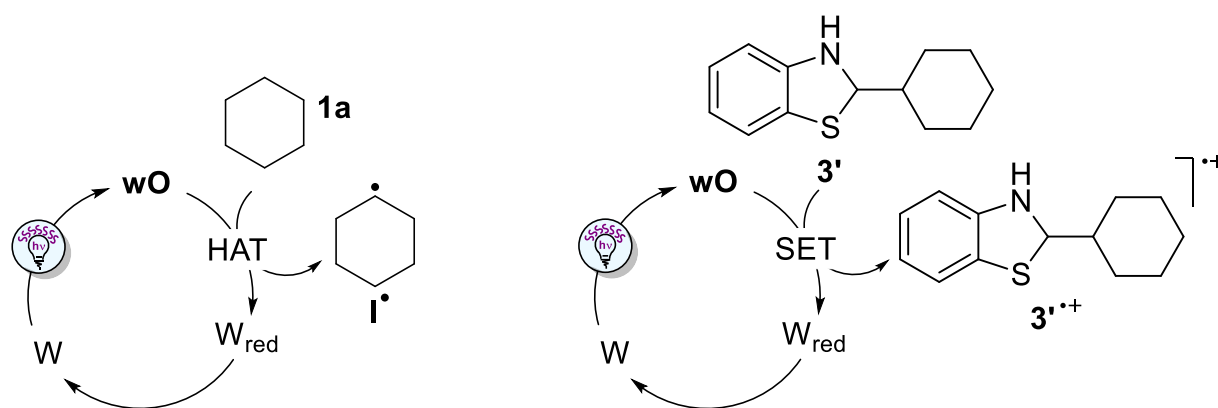


Figure S6. Expected modes of quenching of **wO** by **1a** (left) and **3'** (right).

Indeed, when performing TAS experiments on a 1×10^{-4} M MeCN/H₂O 10:1 solution of TBADT in the presence of LiNTf₂ (0.05 M) upon addition of increasing amounts of **1a** and **3'**, the profiles reported in **Figure S7** were observed.

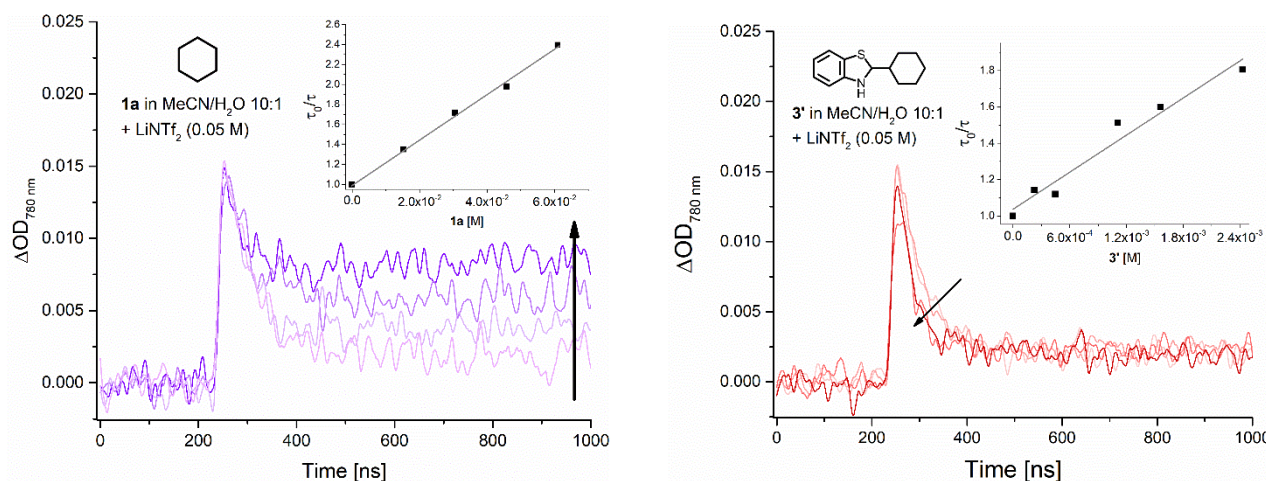
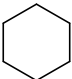
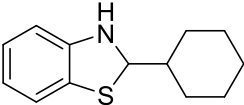


Figure S7. Decay profiles of a MeCN/H₂O 10:1 solution of TBADT (10^{-4} M) in the presence of LiNTf₂ (0.05 M) upon addition of increasing amounts of **1a** (left) and **3'** (right).

It is apparent that the two profiles are different, confirming that the quenching of **wO** by **1a** and **3'** occurs via HAT and SET, respectively. Table S2 summarizes the results of the photophysical quenching experiments reported below in more detail. In particular, the quenching constants of the reactive excited state of the photocatalyst (**wO**) by **1a** and **3'** in different media are given.

Table S2. Quenching constants of **wO** by **1a** and **3'** in MeCN, MeCN/H₂O 10:1 and MeCN/H₂O 10:1 + 0.05 M LiNTf₂.

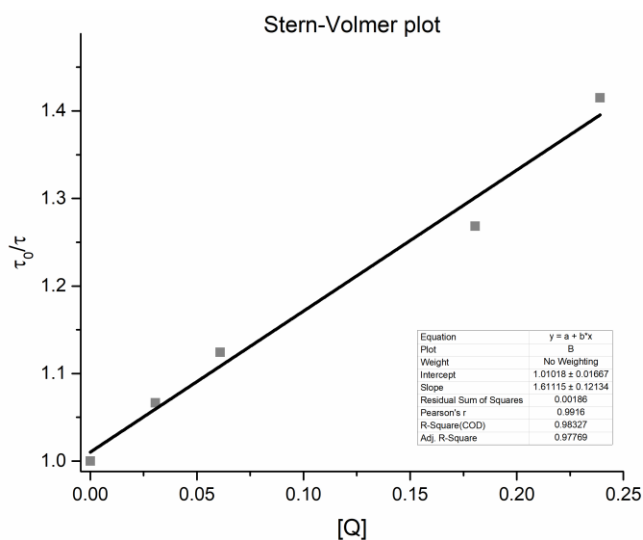
	k_Q (M ⁻¹ s ⁻¹)	τ_0 (ns)	
<div style="text-align: center;">  1a </div>	$2.3 \cdot 10^7$	69 ns	in MeCN
	$8.9 \cdot 10^7$	56 ns	in MeCN/H ₂ O 10:1
	$3.3 \cdot 10^8$	60 ns	in MeCN/H ₂ O 10:1 + 0.05 M LiNTf ₂
<div style="text-align: center;">  3' </div>	$4.7 \cdot 10^9$	70 ns	in MeCN
	$3.7 \cdot 10^9$	57 ns	in MeCN/H ₂ O 10:1
	$7.5 \cdot 10^9$	59 ns	in MeCN/H ₂ O 10:1 + 0.05 M LiNTf ₂

1.4.1 Quenching of wO with cyclohexane in MeCN

- Starting solution: TBADT 10⁻⁴ M in MeCN (3 mL)
- Quenching solution: neat cyclohexane

The Stern-Volmer plot was fitted with the following equation:

$$\frac{\tau_0}{\tau} = 1 + k_Q \tau_0 [Q]$$



$$b = k_Q \times \tau_0$$

$$\tau_0 = 6.9 \times 10^{-8} \text{ s}$$

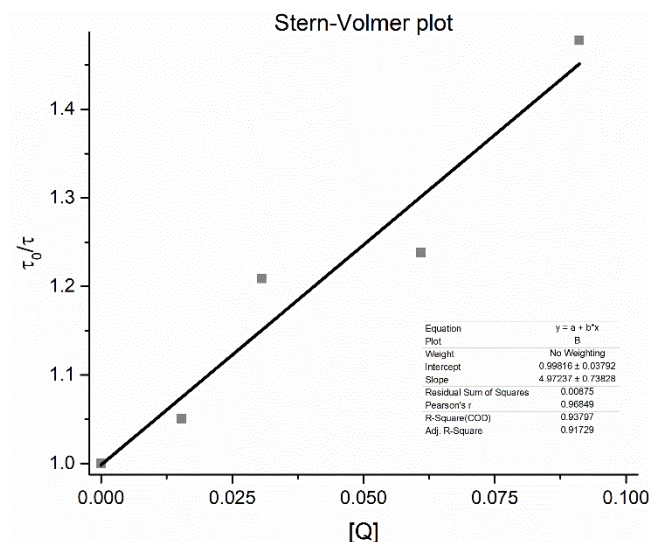
$$k_Q = 2.3 \times 10^7 \text{ M}^{-1} \cdot \text{s}^{-1}$$

1.4.2 Quenching of wO with cyclohexane in MeCN/H₂O 10:1

- Starting solution: TBADT 10⁻⁴ M in MeCN/ H₂O 10:1 (3 mL)
- Quenching solution: neat cyclohexane

The Stern-Volmer plot was fitted with the following equation:

$$\frac{\tau_0}{\tau} = 1 + k_Q \tau_0 [Q]$$



$$b = k_Q \times \tau_0$$

$$\tau_0 = 5.6 \times 10^{-8} \text{ s}$$

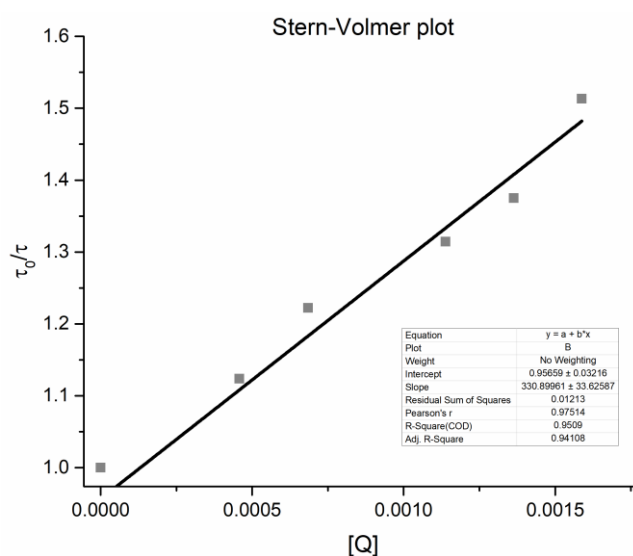
$$k_Q = 8.9 \times 10^7 \text{ M}^{-1} \cdot \text{s}^{-1}$$

1.4.3 Quenching of wO with 3' in MeCN

- Starting solution: TBADT 10⁻⁴ M in MeCN (3 mL)
- Quenching solution: 3' 0.14 M in MeCN

The Stern-Volmer plot was fitted with the following equation:

$$\frac{\tau_0}{\tau} = 1 + k_Q \tau_0 [Q]$$



$$b = k_Q \times \tau_0$$

$$\tau_0 = 7.0 \times 10^{-8} \text{ s}$$

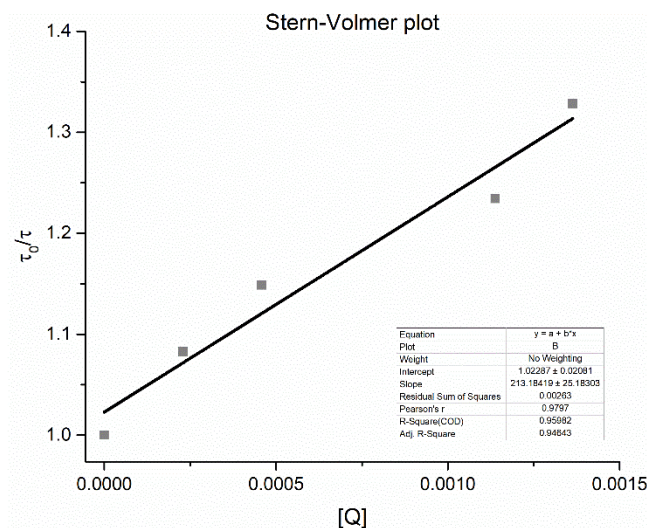
$$k_Q = 4.7 \times 10^9 \text{ M}^{-1} \cdot \text{s}^{-1}$$

1.4.4 Quenching of wO with 3' in MeCN/H₂O 10:1

- Starting solution: TBADT 10⁻⁴ M in MeCN/ H₂O 10:1 (3 mL)
- Quenching solution: neat cyclohexane

The Stern-Volmer plot was fitted with the following equation:

$$\frac{\tau_0}{\tau} = 1 + k_Q \tau_0 [Q]$$



$$b = k_Q \times \tau_0$$

$$\tau_0 = 5.7 \times 10^{-8} \text{ s}$$

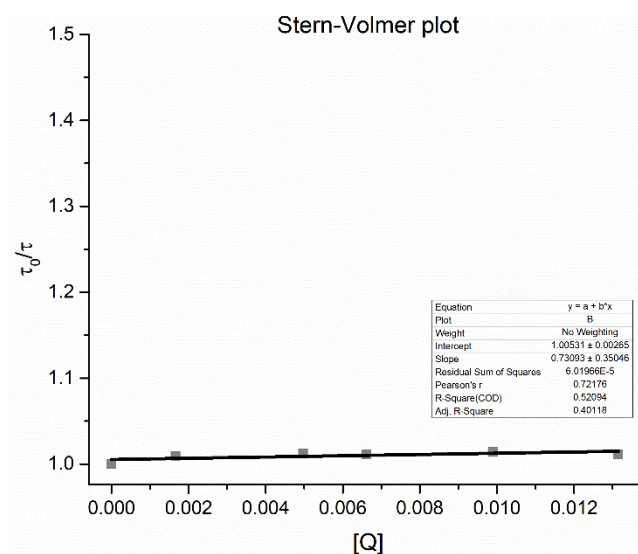
$$k_Q = 3.7 \times 10^9 \text{ M}^{-1} \cdot \text{s}^{-1}$$

1.4.5 Quenching of wO with lithium triflimide in MeCN/H₂O 10:1

- Starting solution: TBADT 10⁻⁴ M in MeCN/H₂O 10:1 (3 mL)
- Quenching solution: lithium triflimide 1.0 M in MeCN/H₂O 10:1

The Stern-Volmer plot was fitted with the following equation:

$$\frac{\tau_0}{\tau} = 1 + k_Q \tau_0 [Q]$$



$$b = k_Q \times \tau_0$$

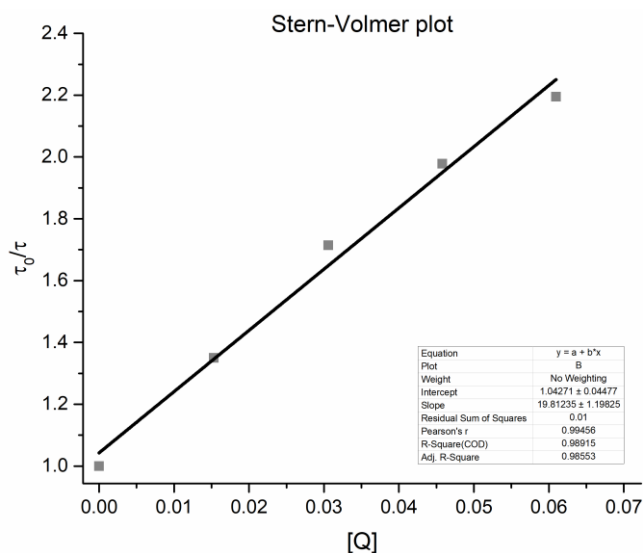
$$\tau_0 = 6.1 \times 10^{-8} \text{ s}$$

$$k_Q = \text{n.d.}$$

1.4.6 Quenching of wO with cyclohexane in MeCN/H₂O 10:1 + 0.05 M lithium triflimide

- Starting solution: TBADT 10⁻⁴ M (+0.05 M LiNTf₂) in MeCN/H₂O 10:1 (3 mL)
- Quenching solution: neat cyclohexane

The Stern-Volmer plot was fitted with the following equation: $\frac{\tau_0}{\tau} = 1 + k_Q \tau_0 [Q]$

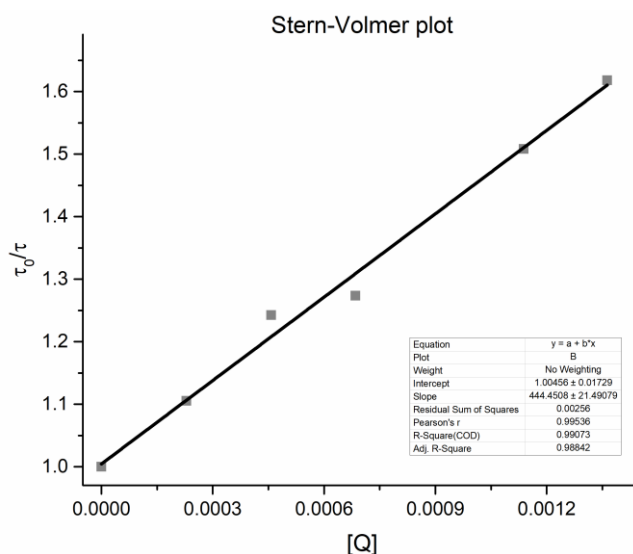


$$b = k_Q \times \tau_0 \quad \tau_0 = 6.0 \times 10^{-8} \text{ s} \quad k_Q = 3.3 \times 10^8 \text{ M}^{-1} \cdot \text{s}^{-1}$$

1.4.7 Quenching of wO with 3' in MeCN/H₂O 10:1 + 0.05 M lithium triflimide

- Starting solution: TBADT 10⁻⁴ M (+0.05 M LiNTf₂) in MeCN/H₂O 10:1 (3 mL)
- Quenching solution: 3' 0.14 M in MeCN/H₂O 10:1

The Stern-Volmer plot was fitted with the following equation: $\frac{\tau_0}{\tau} = 1 + k_Q \tau_0 [Q]$

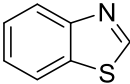
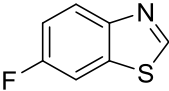
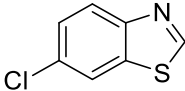
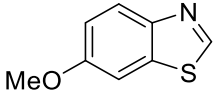
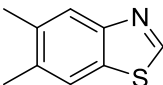
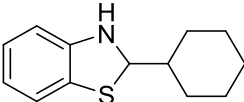


$$b = k_Q \times \tau_0 \quad \tau_0 = 5.9 \times 10^{-8} \text{ s} \quad k_Q = 7.5 \times 10^9 \text{ M}^{-1} \cdot \text{s}^{-1}$$

1.5 Electrochemical data

The electrochemical measurements were carried out by a BASi computer-controlled electrochemical analyzer. Electrochemical measurements (cyclic voltammetry) were performed in a three-electrode cell (3 mL) and acetonitrile or aqueous acetonitrile were used as solvent (see below). As for the electrolyte, it was used in a 0.1 M concentration (see below), while the tested compounds were used in a 5 mM concentration. Electrodes: glassy carbon (diameter 2 mm, BASi) as the working electrode, Pt wire as the auxiliary electrode and Ag/AgCl (sat'd NaCl) as the reference electrode. Scan speed was 100 mV/s. The potentials measured were then referred to SCE by applying the equation: $E \text{ (V vs SCE)} = E \text{ (V vs Ag/AgCl, sat'd NaCl)} - 47 \text{ mV}$.

Table S3. $E_{p/2}^{ox}$ of representative benzothiazoles **2** and benzothiazoline **3'** used in this work, reported against saturated calomel electrode (SCE). Electrolyte: LiClO₄ 0.1 M. Solvent: MeCN.

 2a + 2.08 V vs SCE	 2b + 2.13 V vs SCE	 2c + 2.15 V vs SCE	 2f $E_{offset} > +1.0 \text{ V vs SCE}$
	 2i $E_{offset} > +1.0 \text{ V vs SCE}$	 3' + 0.50 V vs SCE	

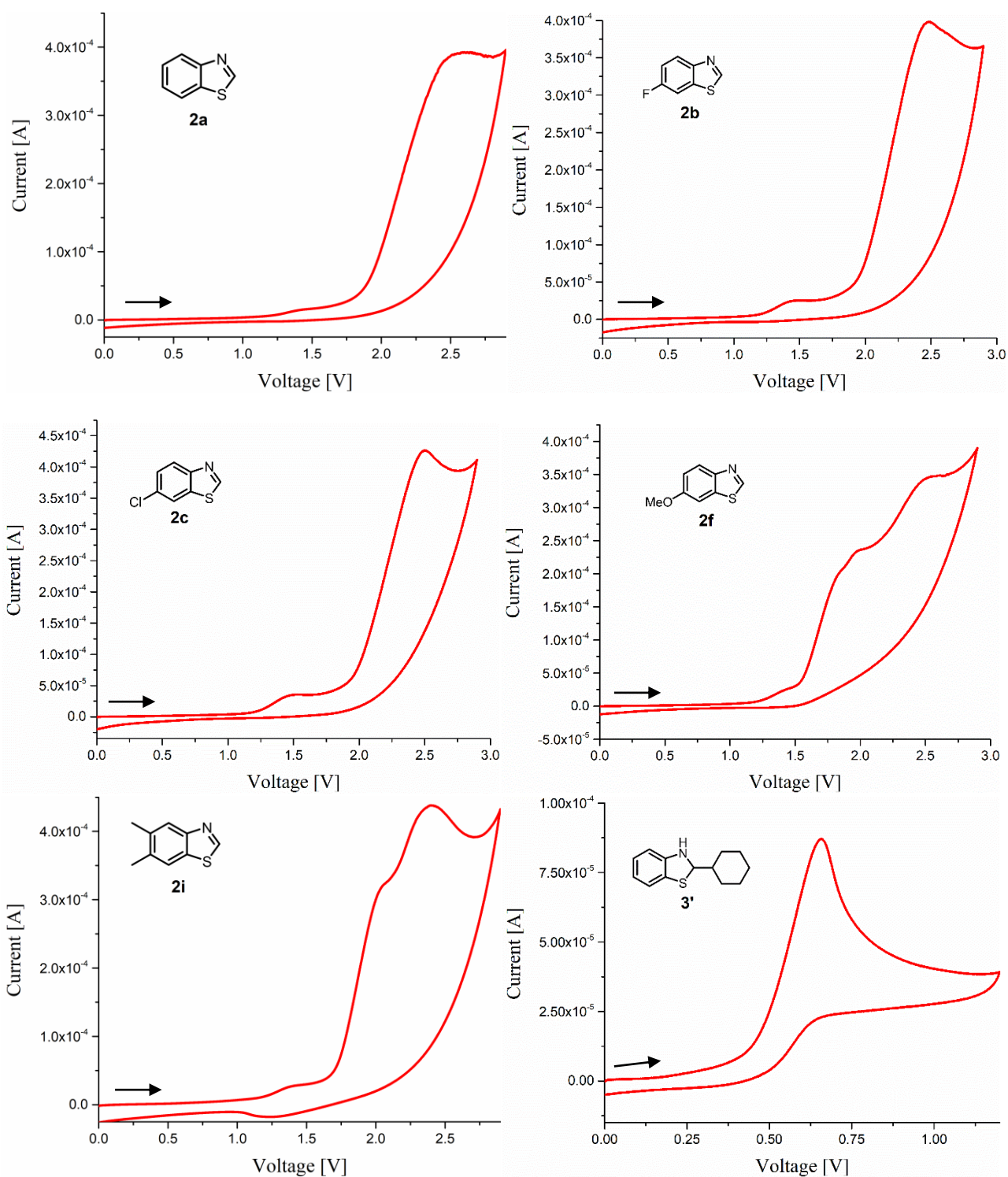


Figure S8. Cyclic voltammetry of compounds **2a**, **2b**, **2c**, **2f**, **2i** and **3'**. Electrolyte: LiClO₄ 0.1 M. Solvent: MeCN. Concentration of the tested compound: 5 mM.

In order to assess the electrocatalytic behavior of TBADT, we evaluated its redox potential along with that of **III'**. In particular, we used protonated product **3** (via addition of 1 equiv of trifluoroacetic acid) and measured its reduction potential, as indicated in the literature.^{S5} In particular, we performed a cyclic voltammogram of **3** alone, of **3** in the presence of 1 equivalent of trifluoroacetic acid (TFA) (to in situ generate the species **3-H**⁺) and of TFA alone (**Figure S9**) in MeCN/H₂O 10:1.

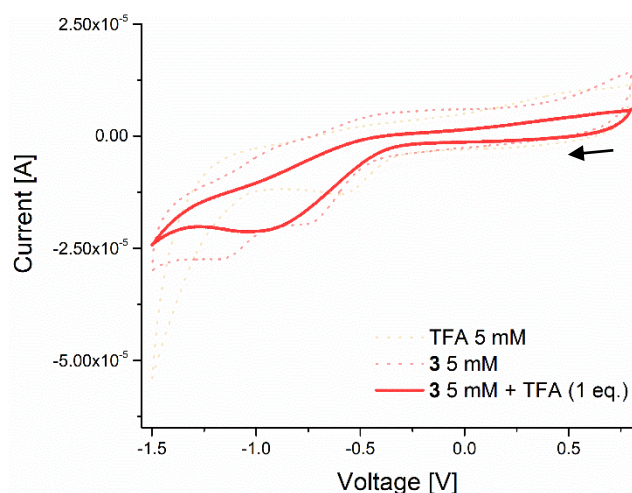
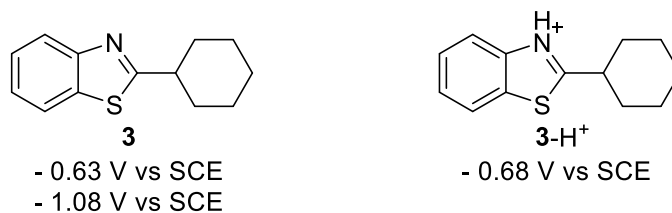


Figure S9. Cyclic voltammetry of TFA, **3** and **3-H**⁺. Electrolyte: TBAClO₄ 0.1 M. Solvent: MeCN/H₂O 10:1. Concentration of the tested compounds: 5 mM.

The attempts to reduce **3** led to the observation of two reductive events at $E_{p/2}^{\text{red}} = -0.63$ V and -1.08 V vs SCE), while the reduction of the protonated product (**3-H**⁺) resulted in one broad peak at -0.68 V vs SCE. As a blank experiment, we also measured the redox potential for the reduction of protons (from TFA), which occurred at $E_{p/2}^{\text{red}} = -0.50$ V vs SCE (see **Figure S9**) in our conditions.

Table S4. $E_{p/2}^{\text{red}}$ of **3** and **3-H**⁺ reported against saturated calomel electrode (SCE).



Finally, we measured the redox potential of TBADT in different conditions: first in MeCN (TBAClO₄ 0.1 M as the electrolyte) and then in MeCN/H₂O 10:1 (LiClO₄ or LiNTf₂ 0.1 M as the electrolyte). Interestingly, we found a completely different redox behavior in the two cases (**Figure S10**):

- $E_{p/2}^{\text{red}} = -0.91 \text{ V vs SCE}$ ([TBADT] = 5 mM, TBAClO₄ 0.1 M, **MeCN**);^{S6}
- $E_{p/2}^{\text{red}} = -0.45 \text{ V vs SCE}$ ([TBADT] = 5 mM, **LiClO₄** 0.1 M, **MeCN/H₂O 10:1**);
- $E_{p/2}^{\text{red}} = -0.52 \text{ V vs SCE}$ ([TBADT] = 5 mM, **LiNTf₂** 0.1 M, **MeCN/H₂O 10:1**);

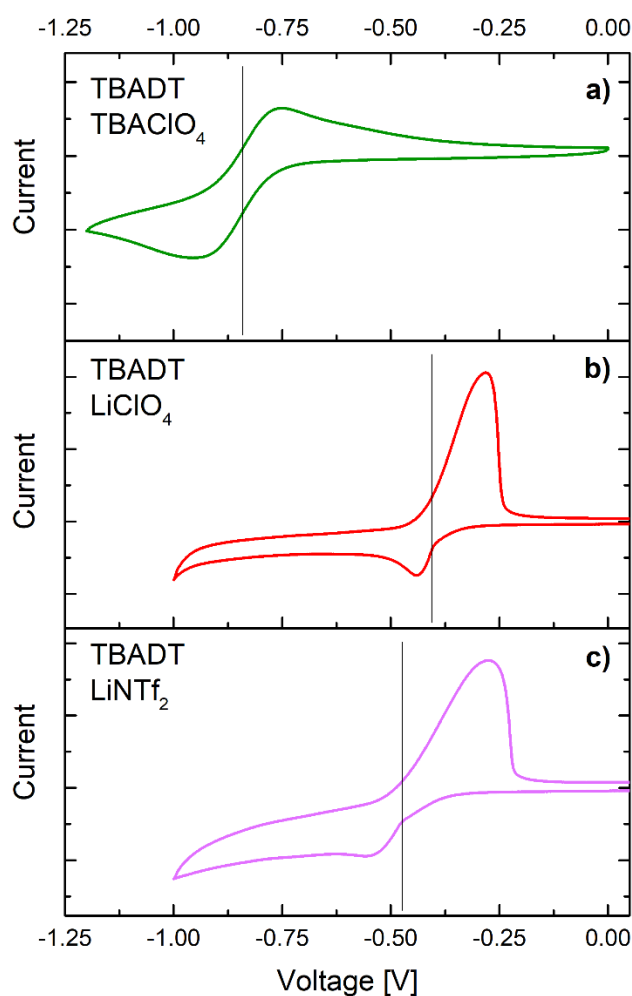


Figure S10. Cyclic voltammetry of: a) a MeCN solution of TBADT (5 mM) and TBAClO₄ (0.1 M), b) a MeCN/H₂O 10:1 solution of TBADT (5 mM) and LiClO₄ (0.1 M), c) a MeCN/H₂O 10:1 solution of TBADT (5 mM) and LiNTf₂ (0.1 M).

The presence of lithium dramatically changes the electrochemical behavior of TBADT, making it a better oxidant for **III**.

2. Experimental section

2.1 General information

Reagents and solvents: All reagents and chemicals used in this work were of analytical grade and purchased from various commercial suppliers (TCI Europe N.V., Sigma Aldrich, Fluorochem). All solvents used were purchased from Carlo Erba, except for ethyl acetate (Sigma Aldrich); THF was freshly distilled before use. TBADT was synthesized according to a procedure reported in the literature.^{S7}

Electrodes: Pt gauze electrodes (guaranteed purity of 999.5 %) were purchased from 8853 S.p.a., Italy. Nafion[®] 117, carbon paper and carbon cloth electrodes were purchased from H2Planet, Italy. Glassy carbon rod electrodes were purchased from Hochttemperatur-Werkstoffe GmbH, Germany. BDD plate electrodes were purchased from CONDIAS GmbH, Germany. Electrolysis reactions were performed on an EC Epsilon EClipse™ Potentiostat/Galvanostat. A PR160-390 nm lamp (40 W) from Kessil Photoredox, USA, was employed as UV light source.

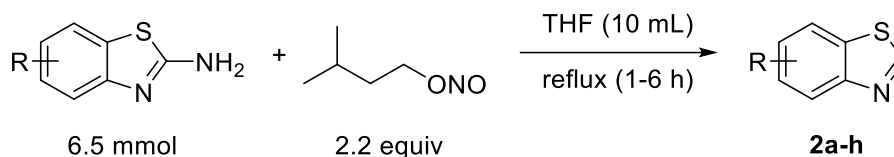
Purification: Column chromatography was performed on an Isolera Spektra One purchased from Biotage, Sweden, using Sepachrom PUREZZA open-load flash cartridges purchased from Sepachrom Srl, Italy. Petroleum ether/cyclohexane and ethyl acetate were used as eluants.

NMR analysis: NMR spectra were recorded on a 376 (for ¹⁹F), 300 or 700 (for ¹H), 75 (for ¹³C) MHz spectrometer, and are internally referenced to residual protio solvent signals (for CDCl₃, referenced at 7.26 and 77.0 ppm, respectively; for CD₃CN, referenced at 2.13 and 118.0 ppm, respectively). Data for ¹H and ¹⁹F NMR are reported as follows: chemical shifts reported in ppm, multiplicity (s = singlet, bs = broad singlet, d = doublet, t = triplet, q = quadruplet, m = multiplet), coupling constant (*J*, Hz) and integration. Data for ¹³C NMR are reported as chemical shifts (ppm).

2.2 General procedure for the synthesis of substituted benzothiazoles

Substituted benzothiazoles (**2b-i**) were not commercially available: **2b**, **2c**, **2d**, **2f**, **2h** and **2i** were prepared following a procedure previously reported in the literature (**Scheme S3**), while **2e** and **2g** were synthesized by adapting the same procedure.^{S8} In particular, a 50 mL round-bottom flask was charged with 10 mL of freshly distilled THF and the chosen 2-aminobenzothiazole derivative (6.5 mmol, 0.65 M). Stirring was applied and isoamyl nitrite (1.9 mL, 14.3 mmol, 2.2 equiv., $\rho = 0.872$ g/mL) was added dropwise. The resulting mixture was then refluxed, depending on the substrate, for a period of time ranging from 1 to 6 hours (see below). The solution was then poured into a

mixture of ice and water, then the aqueous phase was extracted with ethyl acetate (3×30 mL). Organic phases were combined and washed with brine, dried on Na₂SO₄, filtered, then solvent was removed under reduced pressure. Purification was performed by means of column chromatography (SiO₂; cyclohexane/ethyl acetate 95:5). Products were obtained with yields ranging from 40 to 75% (see below).



Scheme S3. Synthesis of benzothiazoles.

2.3 General procedure for the photoelectrochemical cross-dehydrogenative coupling

Preparation and materials of the cell: An H-type cell was used in these experiments (**Figure S11**). A Nafion[®] 117 membrane was used and positioned in between two Teflon[®] rings (7); a flange system (2) was used to seal the juncture between the compartments of the cell (6). The two compartments were capped with silicone septa embedding the required electrodes. In particular, experiments were performed using a 3-electrodes apparatus:

Reference Electrode (RE): Ag/AgCl in sat'd NaCl (3);

Counter Electrode (CE): Pt gauze (4);

Working Electrode (WE): Pt gauze (5).

Two stock solutions were prepared: one for the anodic compartment (anolyte) and one for the cathodic one (catholyte).

Solution for anolyte: benzothiazole (0.05 M), H-Donor (see each case) in MeCN/H₂O 10:1

Solution for catholyte: H₂O

Oxygen was fully removed from both solutions via 3 cycles of freeze-pump-thaw.

Both the anodic and cathodic compartments were charged with LiNTf₂ (1 equiv.), while only the anodic cell was charged with TBADT ((*n*Bu₄N)₄[W₁₀O₃₂]; 4 mol%). Cells were kept under positive flux of Ar for 10 minutes, then 15 mL of the proper solution (see above) were added by means of a syringe through the sealed septum. The potential between WE and RE was set to the desired voltage, then, after a few seconds of electrolysis (*ca.* 5 seconds), the anolyte was irradiated with a 40 W Kessil Lamp (390 nm, full power) placed 5 cm away from the compartment. Current profile

was monitored in time (*potentiostatic mode*) and the reaction was stopped after 20 hours, namely either when the heterocycle was completely consumed (by TLC) or when current intensity values dropped below 5% of the initial value.

After photoelectrolysis, anolyte and catholyte were combined, the cell was thoroughly washed with ethyl acetate (~ 100 mL), the organic phase was in turn washed with water (3×30 mL), brine (3×30 mL) and the organic phase was dried over Na₂SO₄. Solvent was removed under reduce pressure. NMR standard was added (CH₂Br₂) and quantitative NMR analysis was performed in explorative experiments, while purification via column chromatography (cyclohexane/ethyl acetate as the eluants) afforded pure products in preparative experiments.

NOTE: work up of the separated anolyte and catholyte compartments was also carried out to check for reagent migration to the cathodic half-cell, if any. Migration was only rarely observed, however, never exceeding 10%.

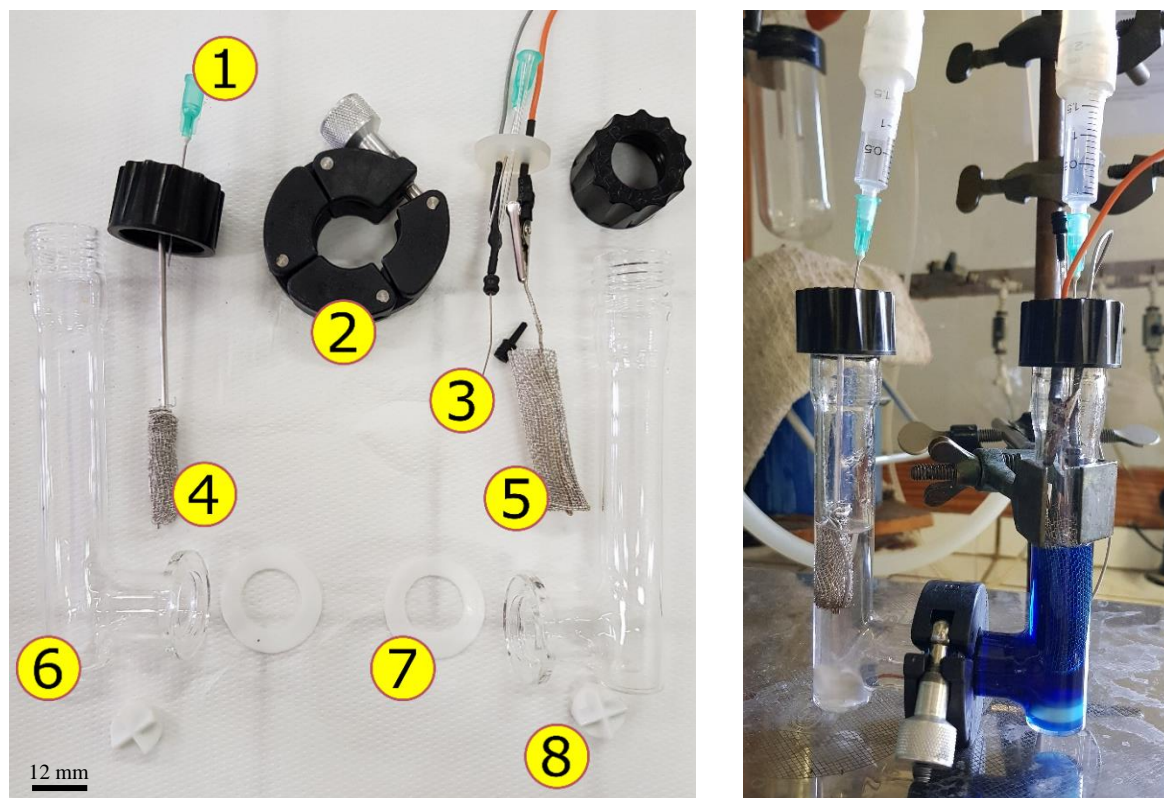


Figure S11. Left part: experimental setup used, including: 1) Argon inlet; 2) flange system; 3) Ag wire for RE; 4) Pt gauze (cathode); 5) Pt gauze (anode); 6) half-cell (7; inner diameter: 15 mm, inner diameter: 18 mm, height: 125 mm) Teflon[®] ring; 8) cross-head magnetic stirrer (diameter: 12 mm). Right part: H-type cell after irradiation; the blue-color of the anolyte is due to the reduced form of the photocatalyst (TBADT).

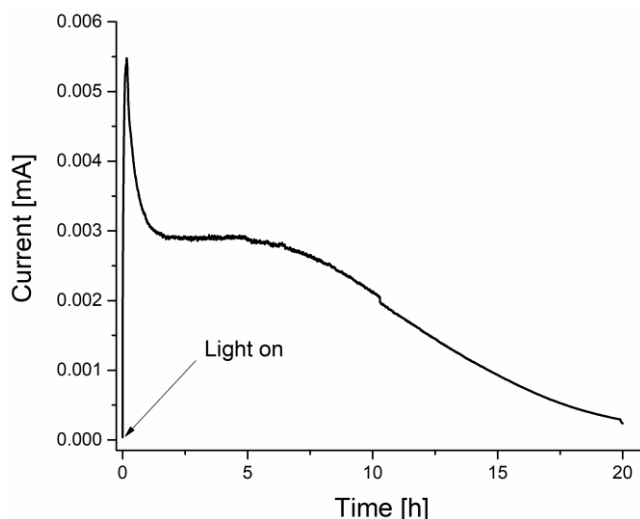


Figure S12. Typical profile for the reaction between **1a** and **2a** performed in the potentiostatic mode ($\Delta E_{WE-RE} = +150$ mV).

Typical experiment with amperostatic mode: Assembly of the reaction setup was performed as indicated above. Current flowing through the cell was set to the desired value (2 mA) and reaction time was fixed to 20 h, allowing to obtain a total charge flow within the cell of 2 F/mol. Work up was performed according to the same procedure indicated above.

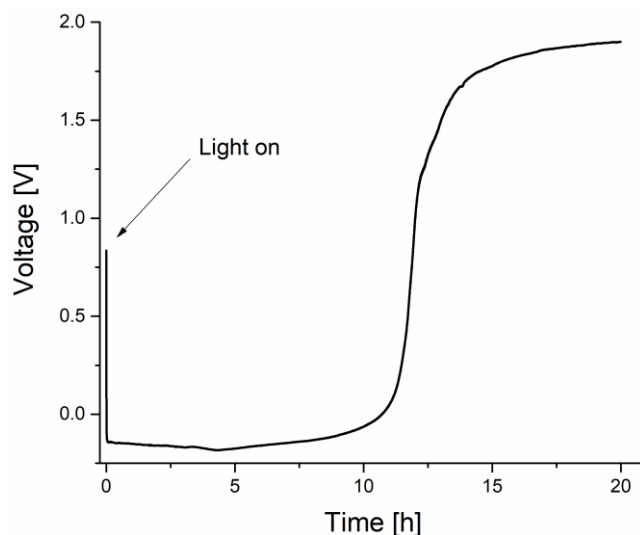


Figure S13. Typical profile for the reaction between **1a** and **2a** performed in the amperostatic mode ($I = 2$ mA).

Typical experiment with undivided setup: a stock solution containing the heterocycle (0.05 M) and the H-Donor (5 equiv.) in MeCN/H₂O 10:1 was prepared in a flask and oxygen was removed via 3 cycles of freeze-pump-thaw.

A 50 mL round-bottom flask was charged with LiNTf₂ (1 equiv.) and TBADT ((*n*Bu₄N)₄[W₁₀O₃₂]; 4 mol%), and sealed with a silicone septum fitted with the required electrodes. The reaction vessel was kept under positive pressure of Ar for 10 minutes before adding 25 mL of stock solution through the septum by means of a syringe. The potential between WE and RE was set to the desired voltage (+150 mV) and the current profile was recorded during time (*potentiostatic mode*). After a few seconds of electrolysis (*ca.* 5 seconds), the flask was irradiated with a 40 W Kessil Lamp (390 nm, full power) placed 5 cm away from the cell. Work up was performed according to the same procedure indicated above.

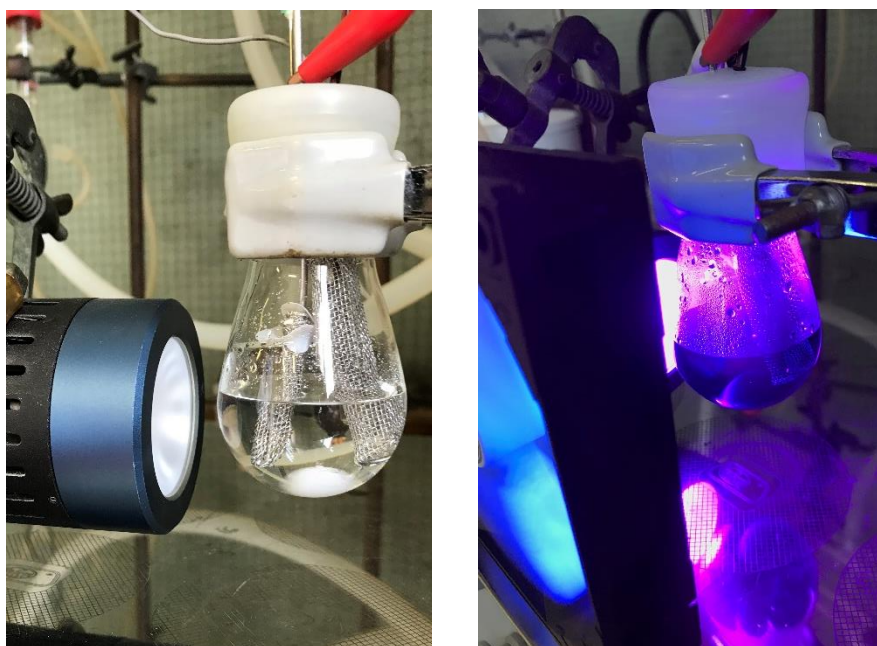


Figure S14. Undivided cell setup: one-neck round bottom flask was used in this experiment.

Typical experiment with a battery: the experimental setup is identical to that reported in **Figure S11**, but two commercially available batteries (1.5 V each) were used in place of the potentiostat (**Figure S15**). The two batteries were connected in series to produce a voltage of 3.0 V overall. The RE was omitted.

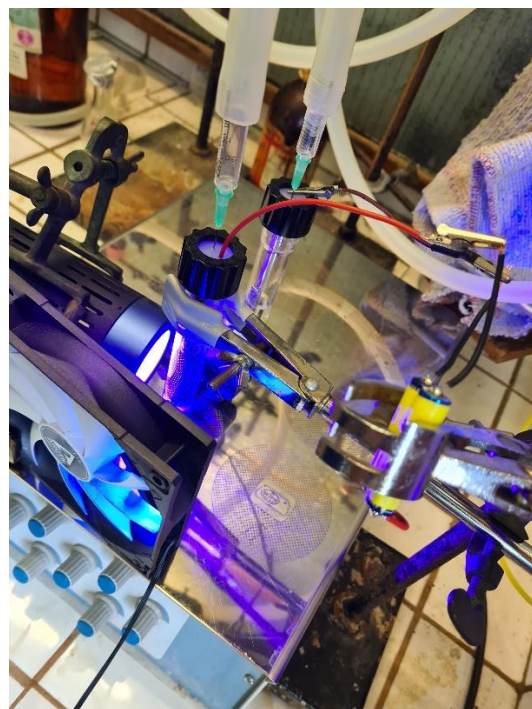
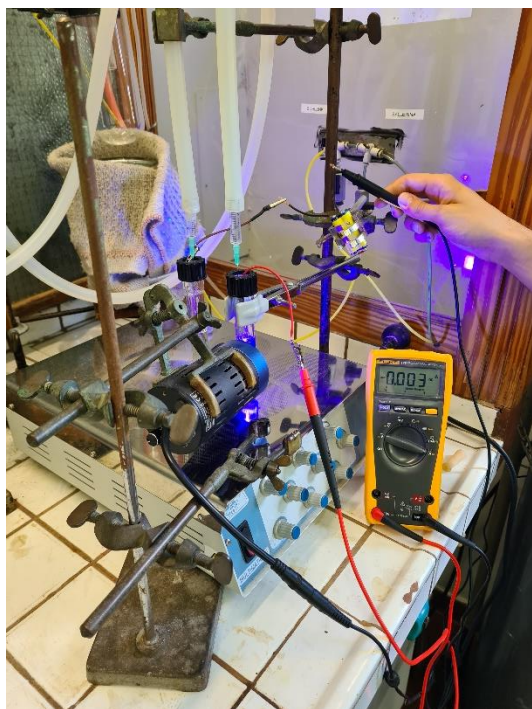
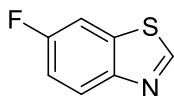


Figure S15. Experimental setup used when using batteries in place of the potentiostat. Left: an amperometer is connected to the circuit to measure the current value at the beginning of the experiment; right: detail of the experimental setup.

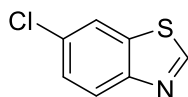
2.4 Characterization of benzothiazoles



6-fluorobenzothiazole (2b): Reaction time: 2 h; white solid (mp 55-56 °C, lit. 58 °C), 51% yield. Characterization data for **2b** are in accordance with the literature.^{S9}

¹H NMR (300 MHz, CDCl₃) δ 8.95 (s, 1H), 8.08 (dd, $J_1 = 9$ Hz, $J_2 = 5$ Hz, 1H), 7.63 (dd, $J_1 = 9$ Hz, $J_2 = 3$ Hz, 1H), 7.26 (td, $J_1 = 9$ Hz, $J_2 = 3$ Hz, 1H).

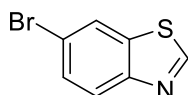
¹³C NMR (75 MHz, CDCl₃) δ 160.9 (d, $J = 246$ Hz), 153.7 (d, $J = 3$ Hz), 149.9 (d, $J = 2$ Hz), 134.9 (d, $J = 11$ Hz), 124.7 (d, $J = 9.5$ Hz), 115.2 (d, $J = 25$ Hz), 108.17 (d, $J = 27$ Hz).



6-chlorobenzothiazole (2c): Reaction time: 1 h; yellowish solid (mp 41-42 °C, lit. 42 °C), 40% yield. Characterization data for **2c** are in accordance with the literature.^{S9}

¹H NMR (300 MHz, CDCl₃) δ 8.99 (s, 1H), 8.05 (d, $J = 9$ Hz, 1H), 7.94 (d, $J = 2$ Hz, 1H), 7.49 (dd, $J_1 = 9$ Hz, $J_2 = 2$ Hz, 1H).

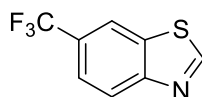
¹³C NMR (75 MHz, CDCl₃) δ 154.3, 151.6, 134.9, 131.7, 127.1, 124.2, 121.4.



6-bromobenzothiazole (2d): Reaction time: 6 h; white solid (mp 51-52 °C, lit. 55 °C), 40 % yield. Characterization data for **2d** are in accordance with the literature.^{S9}

¹H NMR (300 MHz, CDCl₃) δ 8.97 (s, 1H), 8.10 (d, $J = 2$ Hz, 1H), 7.99 (d, $J = 9$ Hz, 1H), 7.62 (dd, $J_1 = 9$ Hz, $J_2 = 2$ Hz, 1H).

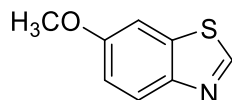
¹³C NMR (75 MHz, CDCl₃) δ 154.2, 152.1, 135.4, 129.7, 124.7, 124.4, 119.3.



6-(trifluoromethyl)benzothiazole (2e): Reaction time: 6 h; yellowish liquid, 38% yield. Characterization data for **2e** are in accordance with the literature.^{S10}

^1H NMR (300 MHz, CDCl_3) δ 9.15 (s, 1H), 8.27–8.25 (m, 1H), 8.23 (d, $J = 9$ Hz, 1H), 7.75 (dd, $J_1 = 9$ Hz, $J_2 = 2$ Hz, 1H).

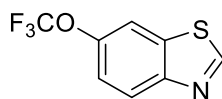
^{13}C NMR (75 MHz, CDCl_3) δ 157.0, 155.2, 134.0, 128.0 (q, $J = 33$ Hz), 124.7 (q, $J = 271$ Hz), 124.2, 123.3 (q, $J = 3$ Hz), 119.8 (q, $J = 4.3$ Hz).



6-methoxybenzothiazole (2f): Reaction time: 6 h; yellowish solid (mp 72-73 °C, lit. 70 °C), 75% yield. Characterization data for **2f** are in accordance with the literature.^{S9}

^1H NMR (300 MHz, CDCl_3) δ 8.84 (s, 1H), 8.01 (dd, $J_1 = 9$ Hz, $J_2 = 1$ Hz, 1H), 7.39 (d, $J = 2$ Hz, 1H), 7.12 (ddd, $J_1 = 9$ Hz, $J_2 = 3$ Hz, $J_3 = 1$ Hz, 1H), 3.88 (s, 3H).

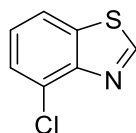
^{13}C NMR (75 MHz, CDCl_3) δ 158.0, 151.3, 147.5, 135.0, 123.8, 115.8, 103.9, 55.7.



6-(trifluoromethoxy)benzothiazole (2g): Reaction time: 1 h; colorless liquid, 72% yield. Characterization data for **2g** are in accordance with the literature.^{S9}

^1H NMR (300 MHz, CDCl_3) δ 9.03 (s, 1H), 8.14 (d, $J = 9$ Hz, 1H), 7.83 (dd, $J_1 = 2$ Hz, $J_2 = 1$ Hz, 1H), 7.50–7.31 (m, 1H).

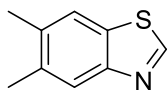
^{13}C NMR (75 MHz, CDCl_3) δ 155.2, 151.9, 147.0 (q, 2 Hz), 134.8, 124.6, 120.7 (q, $J = 257$ Hz), 120.4, 114.5.



4-chlorobenzothiazole (2h): Reaction time: 6 h; pale pink solid (mp 49-51 °C, lit. 42.1-43.8 °C), 70% yield. Characterization data for **2h** are in accordance with the literature.^{S11}

^1H NMR (300 MHz, CDCl_3) δ 9.06 (s, 1H), 7.85 (dd, $J_1 = 8$ Hz, $J_2 = 1$ Hz, 1H), 7.54 (dd, $J_1 = 8$, $J_2 = 1$ Hz, 1H), 7.36 (t, $J = 8$ Hz, 1H).

^{13}C NMR (75 MHz, CDCl_3) δ 154.7, 150.2, 135.2, 128.6, 126.4, 126.1, 120.4.



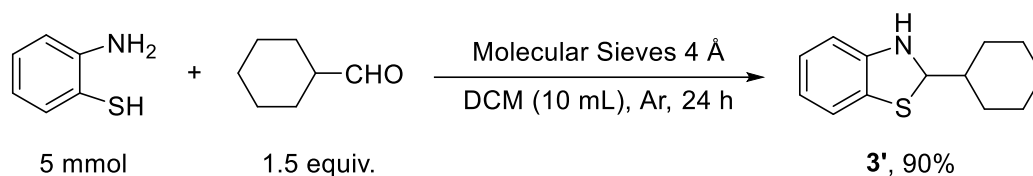
5,6-dimethylbenzothiazole (2i): Reaction time: 6 h; pale pink solid (mp 106-108 °C, lit. 108 °C), 70% yield. Characterization data for **2i** are in accordance with the literature.^{S9}

¹H NMR (300 MHz, CDCl₃) δ 8.89 (s, 1H), 7.91 (s, 1H), 7.69 (s, 1H), 2.41 (s, 3H), 2.40 (s, 3H).

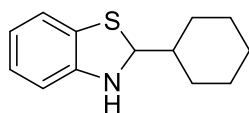
¹³C NMR (75 MHz, CDCl₃) δ 152.8, 151.6, 135.6, 135.2, 130.9, 123.4, 121.6, 20.1.

2.5 Synthesis and characterization of intermediate 2-cyclohexylbenzothiazoline (3')

Compound **3'** was prepared by adapting a procedure reported in the literature (Scheme S4).^{S12} A 100 mL Schlenk flask was charged with 5 g of activated 4Å molecular sieves and inert atmosphere (Argon) was applied. Dichloromethane (10 mL) and cyclohexanecarboxaldehyde (7.5 mmol, 1.5 equiv.) were added under stirring. Then, 2-aminothiophenol (5 mmol, 0.5 M) was added dropwise and the solution was left stirring for 24 hours. Reaction was monitored via TLC to verify 2-aminothiophenol consumption; once completed, the mixture was filtered to remove molecular sieves. Solvent was removed under reduced pressure, then the resulting crude was purified via column chromatography (SiO₂, cyclohexane/ethyl acetate 9:1).



Scheme S4. Synthesis of **3'**.



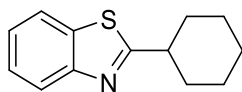
2-cyclohexylbenzothiazoline (3'): white solid. mp: 84-86 °C. lit. 83-85 °C. Spectroscopic data are in accordance with those reported in the literature (registered in CDCl₃).^{S13}

¹H NMR (300 MHz, CD₃CN) δ 6.97 (dd, *J*₁ = 7 Hz, *J*₂ = 1 Hz, 1H), 6.83 (td, *J*₁ = 8 Hz, *J*₂ = 1 Hz, 1H), 6.59 (td, *J*₁ = 8 Hz, *J*₂ = 1 Hz, 1H), 6.54 (d, *J* = 8 Hz, 1H), 5.13 (d, *J* = 7 Hz, 1H), 5.07 (bs, 1H), 1.90-1.55 (m, 6H), 1.35-0.90 (m, 5H).

¹³C NMR (75 MHz, CD₃CN) δ 149.0, 127.0, 126.0, 122.1, 120.0, 110.0, 74.7, 46.5, 29.7, 29.6, 27.1, 26.5, 26.5.

Anal. Calcd. for C₁₃H₁₇NS: C, 71.19; H, 7.81; N, 6.39; Found: C, 71.3; H, 7.8; N, 6.3.

2.6 Characterization of products 3-16



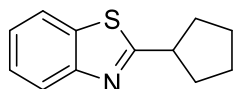
3

2-cyclohexylbenzothiazole (3): colorless liquid, 78% yield. Characterization in accordance with the literature.^{S14}

¹H NMR (300 MHz, CDCl₃) δ 8.00–7.94 (m, 1H), 7.87–7.81 (m, 1H), 7.44 (ddd, $J_1 = 8$ Hz, $J_2 = 7$ Hz, $J_3 = 1$ Hz, 1H), 7.33 (td, $J_1 = 8$ Hz, $J_2 = 1$ Hz, 1H), 3.10 (tt, $J_1 = 12$ Hz, $J_2 = 4$ Hz, 1H), 2.30–2.13 (m, 2H), 1.95–1.54 (m, 5H), 1.54–1.21 (m, 3H).

¹³C NMR (75 MHz, CDCl₃) δ 177.7, 153.2, 134.7, 125.9, 124.6, 122.7, 121.7, 43.6, 33.5, 26.2, 25.9.

Anal. Calcd. for C₁₃H₁₅NS: C, 71.85; H, 6.96; N, 6.45; Found: C, 71.8; H, 7.0; N, 6.4.



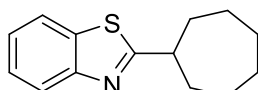
4

2-cyclopentylbenzothiazole (4): colorless liquid, 73% yield. Characterization data are in accordance with the literature.^{S15}

¹H NMR (300 MHz, CDCl₃) δ 7.97 (dd, $J_1 = 8$ Hz, $J_2 = 1$ Hz, 1H), 7.83 (dd, $J_1 = 8$ Hz, $J_2 = 1$ Hz, 1H), 7.44 (ddd, $J_1 = 8$ Hz, $J_2 = 7$ Hz, $J_3 = 1$ Hz, 1H), 7.33 (ddd, $J_1 = 8$ Hz, $J_2 = 7$ Hz, $J_3 = 1$ Hz, 1H), 3.56 (p, $J = 8$ Hz, 1H), 2.34–2.18 (m, 2H), 2.06–1.65 (m, 6H).

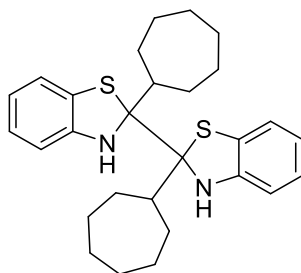
¹³C NMR (75 MHz, CDCl₃) δ 177.3, 153.2, 134.9, 126.0, 124.7, 122.6, 121.6, 44.9, 34.2, 25.7.

Anal. Calcd. for C₁₂H₁₃NS: C, 70.90; H, 6.45; N, 6.89; Found: C, 70.9; H, 6.5; N, 6.9.



5

The reaction between **cycloheptane (1c)** and **benzothiazole (2a)** afforded a mixture of **2-cycloheptylbenzothiazole (5)** and **2,2'-dicycloheptyl-2,2',3,3'-tetrahydro-2,2'-bibenzothiazole (5A)**: in 63% overall yield (**5**, 42% and **5A**, 21%).



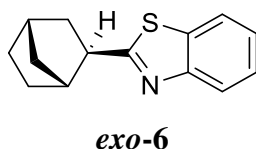
5A

¹H NMR (300 MHz, CDCl₃) δ 7.99 (dd, $J_1 = 8$ Hz, $J_2 = 1$ Hz, 1H), 7.85 (d, $J = 1$ Hz, 1H), 7.45 (td, $J_1 = 8$ Hz, $J_2 = 8$ Hz, $J_3 = 1$ Hz, 1H), 7.33 (td, $J_1 = 8$ Hz, $J_2 = 1$ Hz, 1H), 7.07 (dd, $J_1 = 8$ Hz, $J_2 = 1$ Hz, 1H), 7.03 (dd, $J_1 = 8$ Hz, $J_2 = 1$ Hz, 1H), 6.96–6.84 (m, 2H), 6.77–6.66 (m, 2H), 6.59 (dd, $J_1 = 8$ Hz, $J_2 = 1$ Hz, 1H), 4.03 (bs,

2H), 3.32 (tt, $J_1 = 10$ Hz, $J_2 = 4$ Hz, 1H), 2.38–2.31 (m, 1H), 2.31–2.19 (m, 4H), 2.05–1.77 (m, 13H), 1.77–1.29 (m, 21H).

^{13}C NMR (75 MHz, CDCl_3) δ 178.8, 152.9, 146.3, 146.0, 134.7, 127.1, 126.9, 125.9, 125.9, 124.9, 124.7, 124.6, 122.5, 121.7, 121.6, 121.5, 121.4, 120.2, 120.0, 110.4, 110.1, 89.0, 88.4, 45.5, 45.0, 44.6, 35.4, 30.2, 28.2, 28.1, 27.0, 26.6, 25.9, 25.6, 16.2, 16.1.

The reaction between **norbornane (1d)** and **benzothiazole (2a)** led to the formation of a mixture of 3 different products in 69% overall yield. The three products were identified as: *exo*-2-(bicyclo[2.2.1]heptan-2-yl)benzothiazole (***exo*-6**), *endo*-2-(bicyclo[2.2.1]heptan-2-yl)benzothiazole (***endo*-6**) and 2-(cyclopentylmethyl)benzothiazole (**6A**): their distribution was determined via ^1H -NMR (700 MHz, CDCl_3) to be ***exo*-6** : ***endo*-6** : **6A** = 8: 1 : 1 (see below). Further careful purification of the products mixture allowed to obtain analytically pure samples of each product.

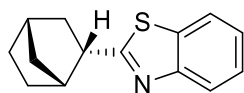


***exo*-2-(bicyclo[2.2.1]heptan-2-yl)benzothiazole (*exo*-6):** colorless liquid, 55% yield. Characterization data are in accordance with the literature.^{S16}

^1H NMR (300 MHz, CDCl_3) δ 7.96 (d, $J = 8$ Hz, 1H), 7.83 (dd, $J_1 = 8$ Hz, $J_2 = 1$ Hz, 1H), 7.47–7.38 (m, 1H), 7.32 (td, $J_1 = 8$ Hz, $J_2 = 1$ Hz, 1H), 3.24–3.14 (m, 1H), 2.67–2.58 (m, 1H), 2.49–2.41 (m, 1H), 2.17–2.07 (m, 1H), 1.88 (ddd, $J_1 = 12$ Hz, $J_2 = 9$ Hz, $J_3 = 2$ Hz, 1H), 1.76–1.54 (m, 3H), 1.52–1.40 (m, 1H), 1.38–1.21 (m, 2H).

^{13}C NMR (75 MHz, CDCl_3) δ 177.7, 153.4, 135.1, 125.9, 124.6, 122.7, 121.5, 47.3, 44.5, 38.4, 36.7, 36.6, 29.9, 28.9.

Anal. Calcd. for $\text{C}_{14}\text{H}_{15}\text{NS}$: C, 73.32; H, 6.59; N, 6.11; Found: C, 73.4; H, 6.6; N, 6.1.



endo-6

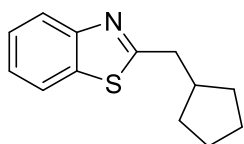
endo-2-(bicyclo[2.2.1]heptan-2-yl)benzothiazole (endo-6):

colorless liquid, 6% yield.

^1H NMR (300 MHz, CDCl_3) δ 8.00 (d, $J = 8$ Hz, 1H), 7.84 (d, $J = 8$ Hz, 1H), 7.49–7.41 (m, 1H), 7.38–7.30 (m, 1H), 3.61 (dddd, $J_1 = 11$ Hz, $J_2 = 6$ Hz, $J_3 = 4$ Hz, $J_4 = 2$ Hz, 1H), 2.81–2.70 (m, 1H), 2.44–2.37 (m, 1H), 2.20–2.05 (m, 1H), 1.96–1.79 (m, 2H), 1.66–1.28 (m, 5H).

^{13}C NMR (75 MHz, CDCl_3) δ 175.9, 153.3, 135.0, 126.0, 124.7, 122.6, 121.6, 46.0, 43.5, 40.4, 37.5, 35.4, 29.8, 23.9.

Anal. Calcd. for $\text{C}_{14}\text{H}_{15}\text{NS}$: C, 73.32; H, 6.59; N, 6.11; Found: C, 73.3; H, 6.7; N, 6.1.



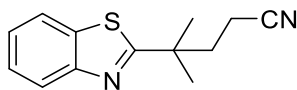
6A

2-(cyclopentylmethyl)benzothiazole (6A): colorless liquid, 8% yield. Characterization data are in accordance with the literature.^{S17}

^1H NMR (300 MHz, CDCl_3) δ 7.97 (d, $J = 8$ Hz, 1H), 7.84 (d, $J = 8$ Hz, 1H), 7.48–7.42 (m, 1H), 7.40–7.29 (m, 1H), 3.12 (d, $J = 8$ Hz, 2H), 2.40 (q, $J = 8$ Hz, 1H), 1.95–1.80 (m, 2H), 1.75–1.45 (m, 4H), 1.40–1.25 (m, 2H).

^{13}C NMR (75 MHz, CDCl_3) δ 172.1, 153.2, 135.3, 126.0, 124.8, 122.6, 121.6, 40.7, 40.5, 32.7, 25.2.

Anal. Calcd. for $\text{C}_{13}\text{H}_{15}\text{NS}$: C, 71.85; H, 6.96; N, 6.45; Found: C, 71.9; H, 7.1; N, 6.4.



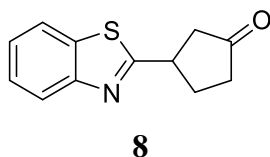
7

4-(benzothiazol-2-yl)-4-methylpentanenitrile (7): colorless liquid, 88% yield.

^1H NMR (300 MHz, CDCl_3) δ 8.09–7.94 (m, 1H), 7.87 (ddd, $J_1 = 8$ Hz, $J_2 = 3$ Hz, $J_3 = 1$ Hz, 1H), 7.53–7.44 (m, 1H), 7.43–7.35 (m, 1H), 2.41–2.32 (m, 2H), 2.30–2.21 (m, 2H), 1.55 (s, 6H).

^{13}C NMR (75 MHz, CDCl_3) δ 178.2, 153.0, 134.8, 126.3, 125.2, 123.0, 121.7, 119.9, 41.0, 38.7, 28.5, 13.2.

Anal. Calcd. for $\text{C}_{13}\text{H}_{14}\text{N}_2\text{S}$: C, 67.79; H, 6.13; N, 12.16; Found: C, 67.8; H, 6.1; N, 12.2.

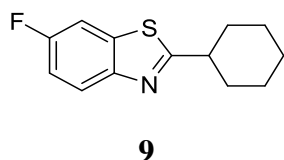


3-(benzothiazol-2-yl)cyclopentanone (8): colorless liquid, 81% yield.

^1H NMR (300 MHz, CDCl_3) δ 7.96 (d, J = 8 Hz, 1H), 7.84 (d, J = 8 Hz, 1H), 7.49–7.41 (m, 1H), 7.39–7.32 (m, 1H), 3.90 (dtd, J_1 = 11 Hz, J_2 = 9 Hz, J_3 = 8 Hz, J_4 = 6 Hz, 1H), 2.85–2.67 (m, 2H), 2.64–2.44 (m, 2H), 2.40–2.24 (m, 2H).

^{13}C NMR (75 MHz, CDCl_3) δ 216.3, 173.0, 153.1, 134.8, 126.3, 125.1, 122.9, 121.7, 44.6, 41.1, 38.0, 30.4.

Anal. Calcd. for $\text{C}_{12}\text{H}_{11}\text{NOS}$: C, 66.33; H, 5.10; N, 6.45; Found: C, 66.3; H, 5.1; N, 6.5.



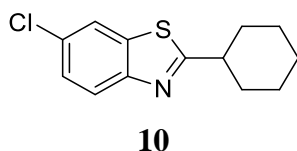
2-cyclohexyl-6-fluorobenzothiazole (9): pale yellow solid, 80% yield. mp: 48–50 °C. Characterization in accordance with the literature.^{S15}

^1H NMR (300 MHz, CDCl_3) δ 7.87 (dd, J_1 = 9 Hz, J_2 = 5 Hz, 1H), 7.48 (dd, J_1 = 8 Hz, J_2 = 3 Hz, 1H), 7.14 (td, J_1 = 9 Hz, J_2 = 3 Hz, 1H), 3.05 (tt, J_1 = 11 Hz, J_2 = 4 Hz, 1H), 2.23–2.08 (m, 2H), 1.91–1.80 (m, 2H), 1.80–1.68 (m, 1H), 1.68–1.52 (m, 2H), 1.51–1.19 (m, 3H).

^{13}C NMR (75 MHz, CDCl_3) δ 177.3 (d, J = 3 Hz), 160.2 (d, J = 245 Hz), 149.8 (d, J = 2 Hz), 135.6 (d, J = 11 Hz), 123.4 (d, J = 9 Hz), 114.4 (d, J = 25 Hz), 107.8 (d, J = 27 Hz), 43.4, 33.4, 26.1, 25.8.

^{19}F NMR (376 MHz, CDCl_3) δ –117.6 (td, J_1 = 8 Hz, J_2 = 5 Hz).

Anal. Calcd. for $\text{C}_{13}\text{H}_{14}\text{FNS}$: C, 66.35; H, 6.00; N, 5.95; Found: C, 66.3; H, 6.1; N, 5.9.



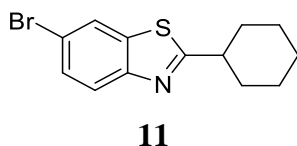
6-chloro-2-cyclohexylbenzothiazole (10): pale yellow solid, 61% yield. mp: 64–66 °C. Characterization in accordance with the literature.^{S18}

^1H NMR (300 MHz, CDCl_3) δ 7.86 (d, J = 9 Hz, 1H), 7.79 (d, J = 2 Hz, 1H), 7.38 (dd, J_1 = 9 Hz, J_2 = 2 Hz, 1H), 3.07 (tt, J_1 = 11 Hz, J_2 = 4 Hz, 1H), 2.23–2.13 (m, 2H), 1.93–1.83 (m, 2H), 1.81–

1.70 (m, 1H), 1.70–1.54 (m, 2H), 1.51–1.20 (m, 3H).

^{13}C NMR (75 MHz, CDCl_3) δ 178.3, 151.7, 135.8, 130.5, 126.7, 123.4, 121.3, 43.5, 33.4, 26.1, 25.8.

Anal. Calcd. for $\text{C}_{13}\text{H}_{14}\text{ClNS}$: C, 62.02; H, 5.61; N, 5.56; Found: C, 62.0; H, 5.7; N, 5.6.

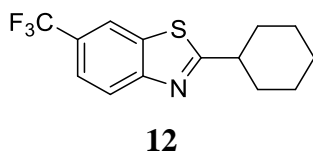


6-bromo-2-cyclohexylbenzothiazole (11): pale yellow solid, 26% yield. mp: 77–79 °C. Characterization in accordance with the literature.^{S19}

^1H NMR (300 MHz, CDCl_3) δ 7.97 (d, $J = 2$ Hz, 1H), 7.81 (d, $J = 9$ Hz, 1H), 7.53 (dd, $J_1 = 9$ Hz, $J_2 = 2$ Hz, 1H), 3.08 (tt, $J_1 = 12$ Hz, $J_2 = 4$ Hz, 1H), 2.24–2.15 (m, 2H), 1.94–1.84 (m, 2H), 1.81–1.72 (m, 1H), 1.71–1.54 (m, 2H), 1.55–1.23 (m, 3H).

^{13}C NMR (75 MHz, CDCl_3) δ 178.4, 152.1, 136.4, 129.4, 124.2, 123.8, 118.2, 43.5, 33.4, 26.1, 25.9.

Anal. Calcd. for $\text{C}_{13}\text{H}_{14}\text{BrNS}$: C, 52.71; H, 4.76; N, 4.73; Found: C, 52.7; H, 4.8; N, 4.7.



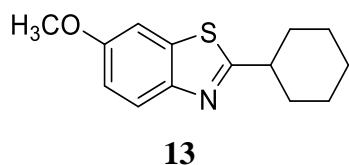
6-trifluoromethyl-2-cyclohexylbenzothiazole (12): pale yellow solid. 50% yield. mp: 47–49 °C.

^1H NMR (300 MHz, CDCl_3) δ 8.14 (s, 1H), 8.05 (d, $J = 8$ Hz, 1H), 7.68 (dd, $J_1 = 9$ Hz, $J_2 = 2$ Hz, 1H), 3.14 (tt, $J_1 = 11$ Hz, $J_2 = 4$ Hz, 1H), 2.29–2.15 (m, 2H), 1.97–1.83 (m, 2H), 1.82–1.58 (m, 3H), 1.56–1.24 (m, 3H).

^{13}C NMR (75 MHz, CDCl_3) δ 181.1, 155.2, 134.8, 126.9 (q, $J = 32$ Hz), 124.4 (q, $J = 271$ Hz), 123.0, 123.0, 119.4 (q, $J = 4$ Hz), 43.7, 33.5, 26.1, 25.9.

^{19}F NMR (376 MHz, CDCl_3) δ –61.7 (s).

Anal. Calcd. for $\text{C}_{14}\text{H}_{14}\text{F}_3\text{NS}$: C, 58.93; H, 4.95; N, 4.91; Found: C, 58.9; H, 4.9; N, 4.9.

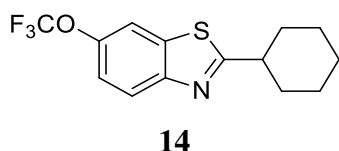


2-cyclohexyl-6-methoxybenzothiazole (13): pale yellow solid, 50% yield. mp: 44–46 °C. Characterization in accordance with the literature.^{S8}

¹H NMR (300 MHz, CDCl₃) δ 7.84 (d, *J* = 9 Hz, 1H), 7.29 (d, *J* = 3 Hz, 1H), 7.03 (dd, *J*₁ = 9 Hz, *J*₂ = 3 Hz, 1H), 3.84 (s, 3H), 3.05 (tt, *J*₁ = 12 Hz, *J*₂ = 4 Hz, 1H), 2.29–2.11 (m, 2H), 1.95–1.81 (m, 2H), 1.79–1.71 (m, 1H), 1.69–1.53 (m, 2H), 1.51–1.20 (m, 3H).

¹³C NMR (75 MHz, CDCl₃) δ 175.2, 157.3, 147.5, 135.8, 123.0, 115.0, 104.4, 55.9, 43.4, 33.5, 26.2, 25.9.

Anal. Calcd. for C₁₄H₁₇NOS: C, 67.98; H, 6.93; N, 5.66; Found: C, 68.0; H, 6.9; N, 5.6.

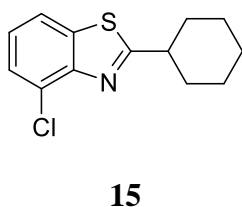


6-(trifluoromethoxy)benzothiazole (14): yellowish solid. 75% yield. mp: 57–60 °C.

¹H NMR (300 MHz, CDCl₃) δ 7.95 (d, *J* = 9 Hz, 1H), 7.73–7.69 (m, 1H), 7.35–7.28 (m, 1H), 3.10 (tt, *J*₁ = 12 Hz, *J*₂ = 4 Hz, 1H), 2.30–2.15 (m, 2H), 1.96–1.83 (m, 2H), 1.83–1.71 (m, 1H), 1.71–1.55 (m, 2H), 1.55–1.23 (m, 3H). ¹³C NMR (75 MHz, CDCl₃) δ 179.1, 151.7, 146.2, 146.2, 135.5, 120.7 (q, *J* = 257 Hz), 119.9, 114.4, 43.6, 33.5, 26.1, 25.9.

¹⁹F NMR (376 MHz, CDCl₃) δ –58.5 (t, *J* = 1 Hz).

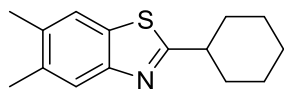
Anal. Calcd. for C₁₄H₁₄F₃NOS: C, 55.80; H, 4.68; N, 4.65; Found: C, 55.8; H, 4.7; N, 4.6.



4-chloro-2-cyclohexylbenzothiazole (15): colorless liquid, 67% yield.

¹H NMR (300 MHz, CDCl₃) δ 7.73 (dd, *J*₁ = 8 Hz, *J*₂ = 1 Hz, 1H), 7.45 (dd, *J*₁ = 8 Hz, *J*₂ = 1 Hz, 1H), 7.25 (t, *J* = 8 Hz, 1H), 3.21 (tt, *J*₁ = 12 Hz, *J*₂ = 4 Hz, 1H), 2.26–2.15 (m, 2H), 1.94–1.84 (m, 2H), 1.82–1.72 (m, 1H), 1.69–1.26 (m, 5H). ¹³C NMR (75 MHz, CDCl₃) δ 179.2, 150.1, 136.2, 127.4, 126.2, 125.1, 120.2, 43.8, 33.8, 26.1, 25.8.

Anal. Calcd. for C₁₃H₁₄ClNS: C, 62.02; H, 5.61; N, 5.56; Found: C, 62.0; H, 5.6; N, 5.6.



16

2-cyclohexyl-5,6-dimethylbenzothiazole (16): white thick paste, 47% yield.

^1H NMR (300 MHz, CDCl_3) δ 7.74 (s, 1H), 7.57 (s, 1H), 3.07 (tt, $J_1 = 12$ Hz, $J_2 = 4$ Hz, 1H), 2.37 (s, 3H), 2.35 (s, 3H), 2.24–2.13 (m, 2H), 1.97 – 1.15 (m, 8H). ^{13}C NMR (75 MHz, CDCl_3) δ 176.7, 151.8, 135.1, 134.0, 131.9, 122.8, 121.6, 43.4, 33.5, 26.2, 25.9, 20.3, 20.2.

Anal. Calcd. for $\text{C}_{15}\text{H}_{19}\text{NS}$: C, 73.42; H, 7.80; N, 5.71; Found: C, 73.4; H, 7.9; N, 5.7.

2.7 Crude 700 MHz ^1H -NMR for the reaction with norbornane

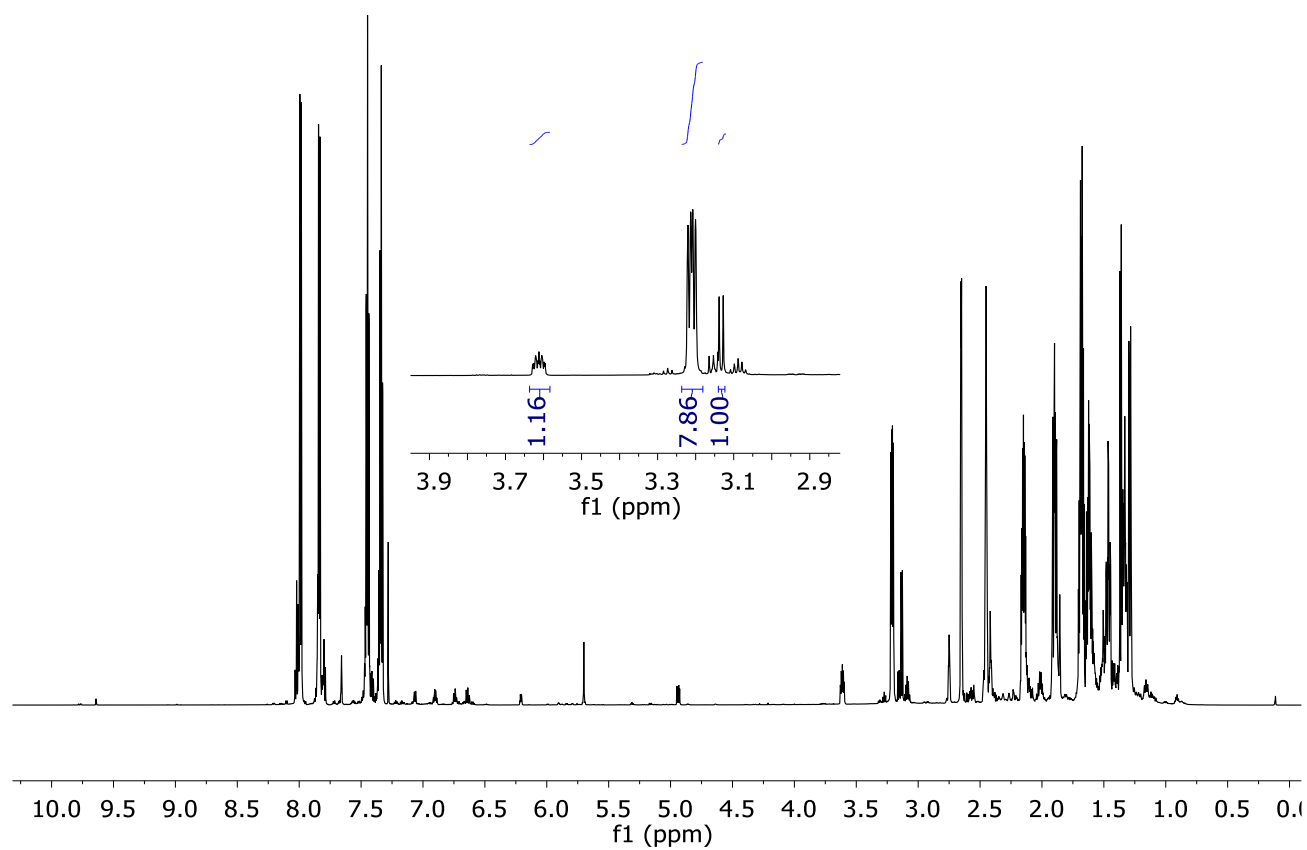
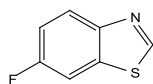


Figure S16. 700 MHz ^1H -NMR of the crude reaction mixture in the process between norbornane and benzothiazole.

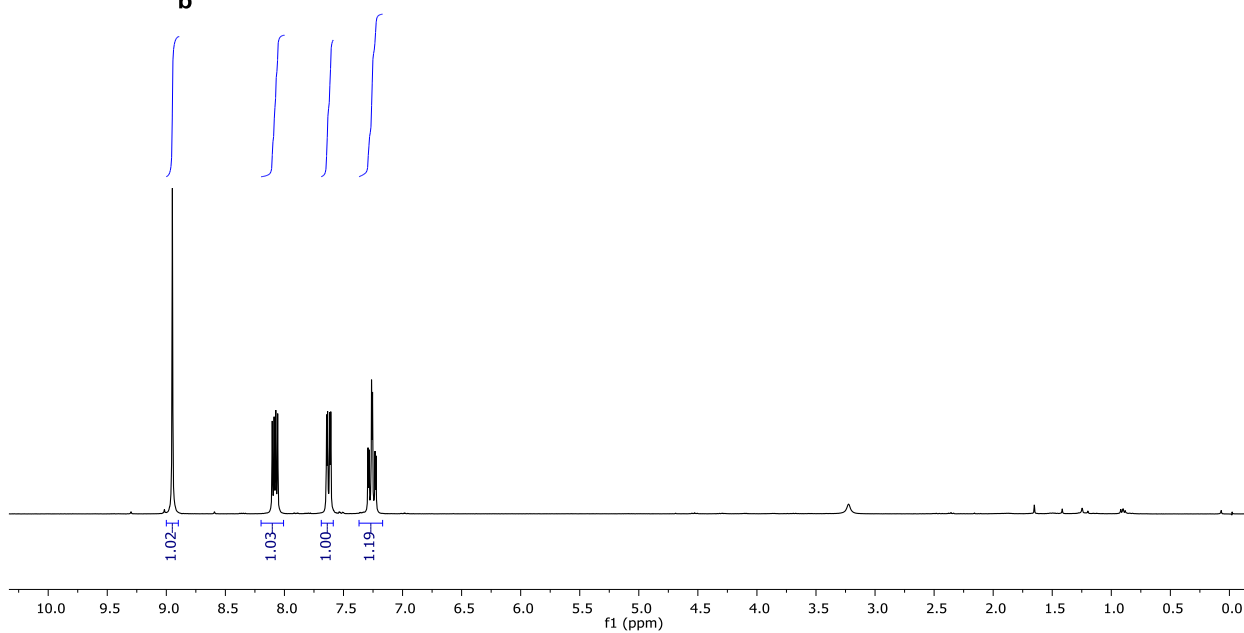
3 References

- S1 For a review, see: C. Tanielian, *Coord. Chem. Rev.*, 1998, **178–180**, 1165–1181 and references therein.
- S2 D. C. Duncan, T. L. Netzel and C. L. Hill, *Inorg. Chem.*, 1995, **34**, 4640–4646.
- S3 I. Texier, J. A. Delaire and C. Giannotti, *Phys. Chem. Chem. Phys.*, 2000, **2**, 1205–1212.
- S4 D. Dondi, M. Fagnoni and A. Albini, *Chem. Eur. J.*, 2006, **12**, 4153–4163.
- S5 H. Yan, Z. Hou and H. Xu, *Angew. Chem. Int. Ed.*, 2019, **58**, 4592–4595.
- S6 An analogous value has been previously reported. See: R. F. Renneke, M. Pasquali and C. L. Hill, *J. Am. Chem. Soc.*, 1990, **112**, 6585–6594.
- S7 S. Protti, D. Ravelli, M. Fagnoni and A. Albini, *Chem. Commun.*, 2009, 7351–7353.
- S8 Z. L. Li, L. K. Jin and C. Cai, *Org. Chem. Front.*, 2017, **4**, 2039–2043.
- S9 S. Chun, S. Yang and Y. K. Chung, *Tetrahedron*, 2017, **73**, 3438–3442.
- S10 B. L. Mylari, E. R. Larson, T. A. Beyer, W. J. Zembrowski, C. E. Aldinger, M. F. Dee, T. W. Siegel and D. H. Singleton, *J. Med. Chem.*, 1991, **34**, 108–122.
- S11 A. R. Katritzky, B. V. Rogovoy, C. Chassaing, V. Vvedensky, B. Forood, B. Flatt and H. Nakai, *J. Heterocycl. Chem.*, 2000, **37**, 1655–1658.
- S12 W. Waengdongbung, V. Hahnvajjanawong and P. Theramongkol, *Orient. J. Chem.*, 2016, **32**, 941–945.
- S13 G. Ikarashi, T. Morofuji and N. Kano, *Chem. Commun.*, 2020, **56**, 10006–10009.
- S14 T. Yao, K. Hirano, T. Satoh and M. Miura, *Angew. Chem. Int. Ed.*, 2012, **51**, 775–779.
- S15 Y. Ma, J. Cammarata and J. Cornella, *J. Am. Chem. Soc.*, 2019, **141**, 1918–1922.
- S16 G.-X. Li, X. Hu, G. He and G. Chen, *ACS Catal.*, 2018, **8**, 11847–11853.
- S17 V. V. Chernyshov, O. I. Yarovaya, S. Z. Vatsadze, S. S. Borisevich, S. N. Trukhan, Y. V. Gatilov, R. Yu. Peshkov, I. V. Eltsov, O. N. Martyanov and N. F. Salakhutdinov, *Eur. J. Org. Chem.*, 2021, **2021**, 452–463.
- S18 A. N. Dinh, A. D. Nguyen, E. M. Aceves, S. T. Albright, M. R. Cedano, D. K. Smith and J. L. Gustafson, *Synlett*, 2019, **30**, 1648–1655.
- S19 W.-C. Yang, K. Wei, X. Sun, J. Zhu and L. Wu, *Org. Lett.*, 2018, **20**, 3144–3147.

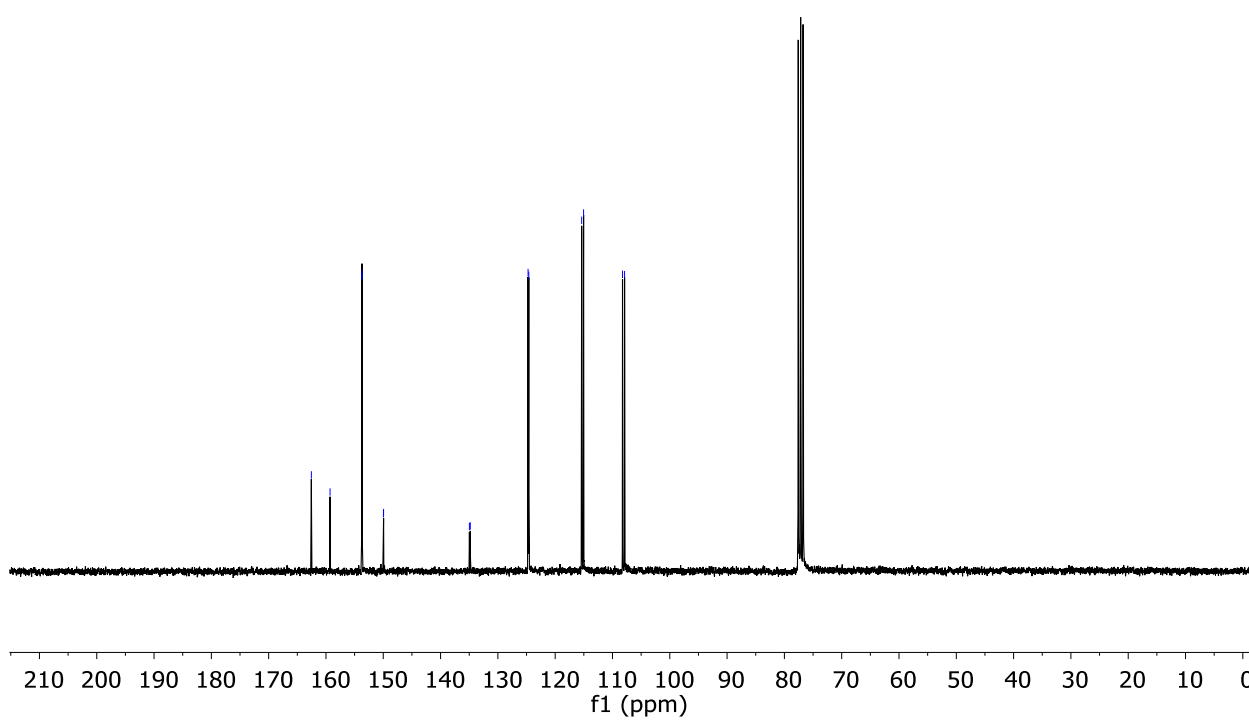
4 ^1H , ^{19}F and ^{13}C NMR spectra

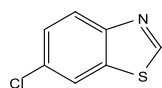


2
b

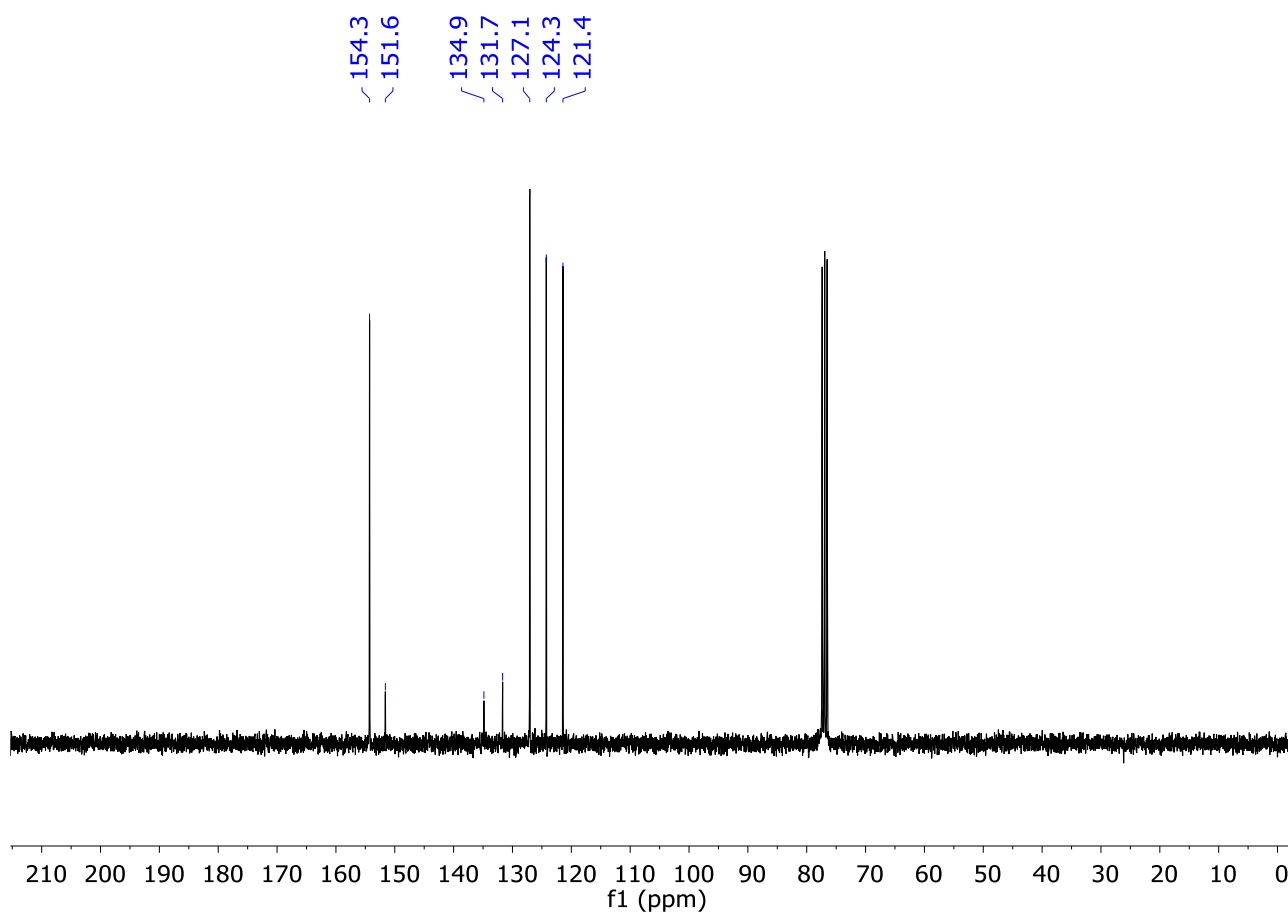
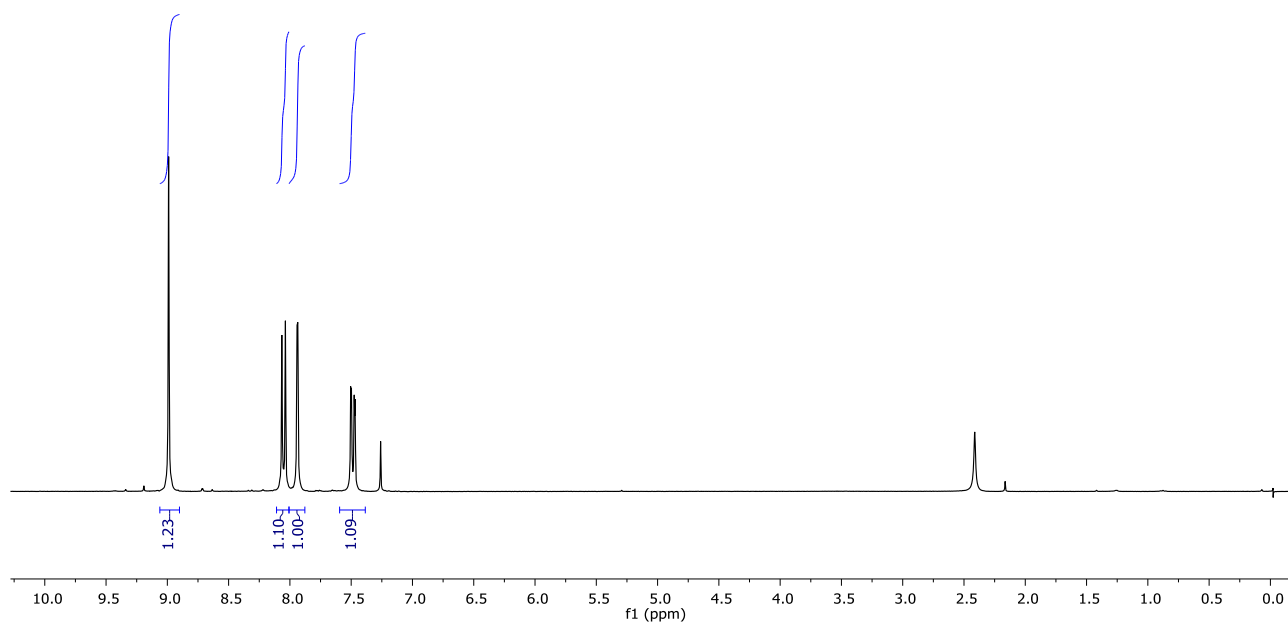


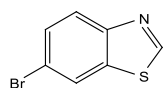
162.5
159.3
153.7
153.7
150.0
149.9
135.0
134.8
124.7
124.6
115.4
115.0
108.2
107.9



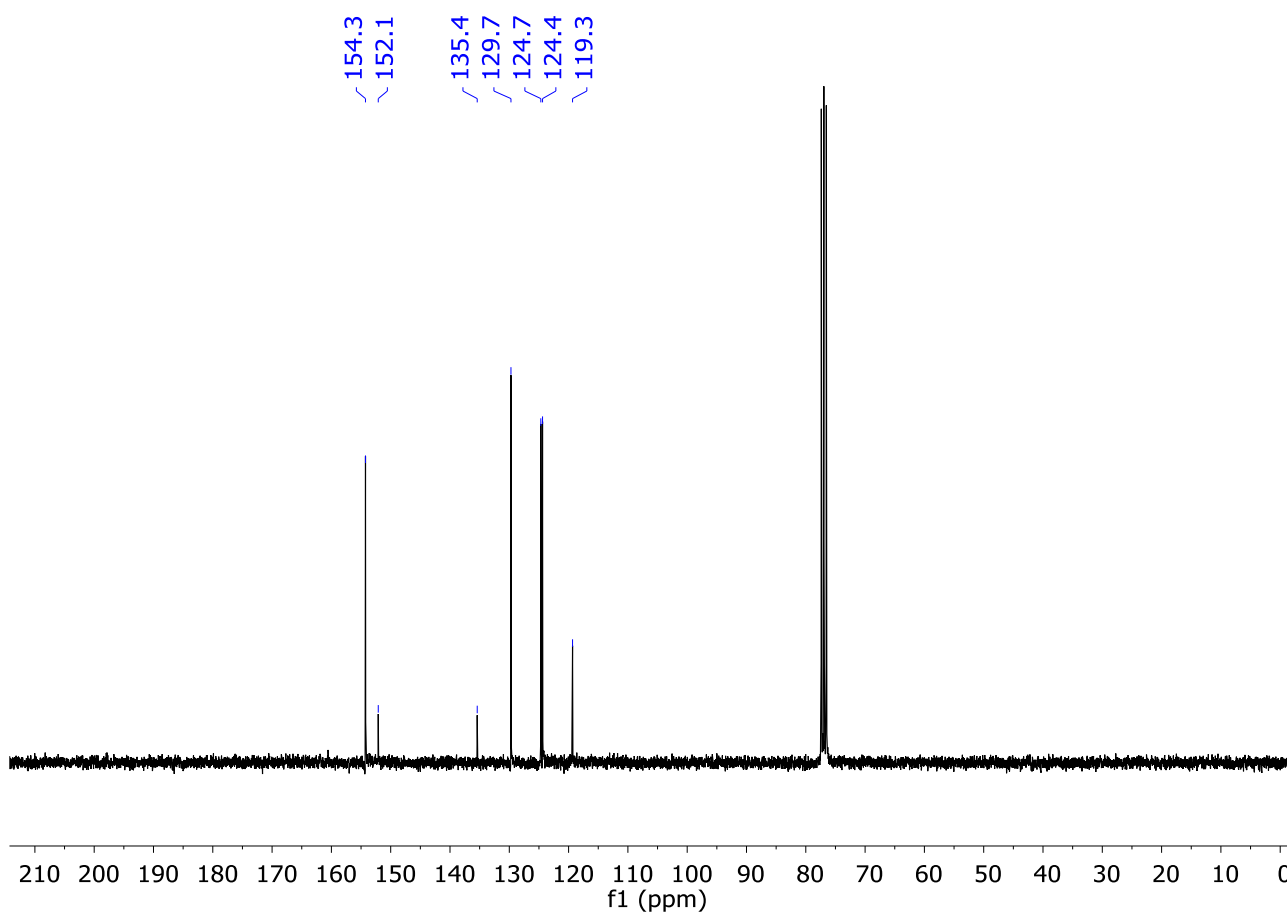
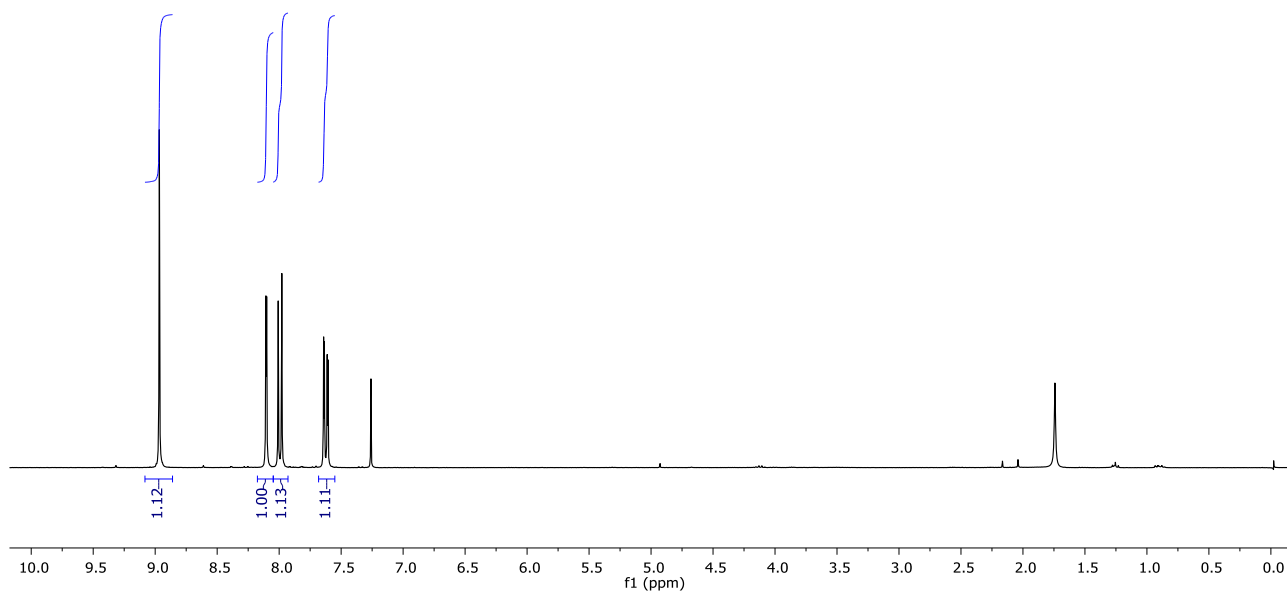


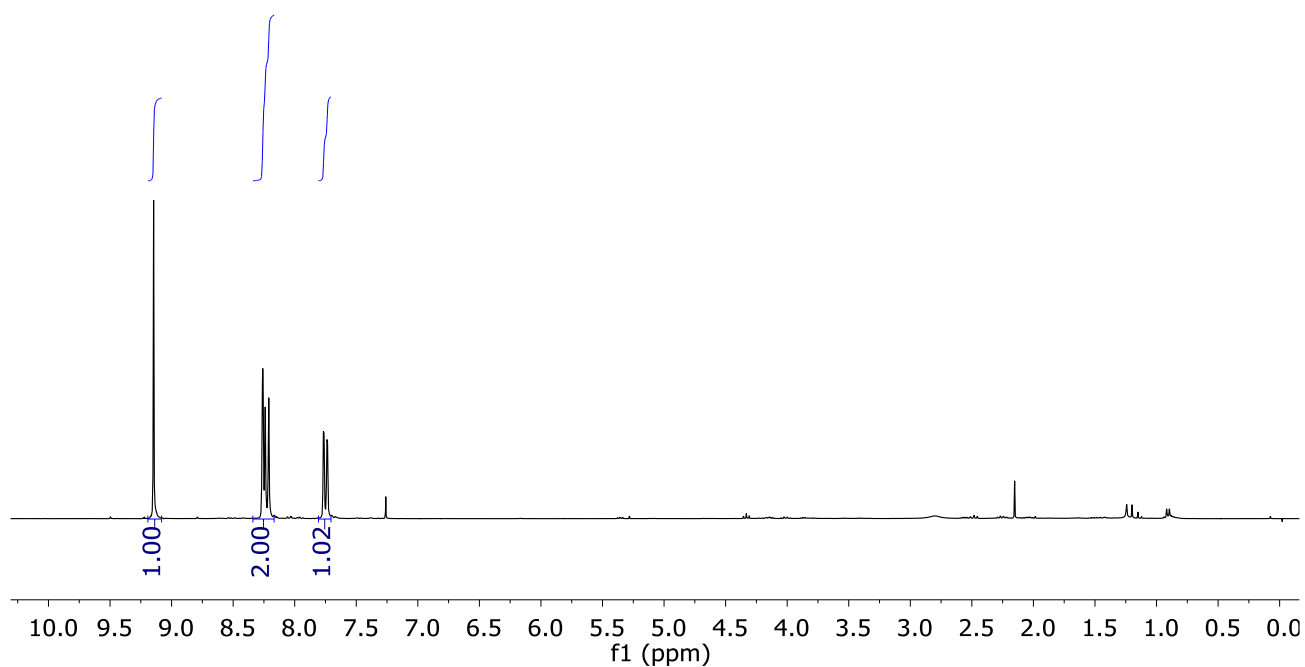
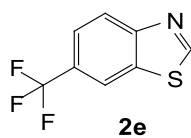
2c



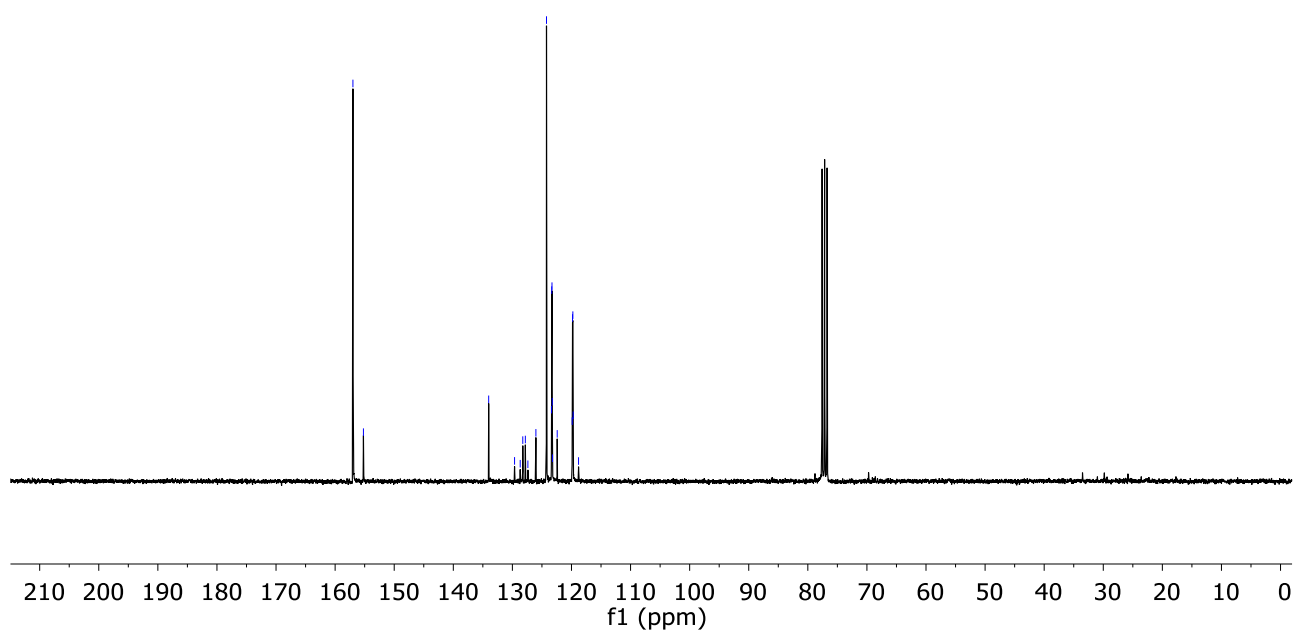


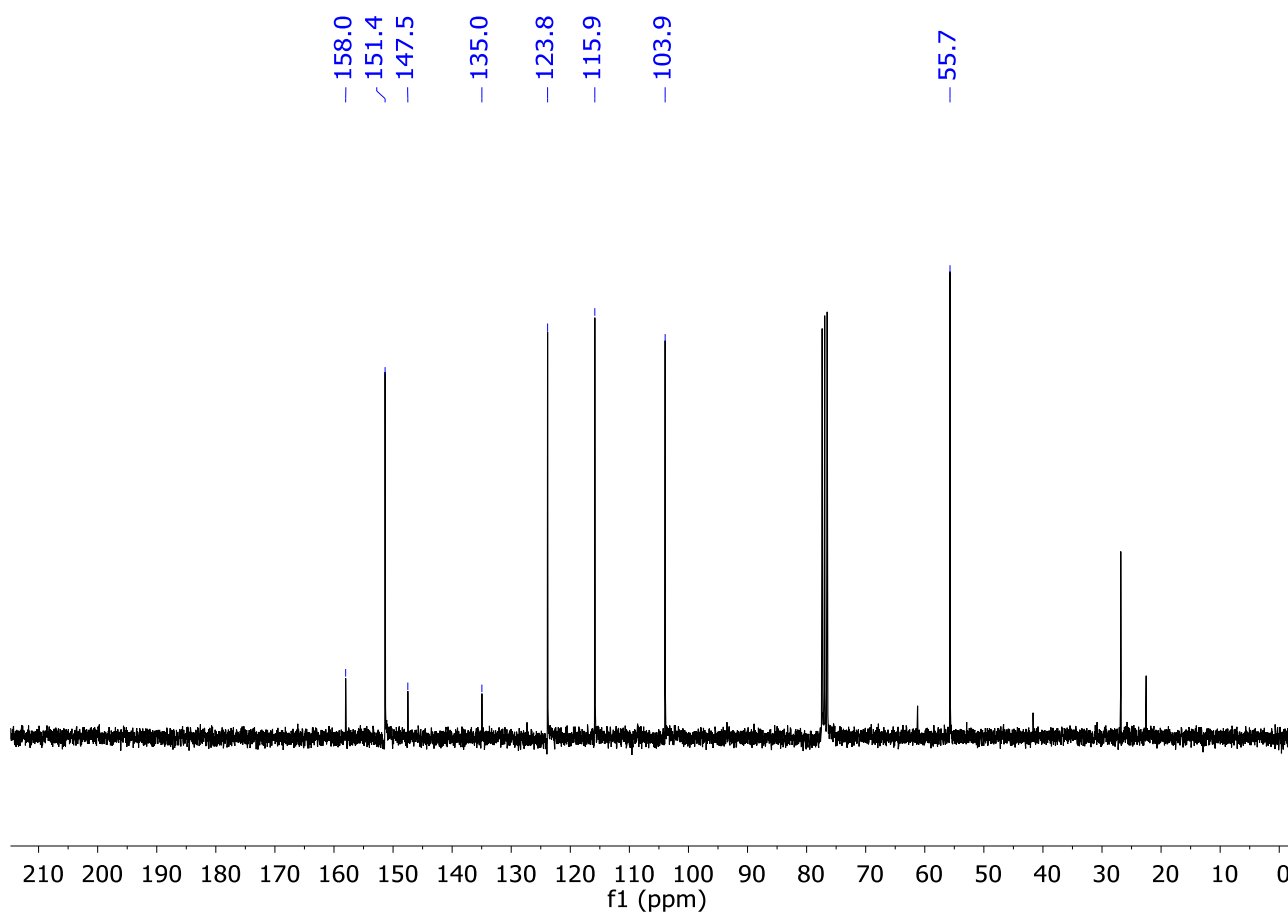
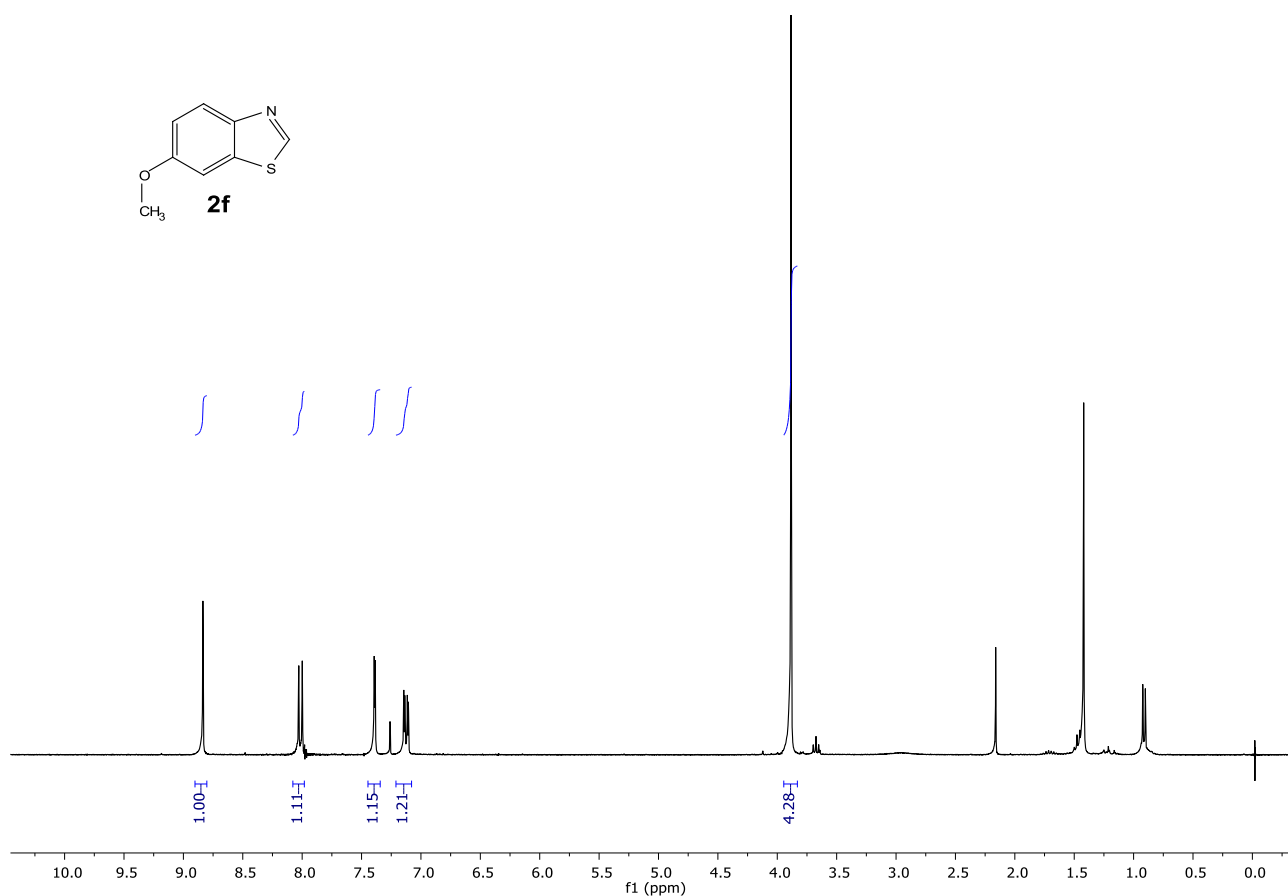
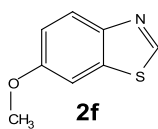
2d

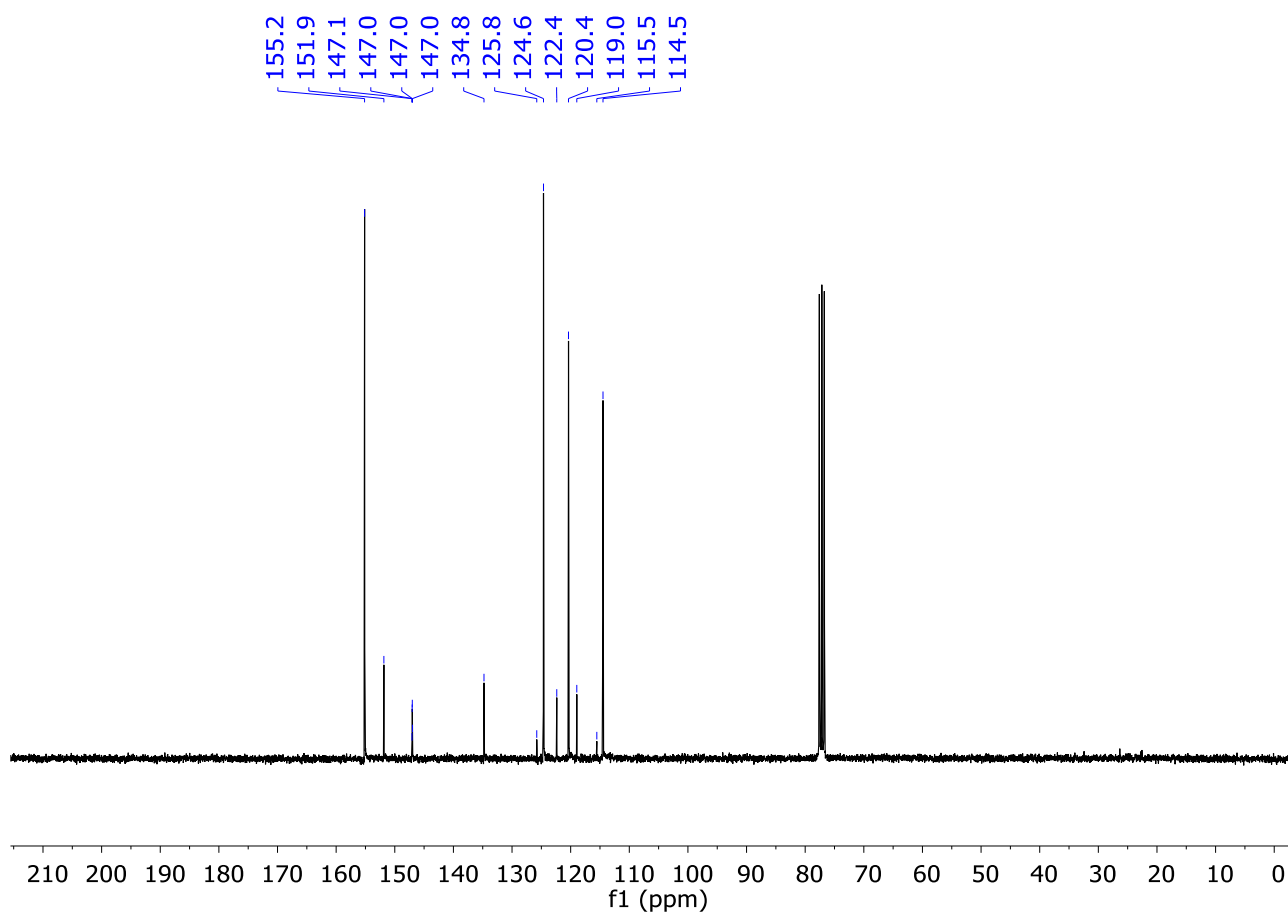
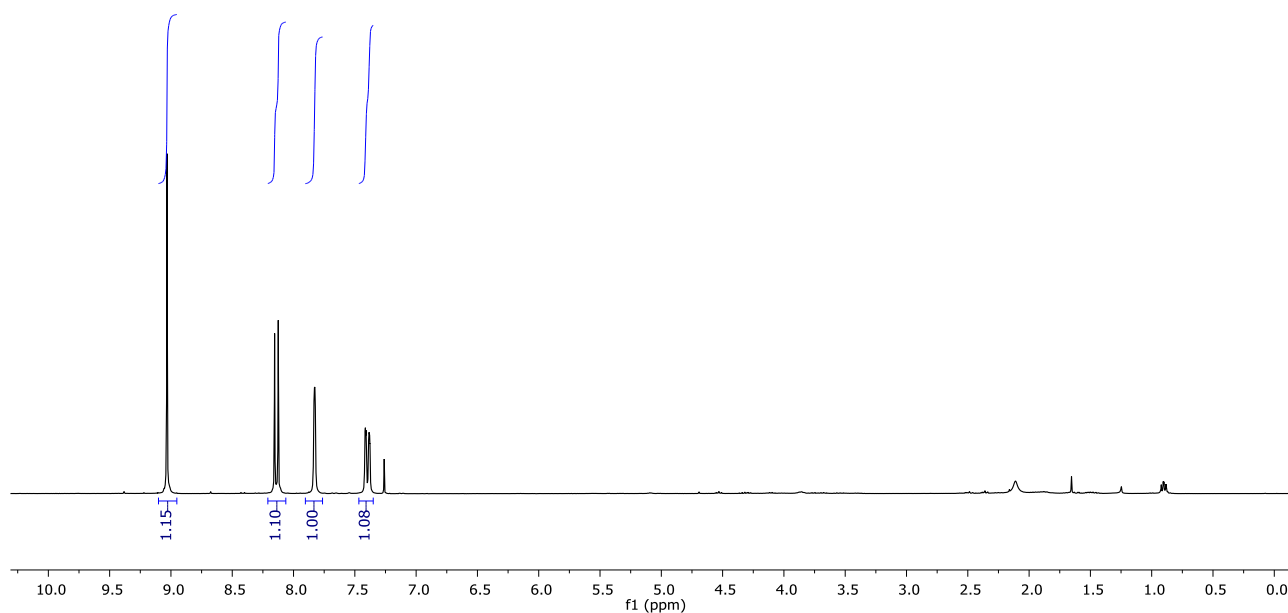
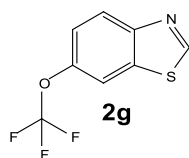


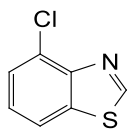


157.0
155.2
134.0
129.6
128.7
128.2
127.8
127.4
126.0
124.2
123.4
123.3
123.3
123.3
123.2
122.4
119.9
119.8
119.8
119.7
118.8

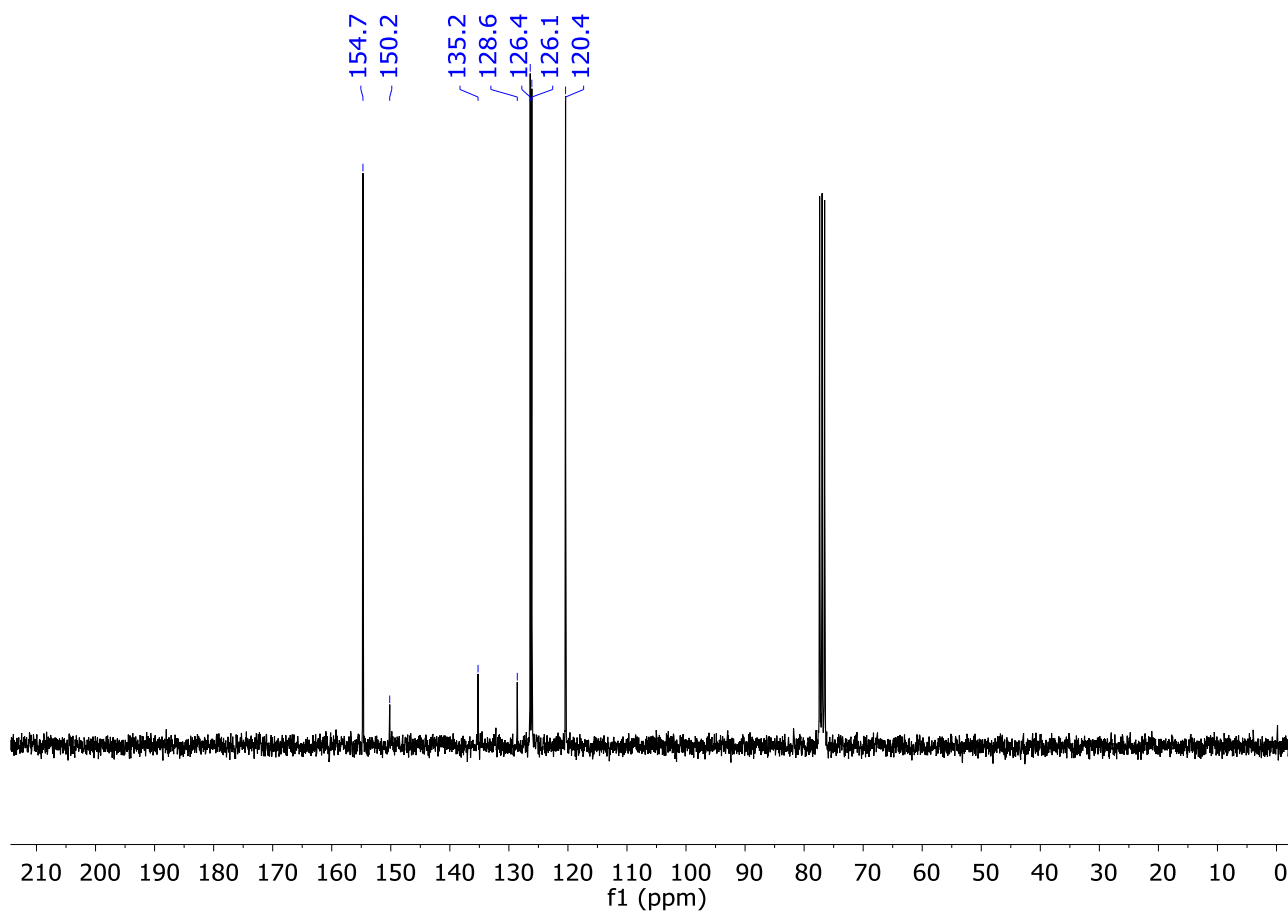
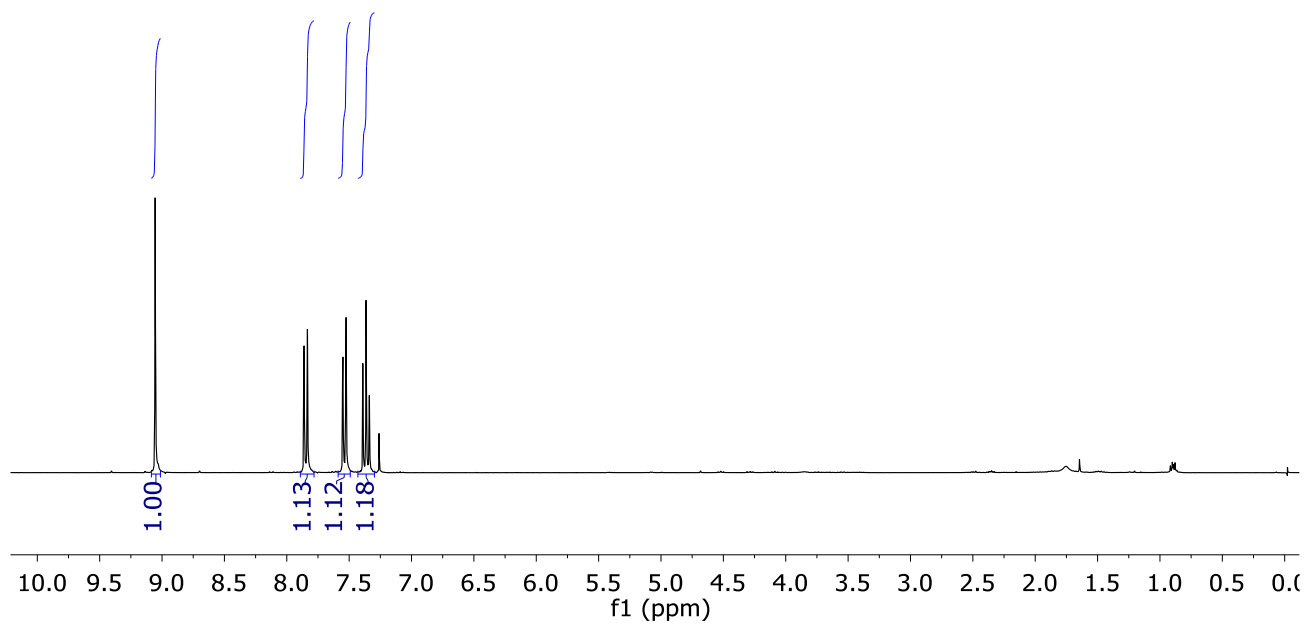


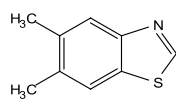




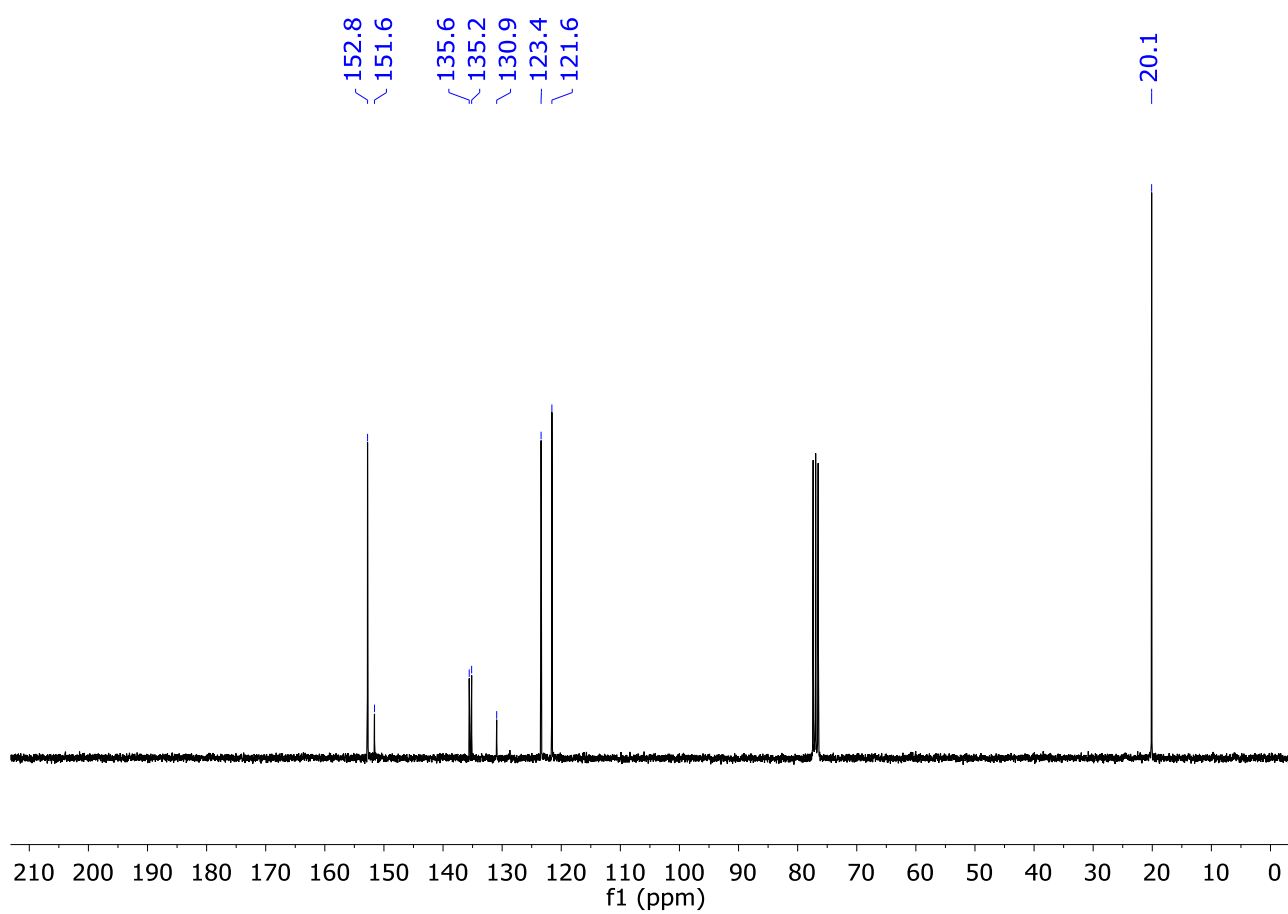
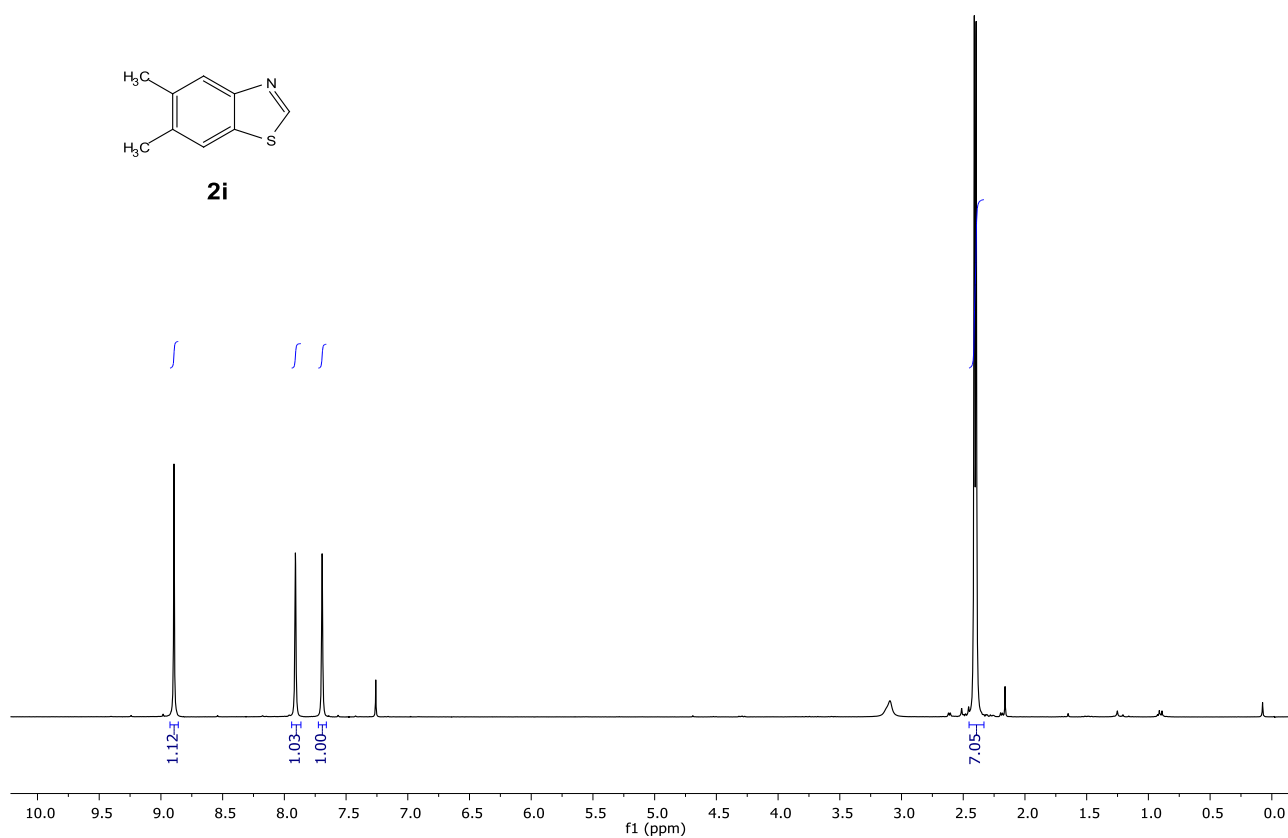


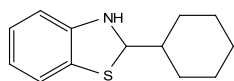
2h



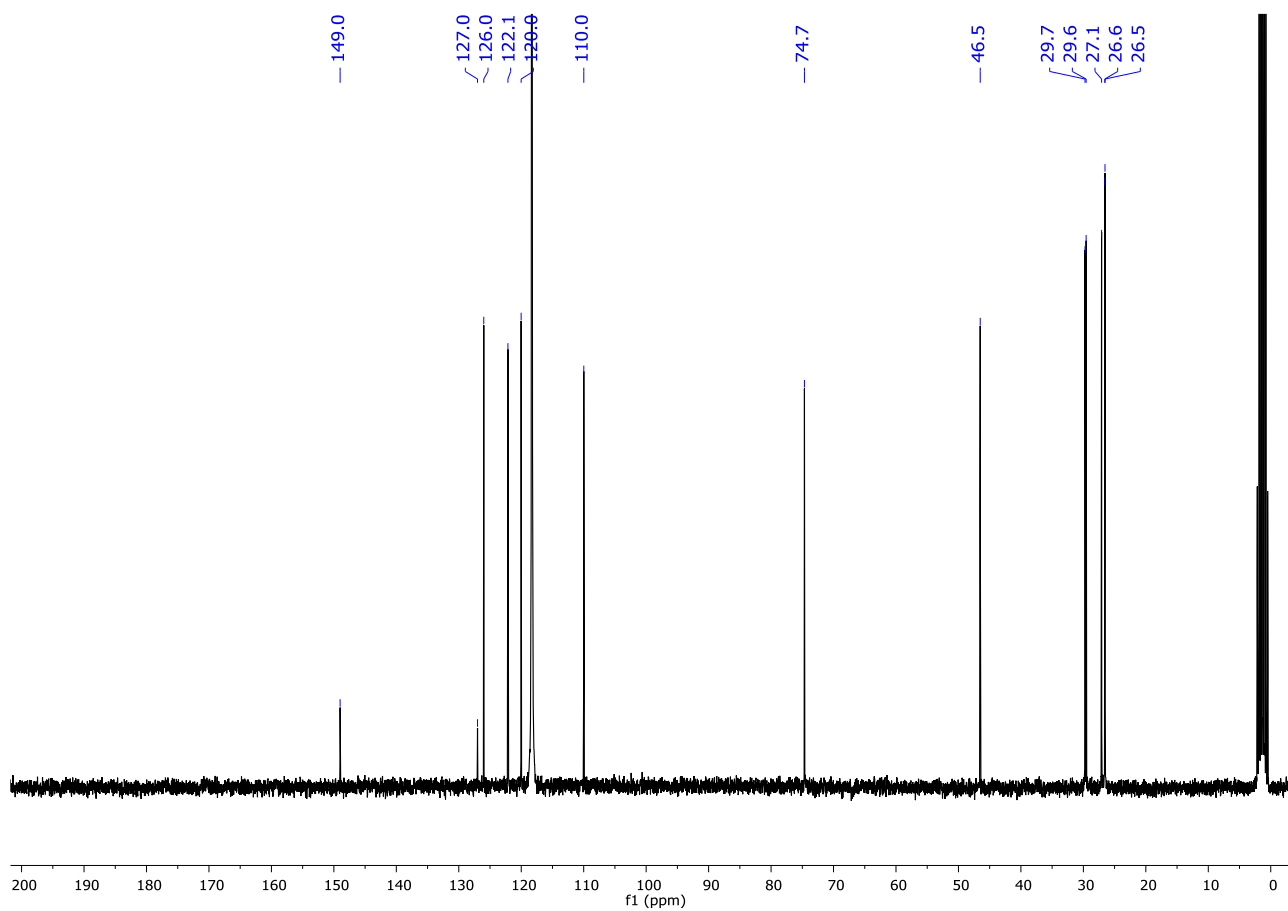
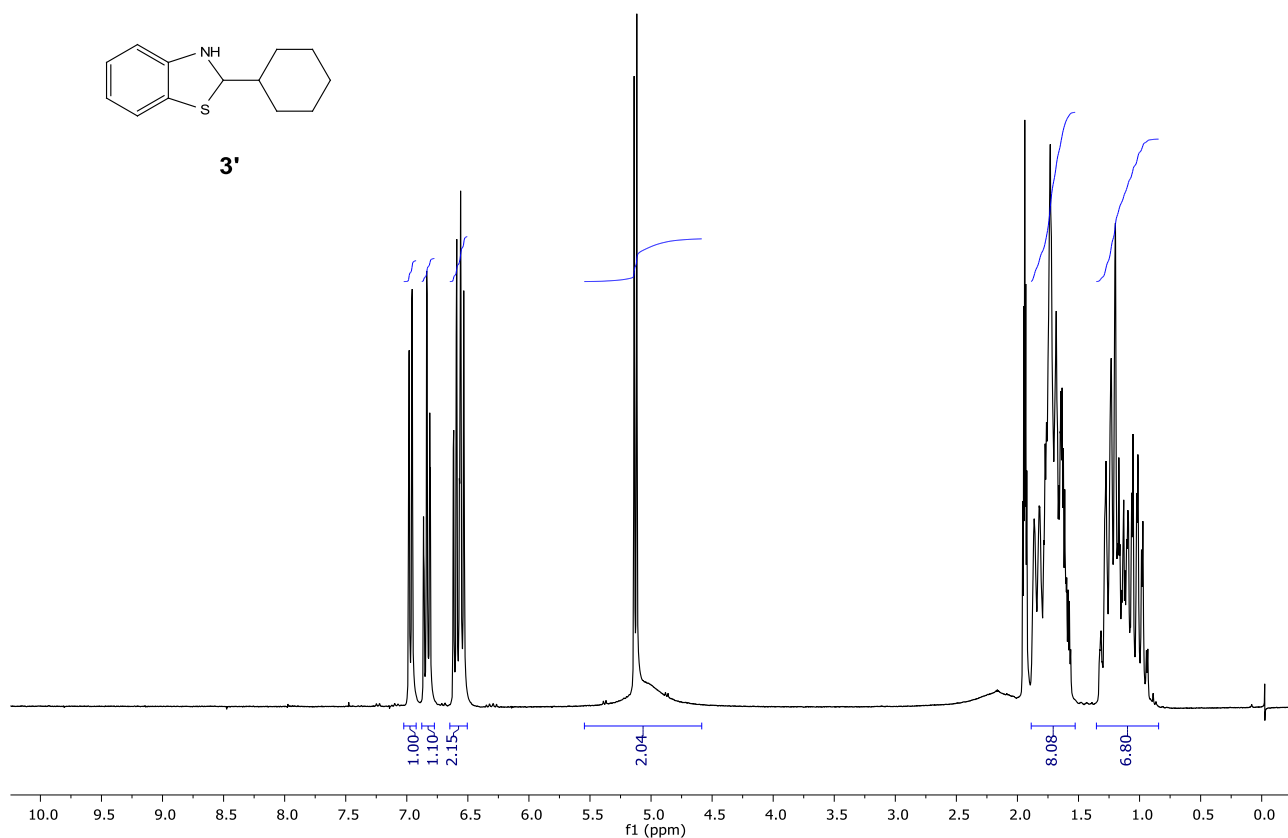


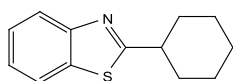
2i



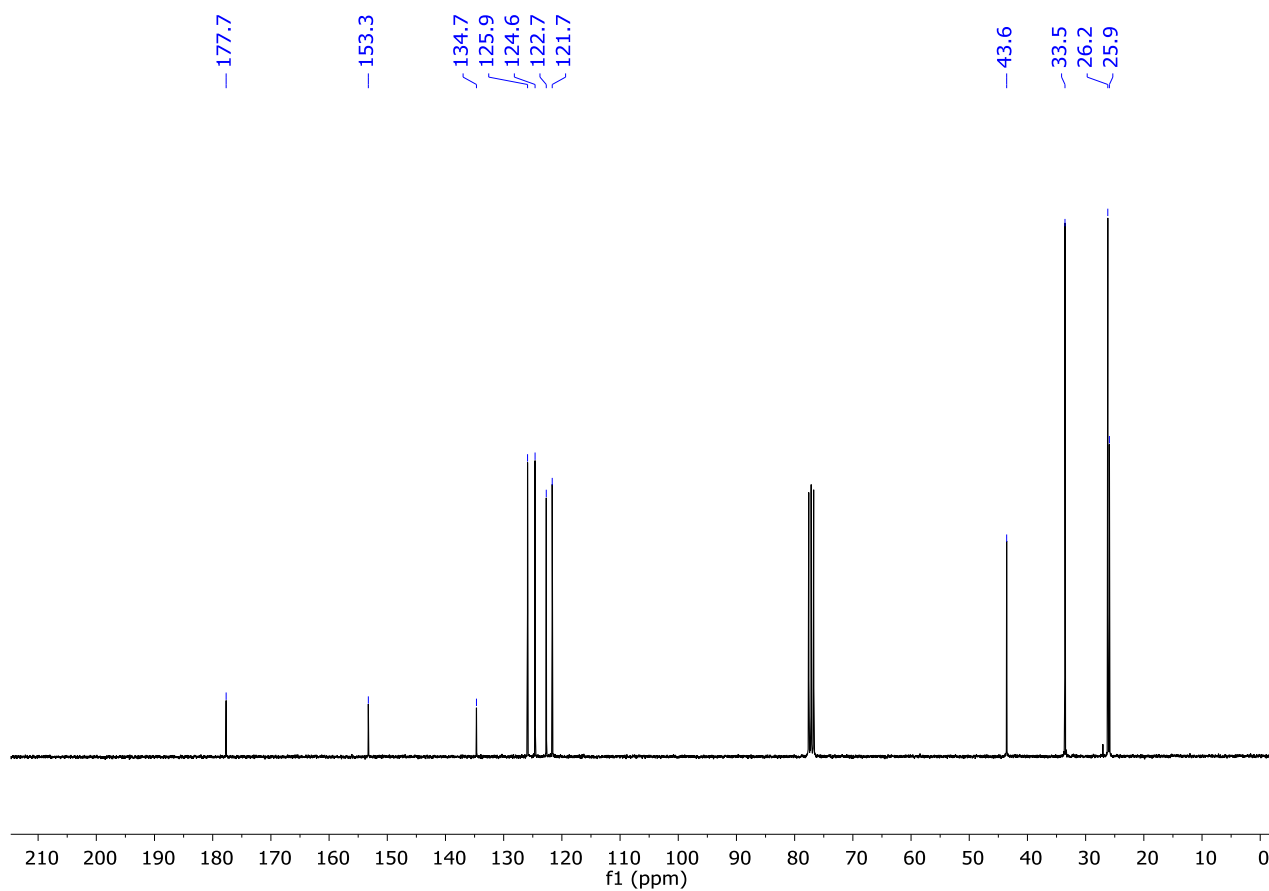
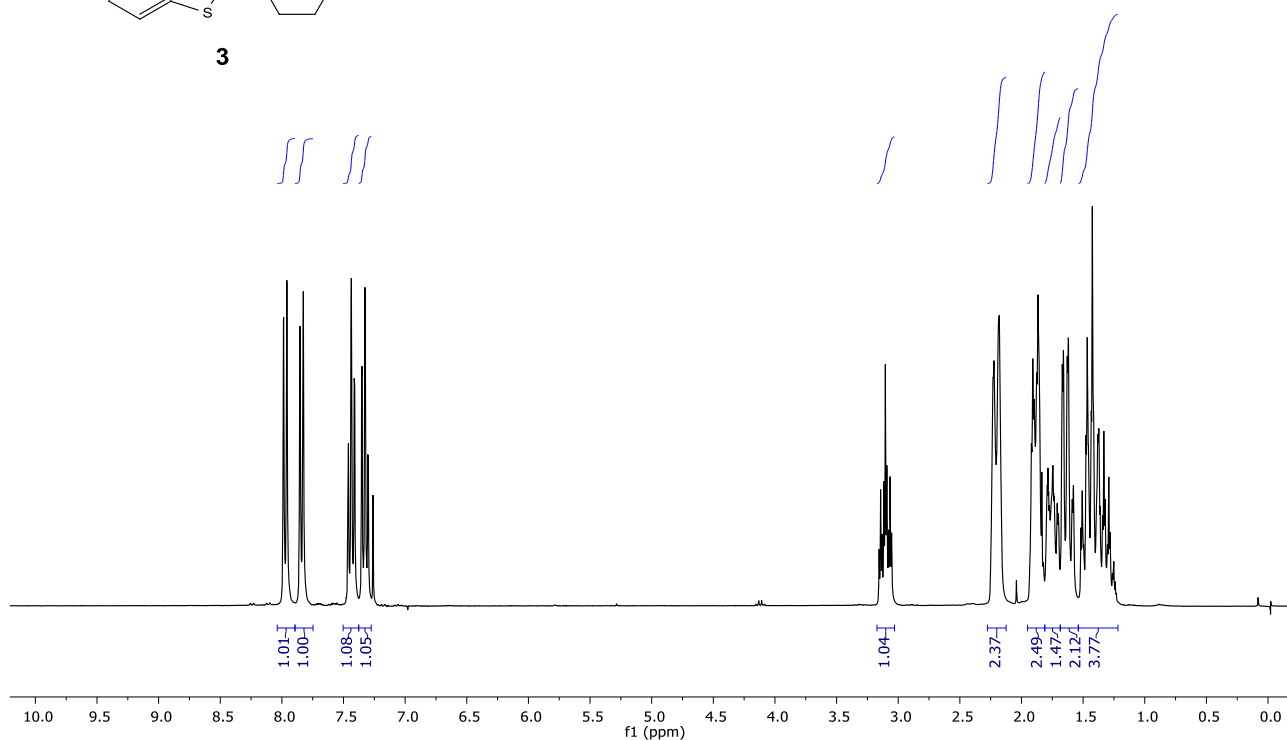


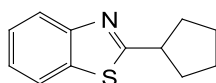
3'



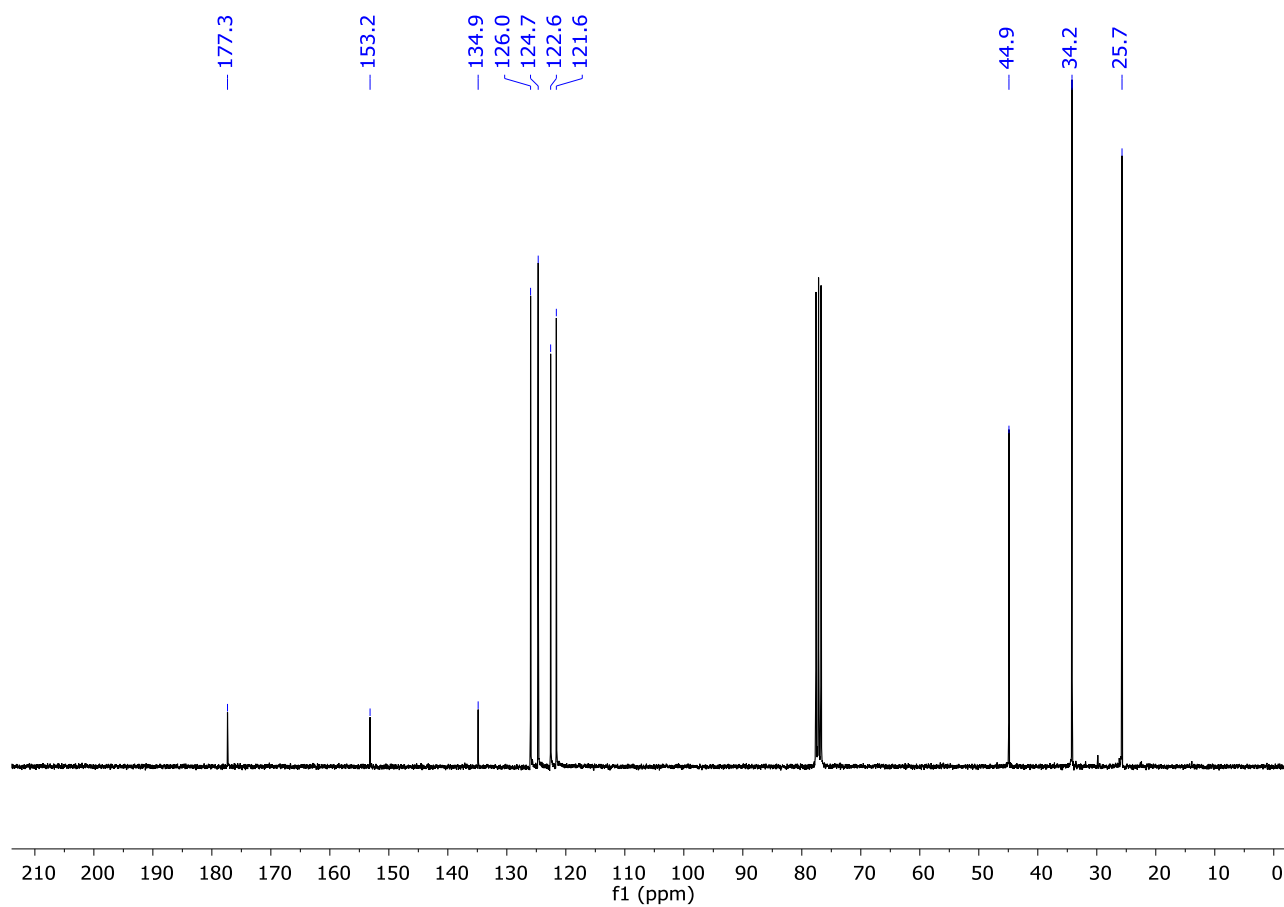
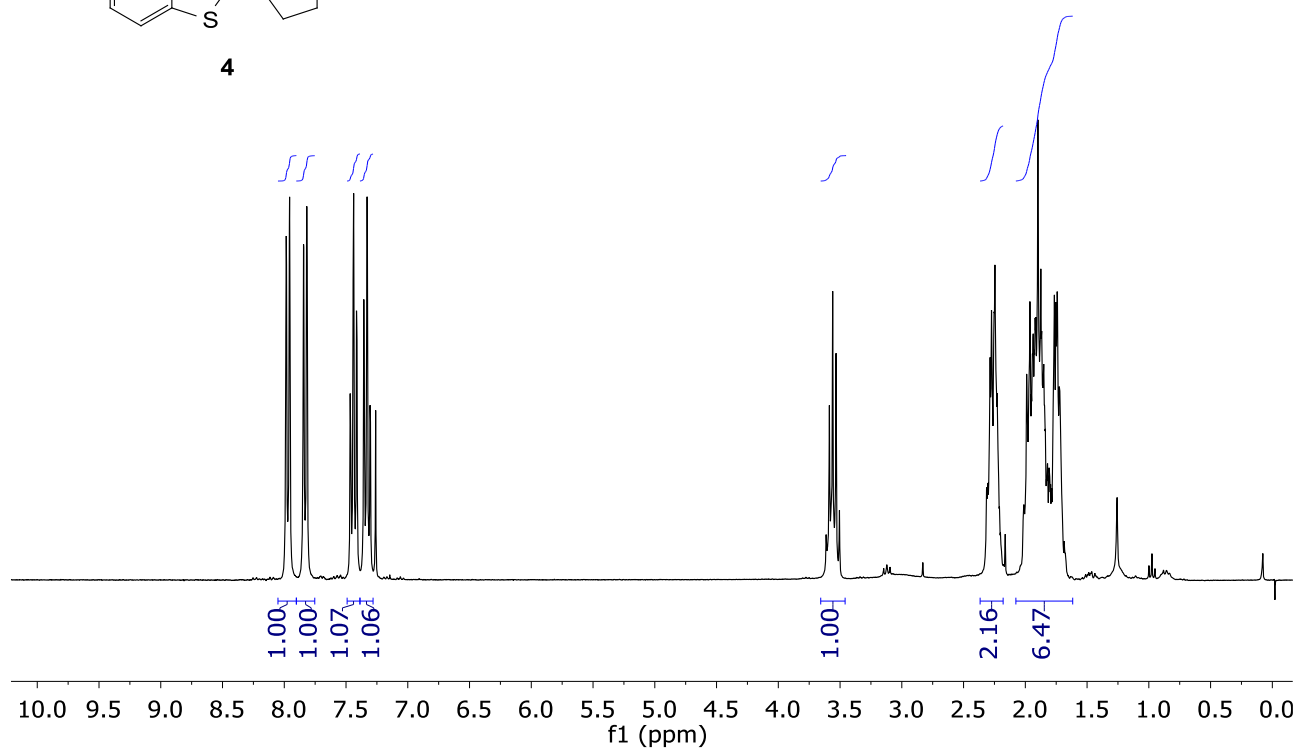


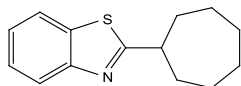
3



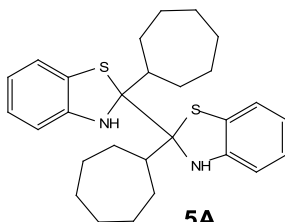


4

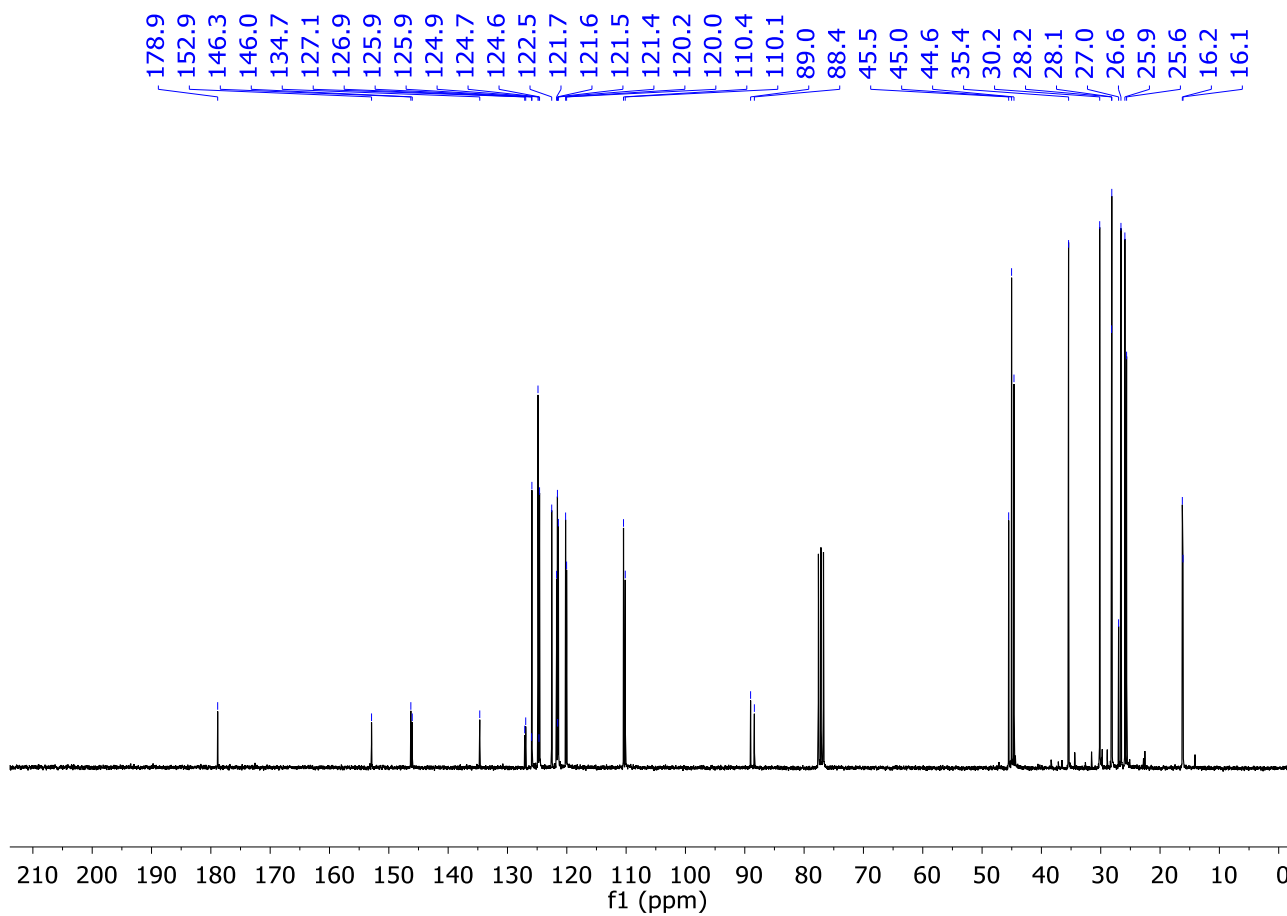
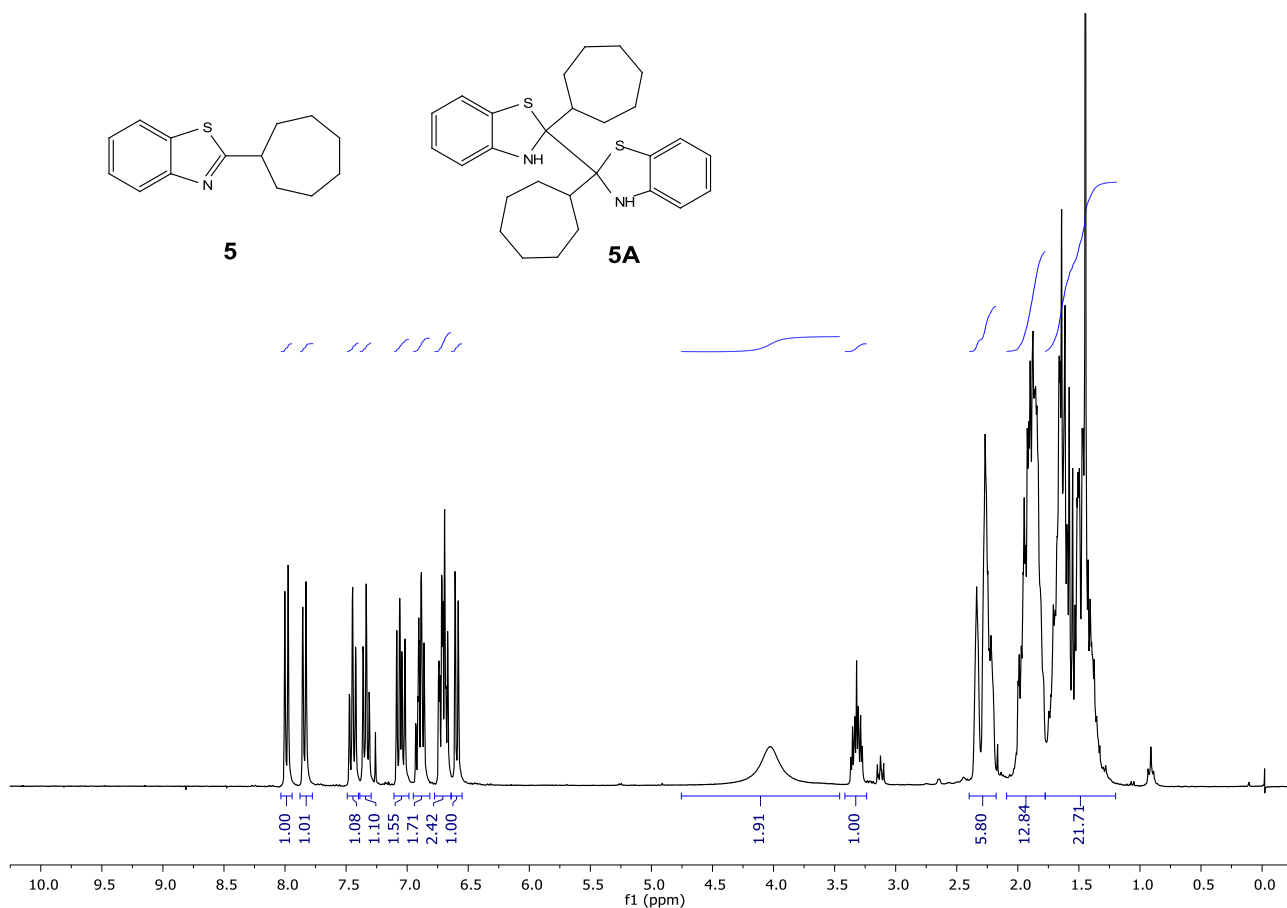


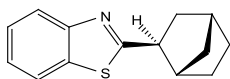


5

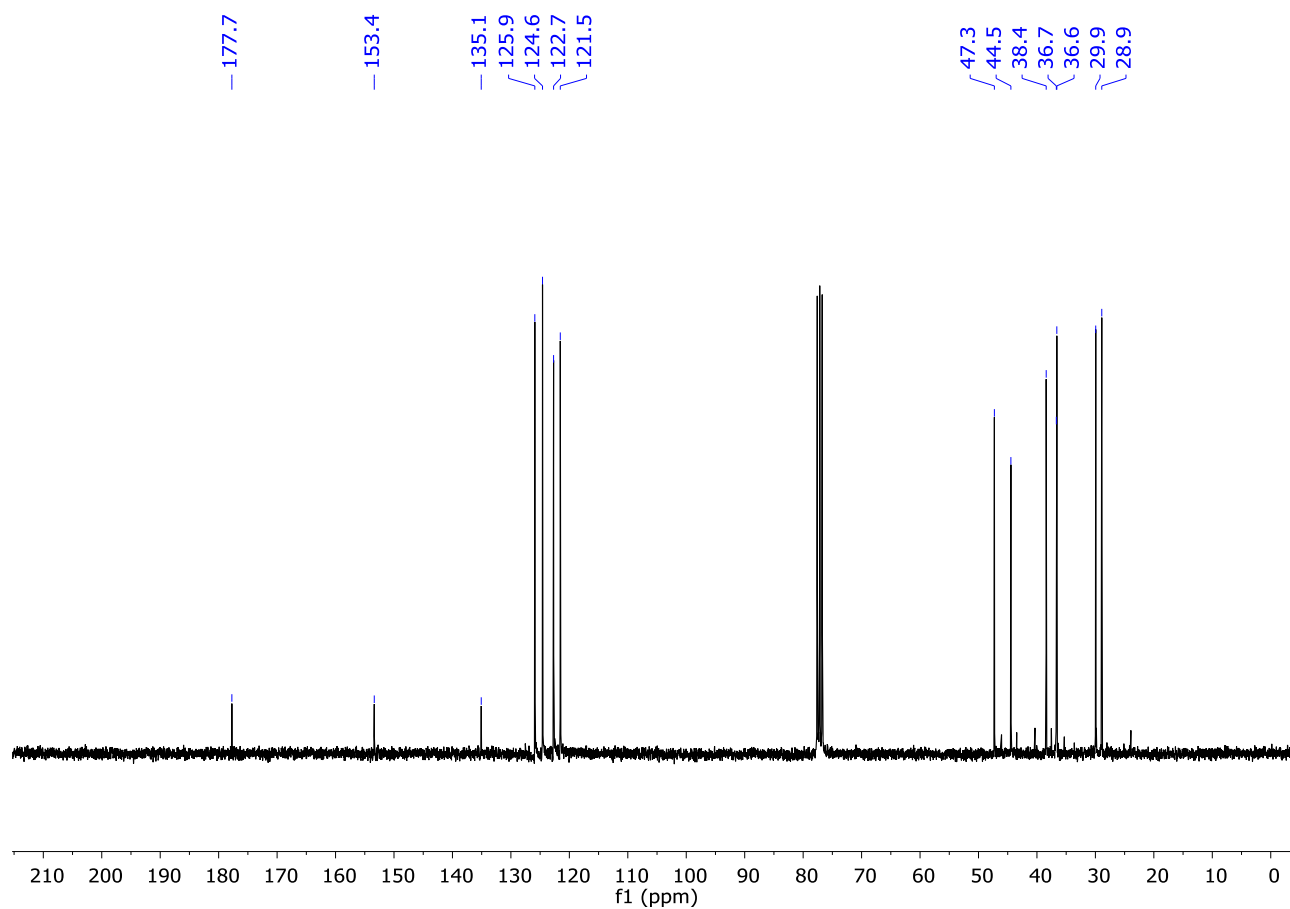
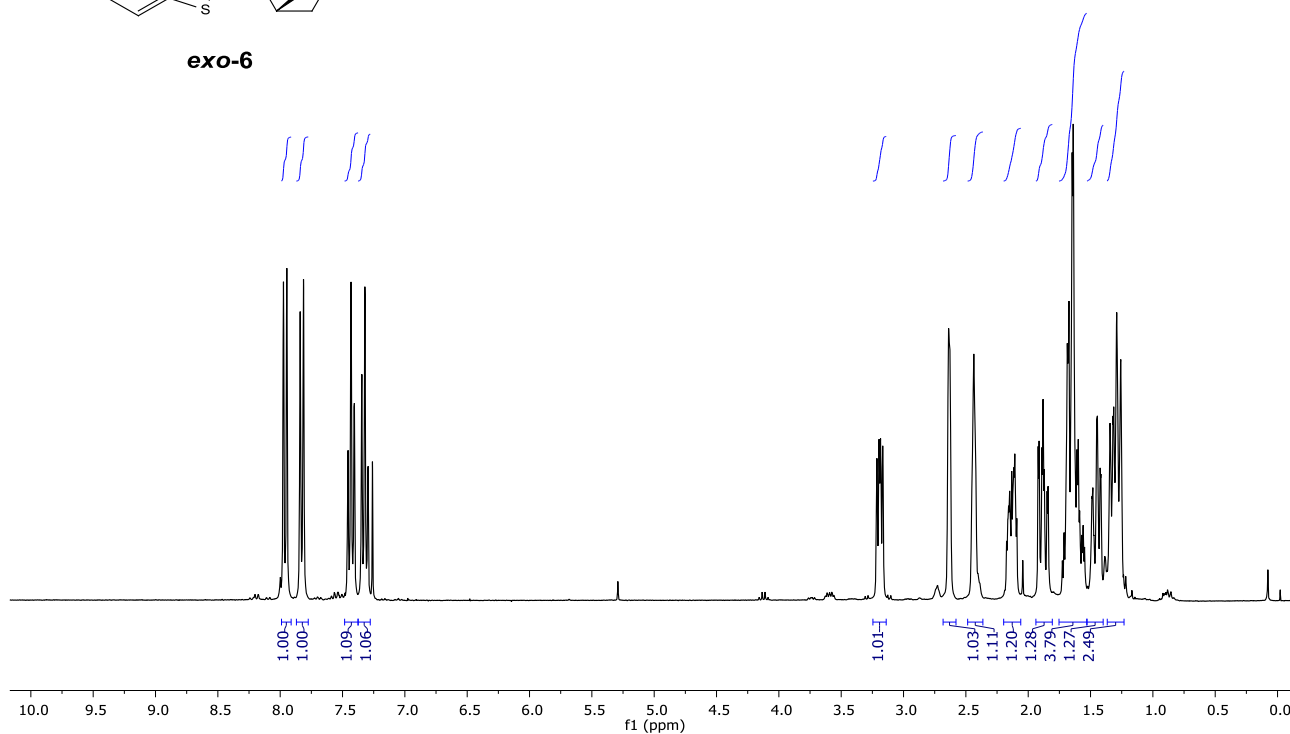


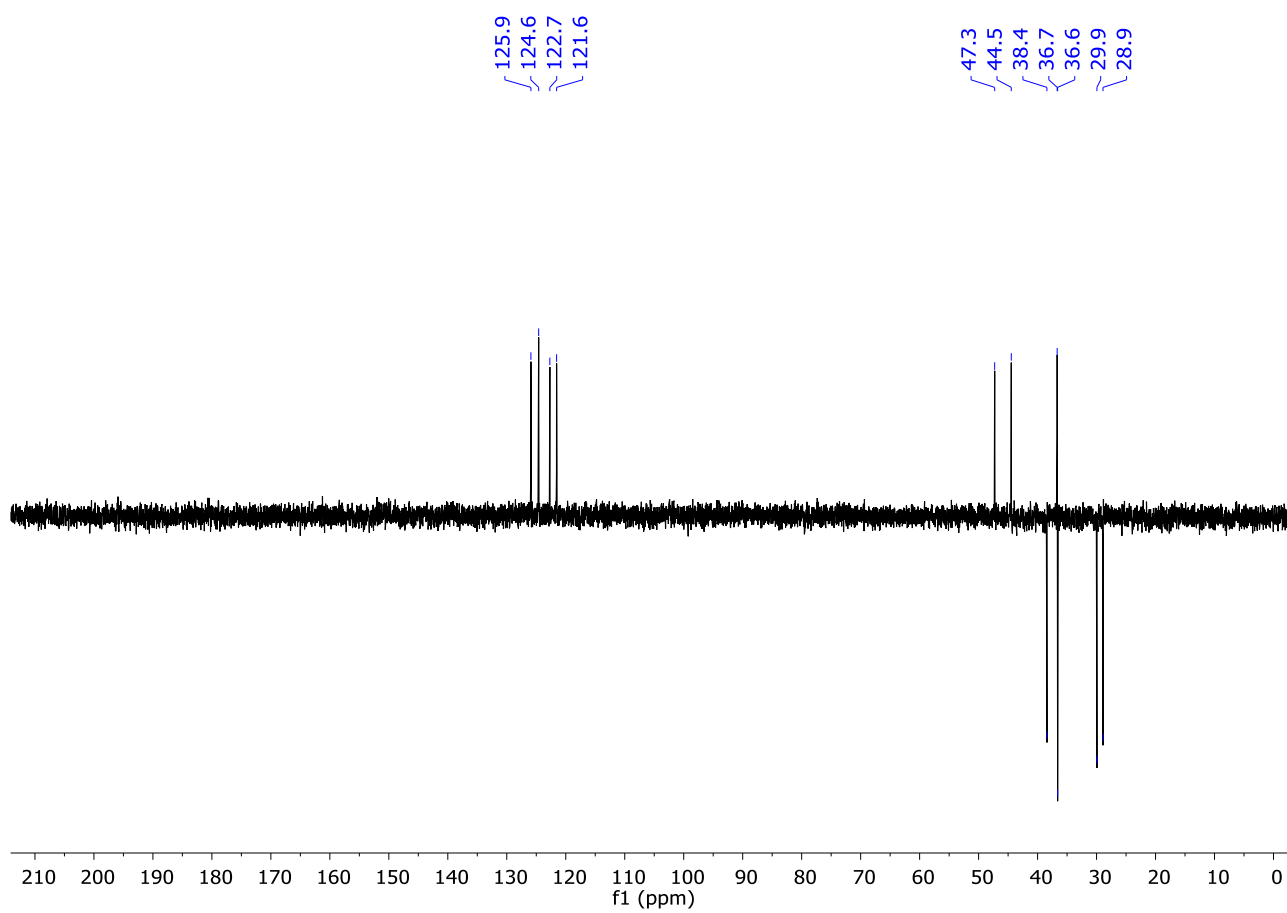
5A

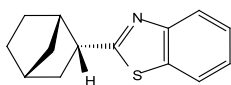




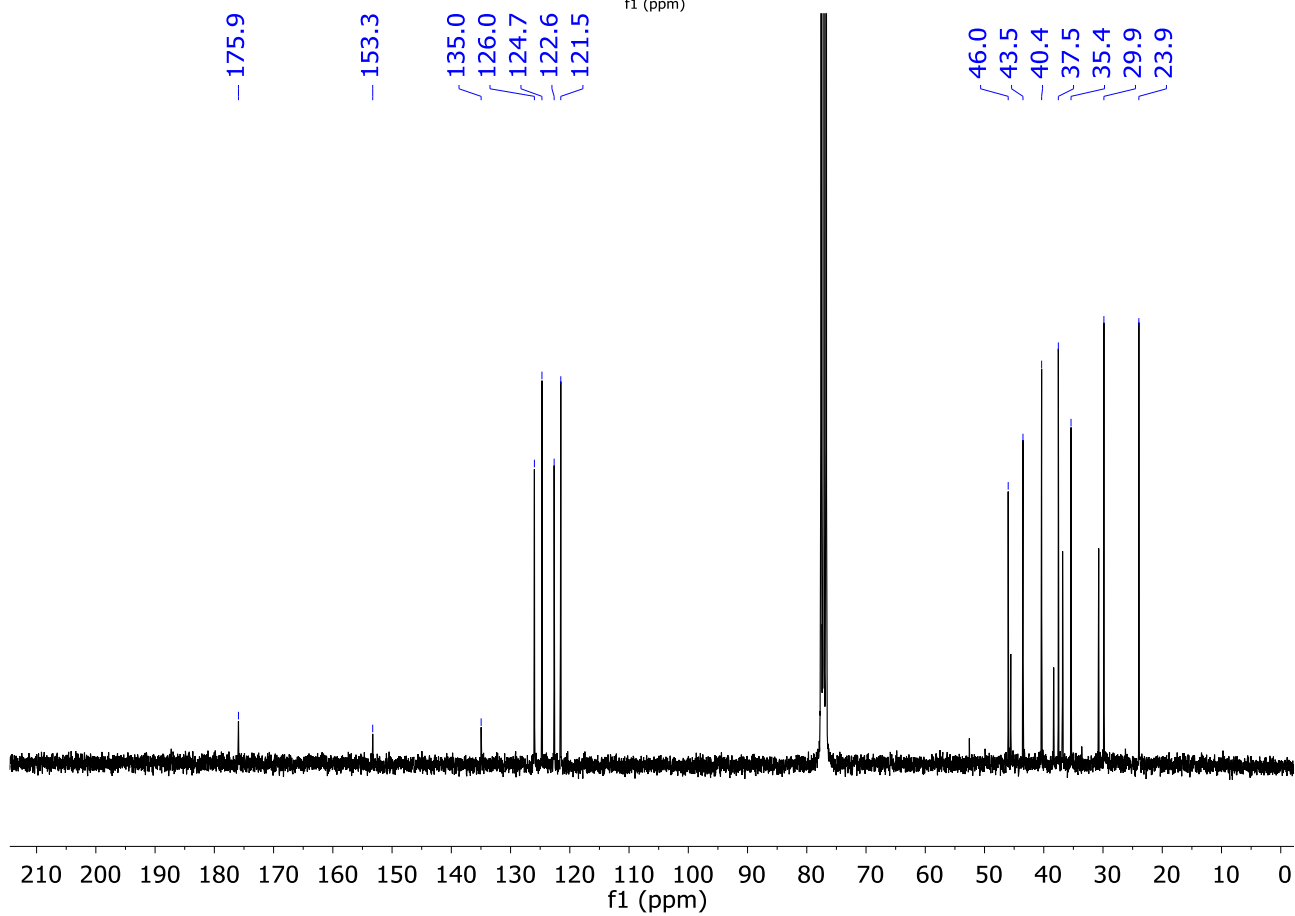
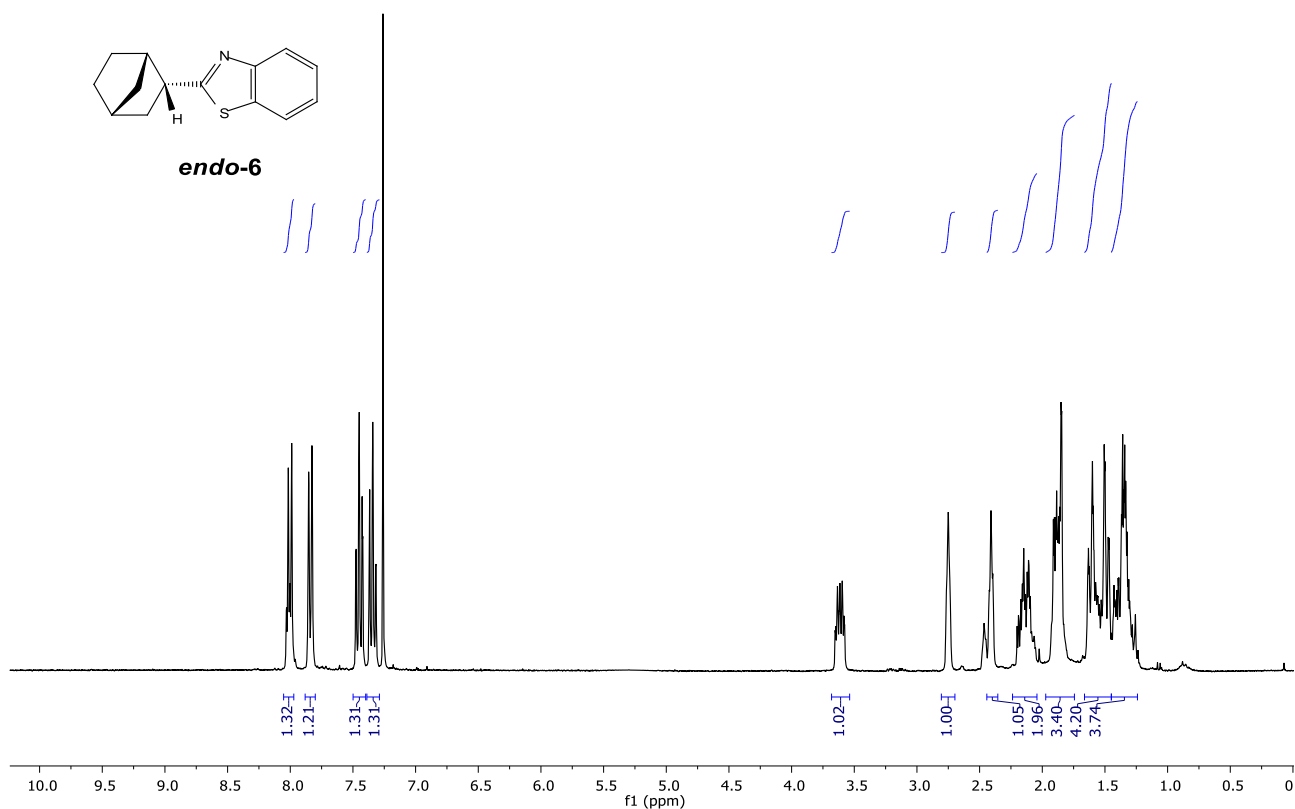
exo-6

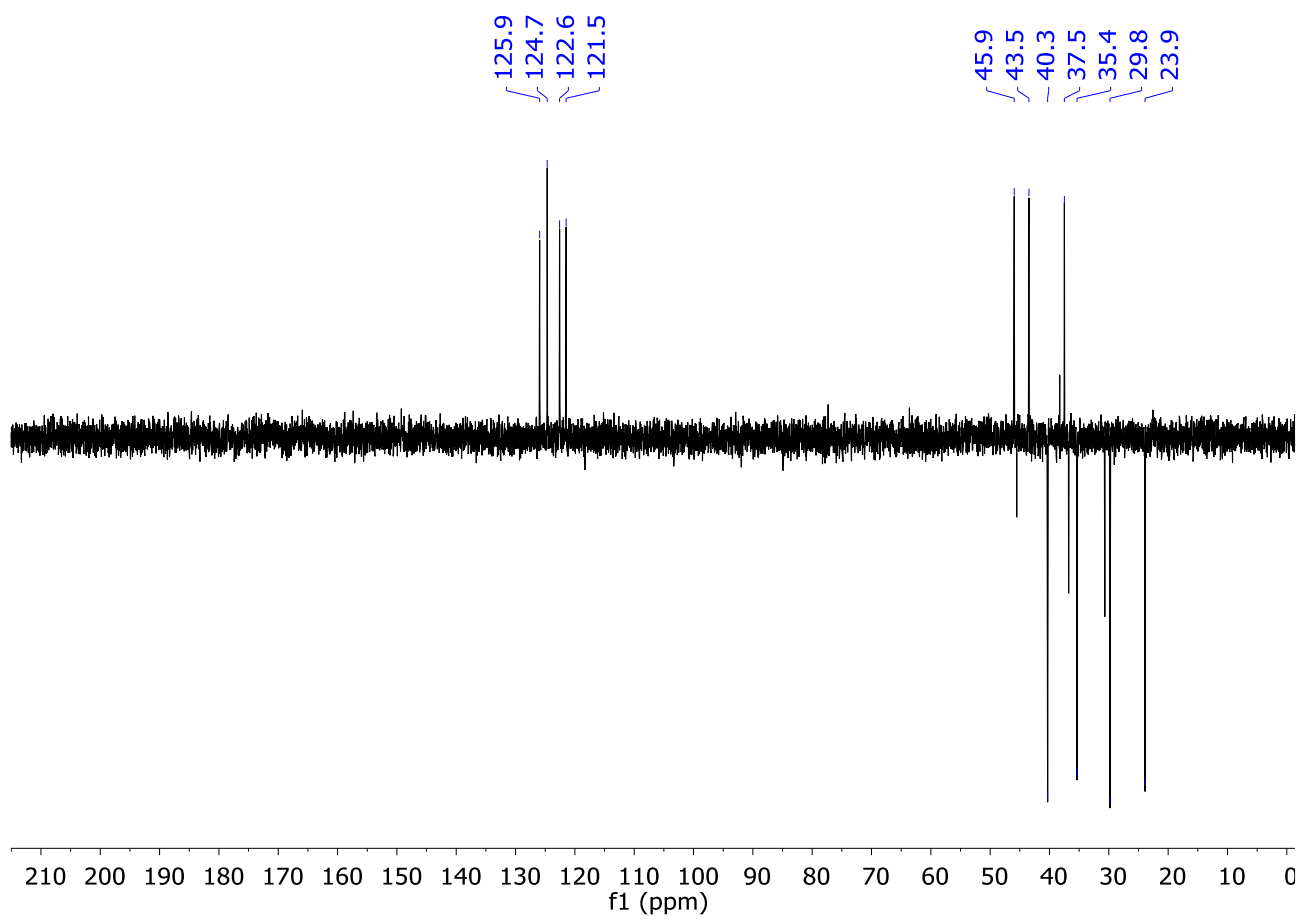


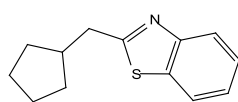




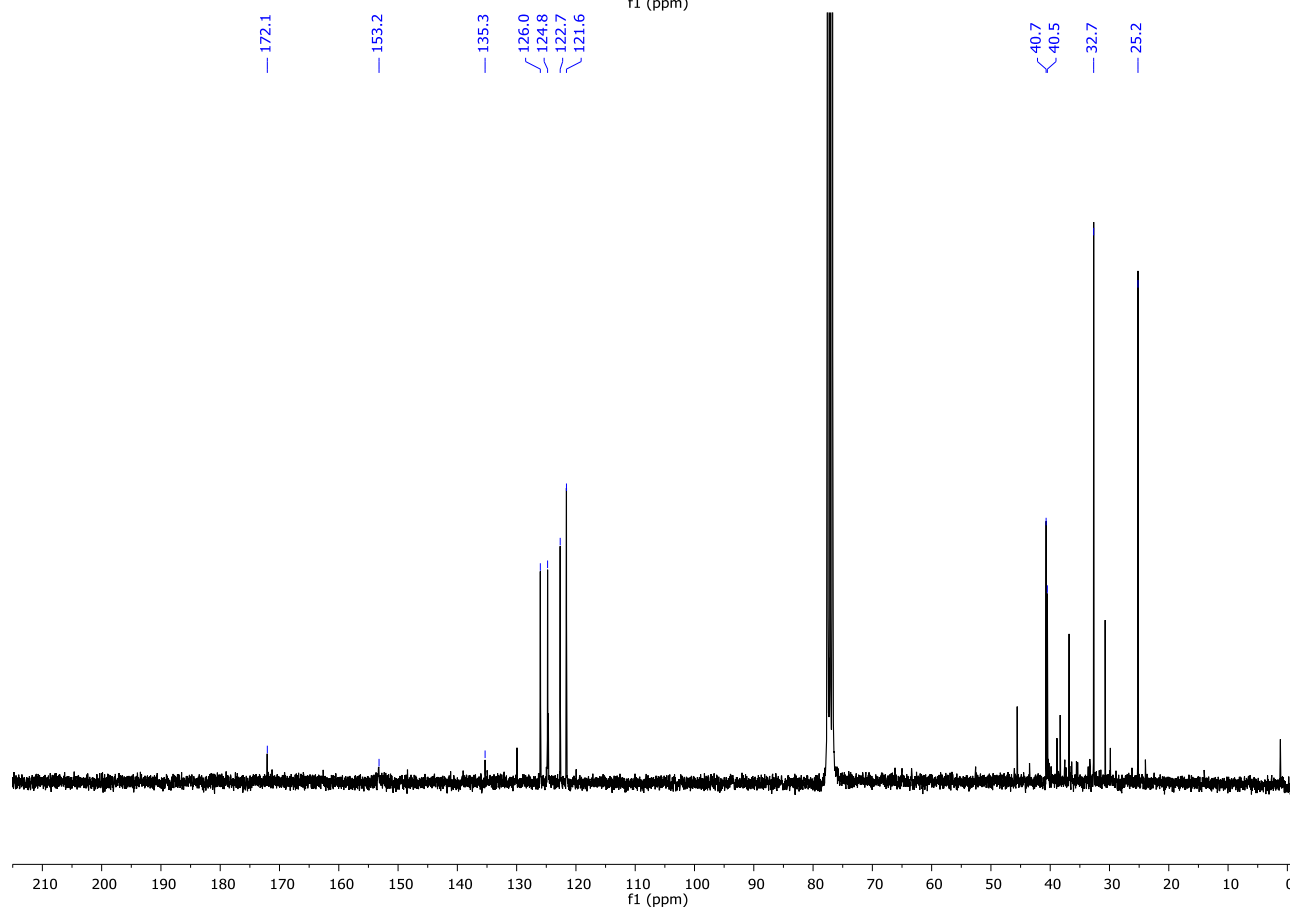
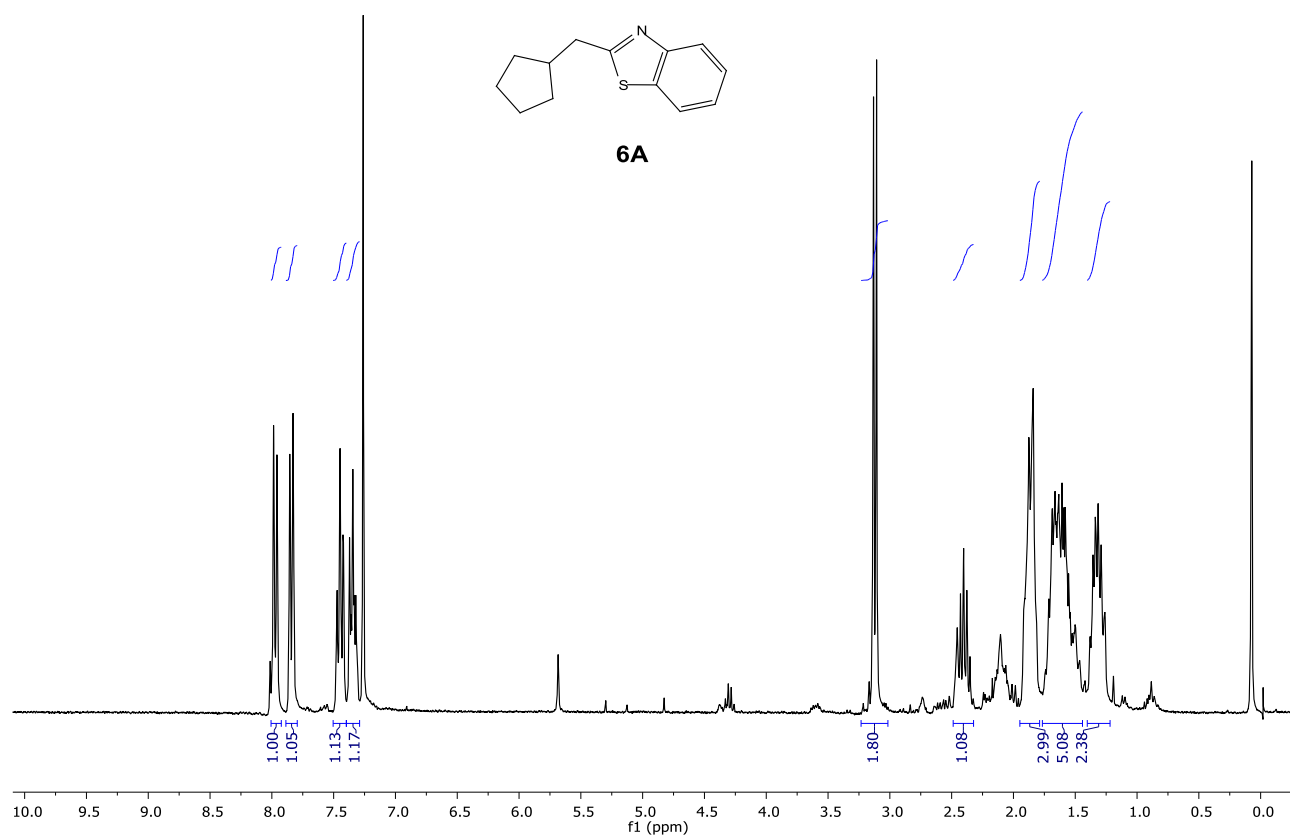
endo-6

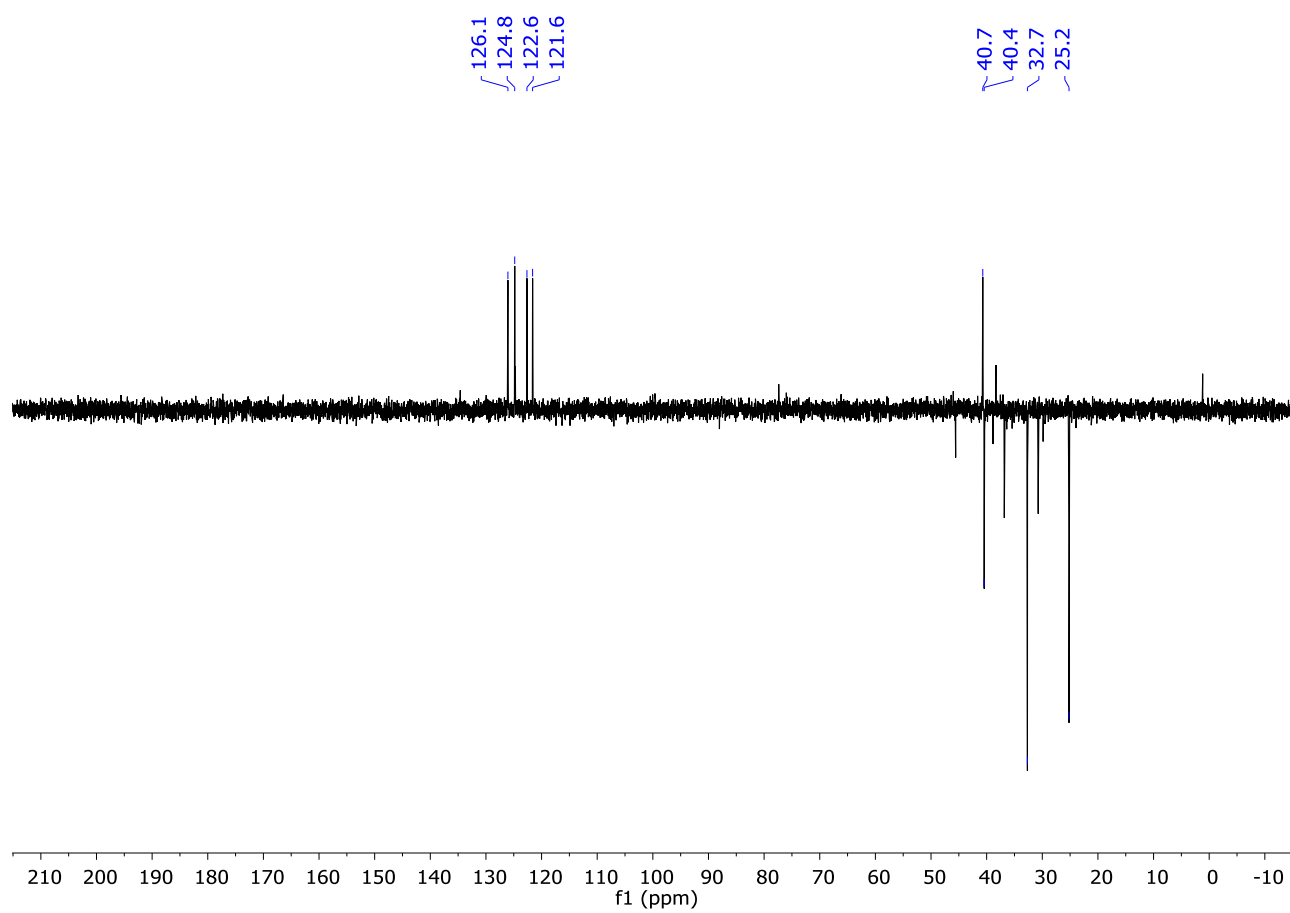


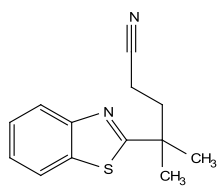




6A



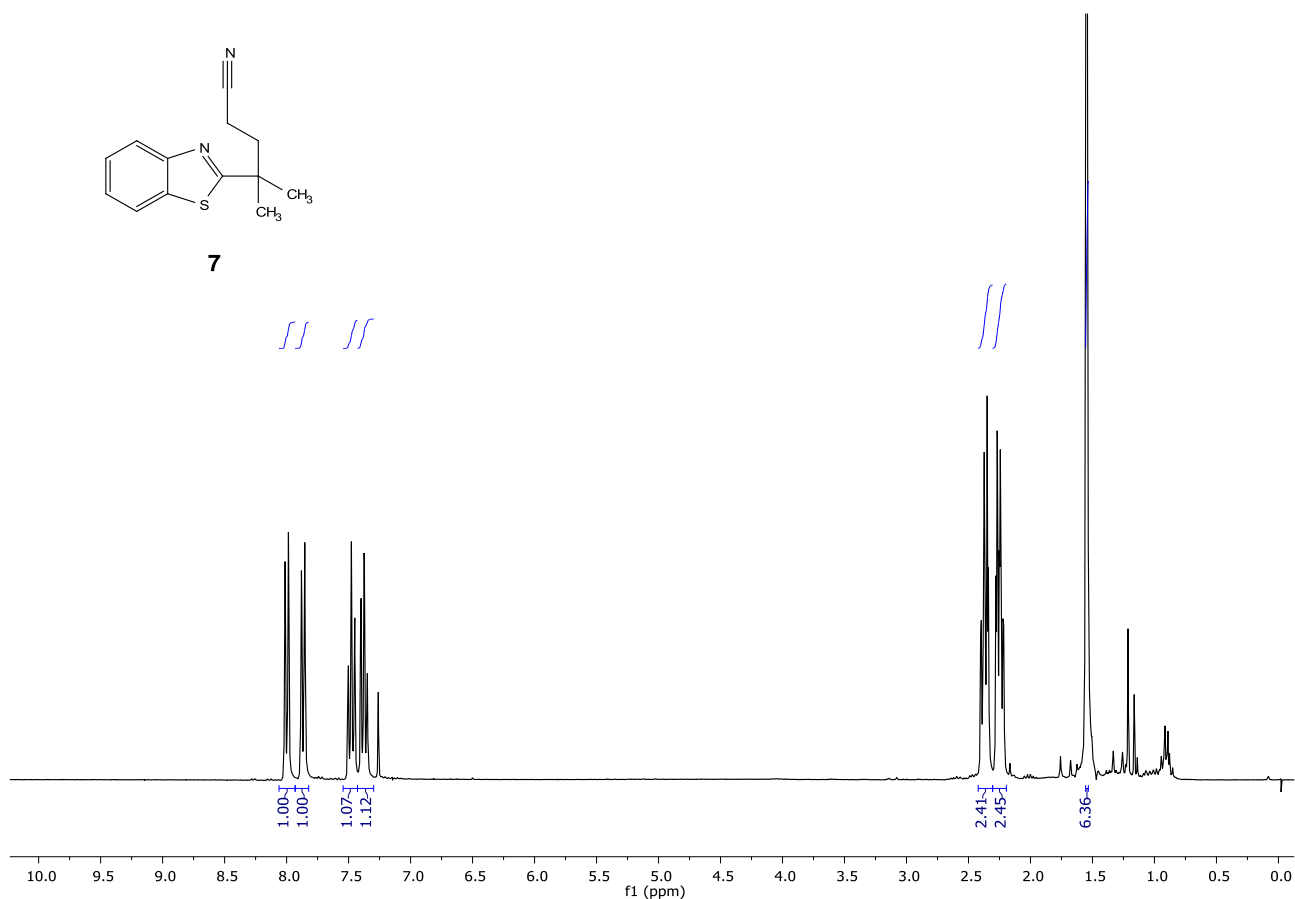




7

// //

//



— 178.2

— 153.0

134.8

126.3

125.2

123.0

121.7

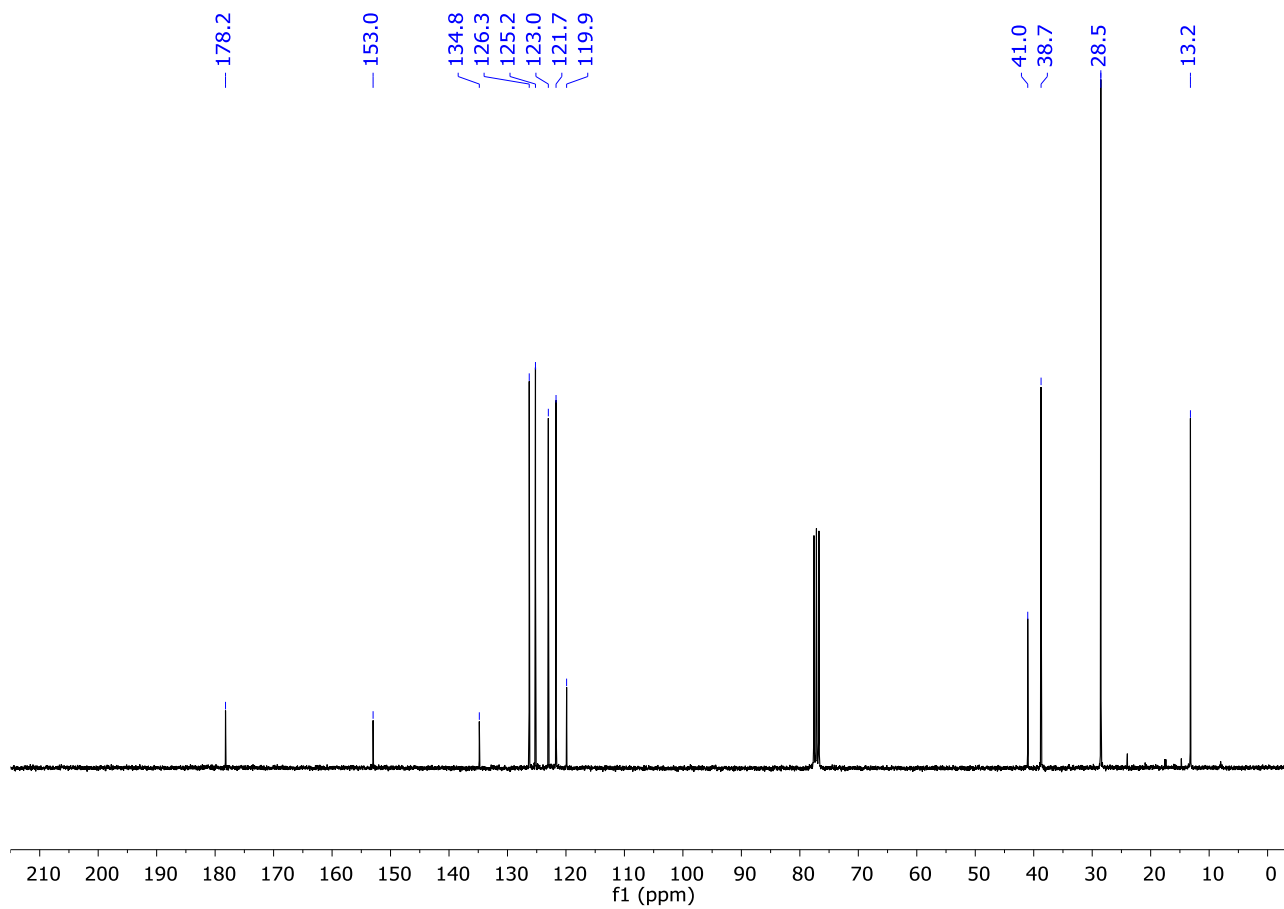
119.9

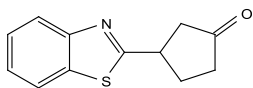
41.0

38.7

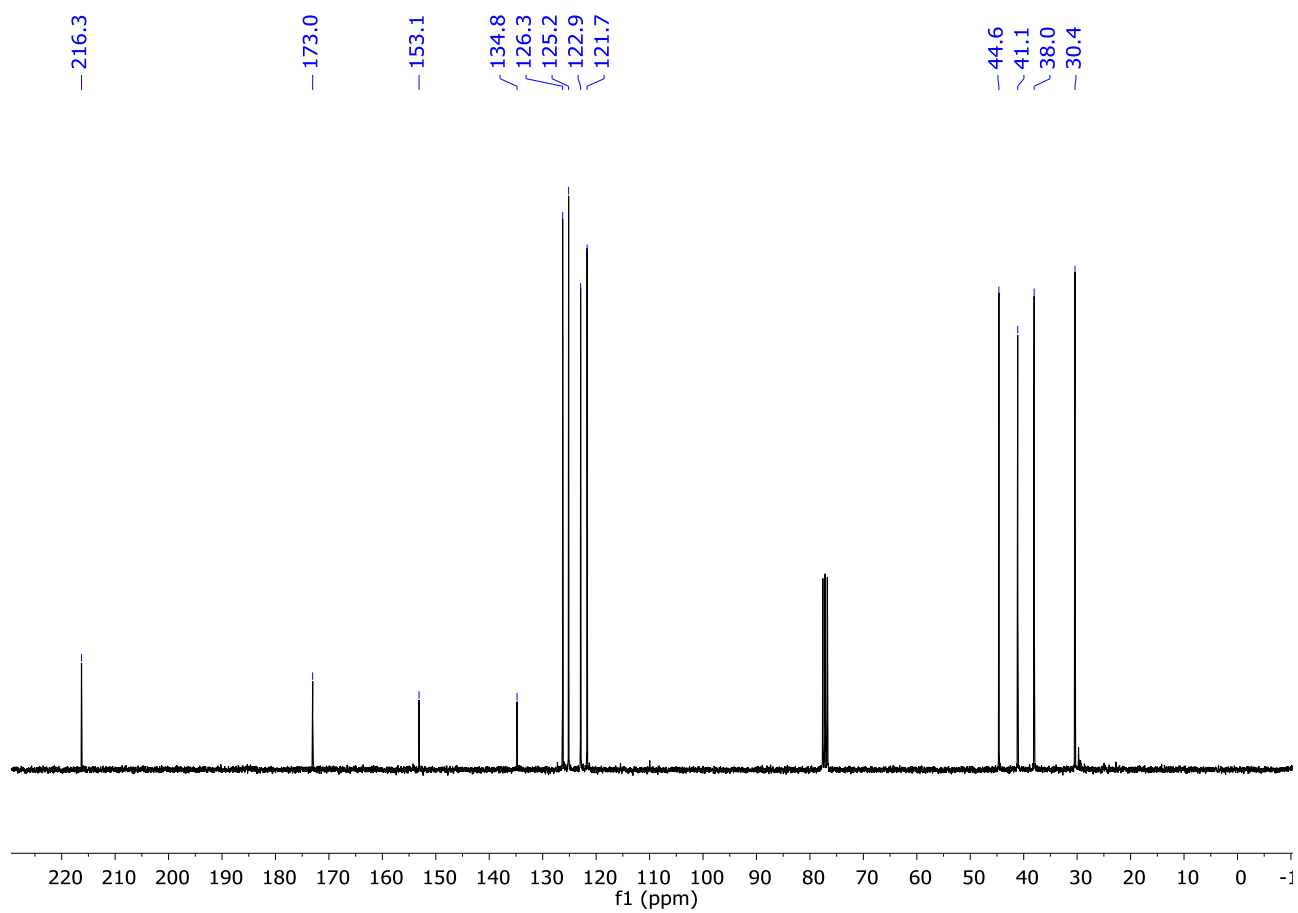
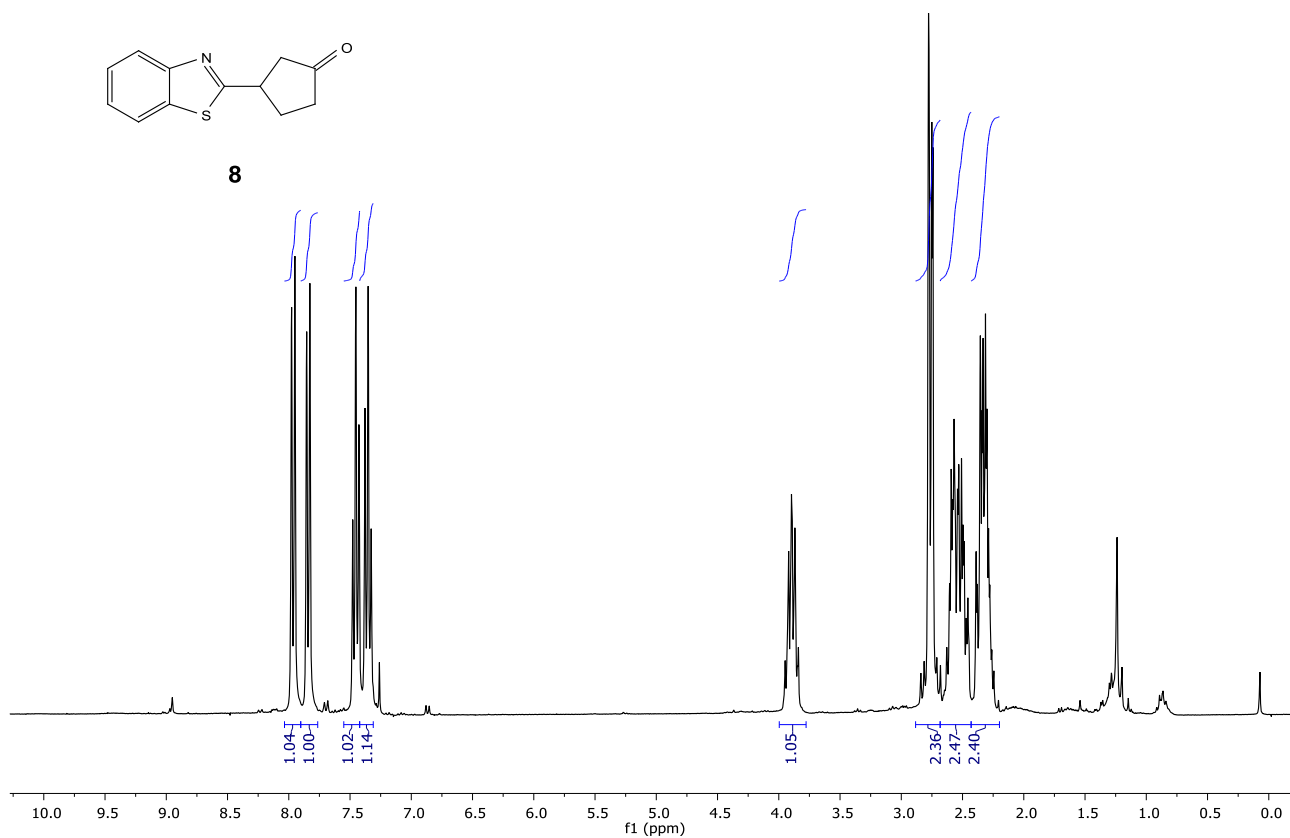
28.5

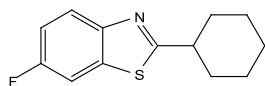
— 13.2



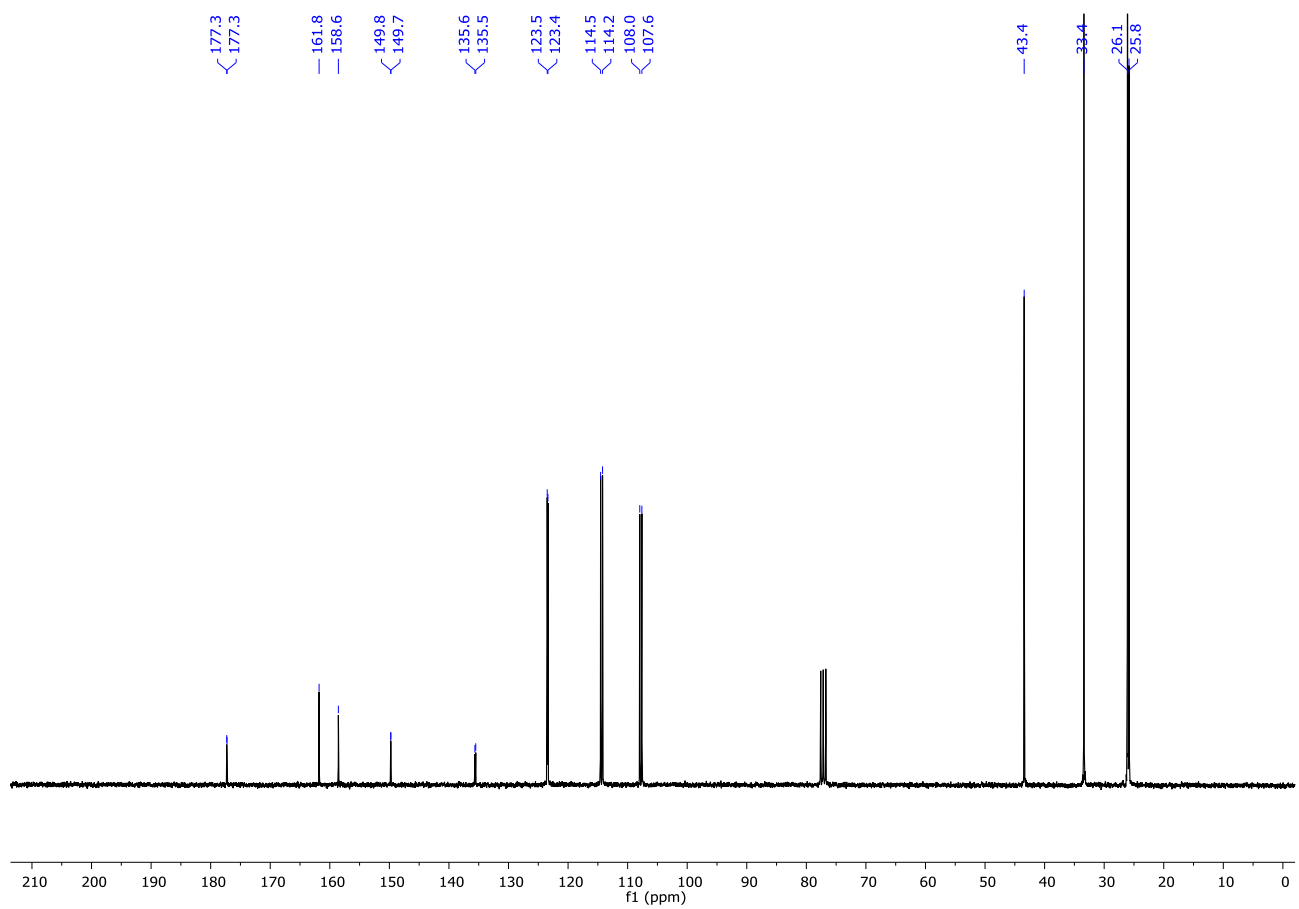
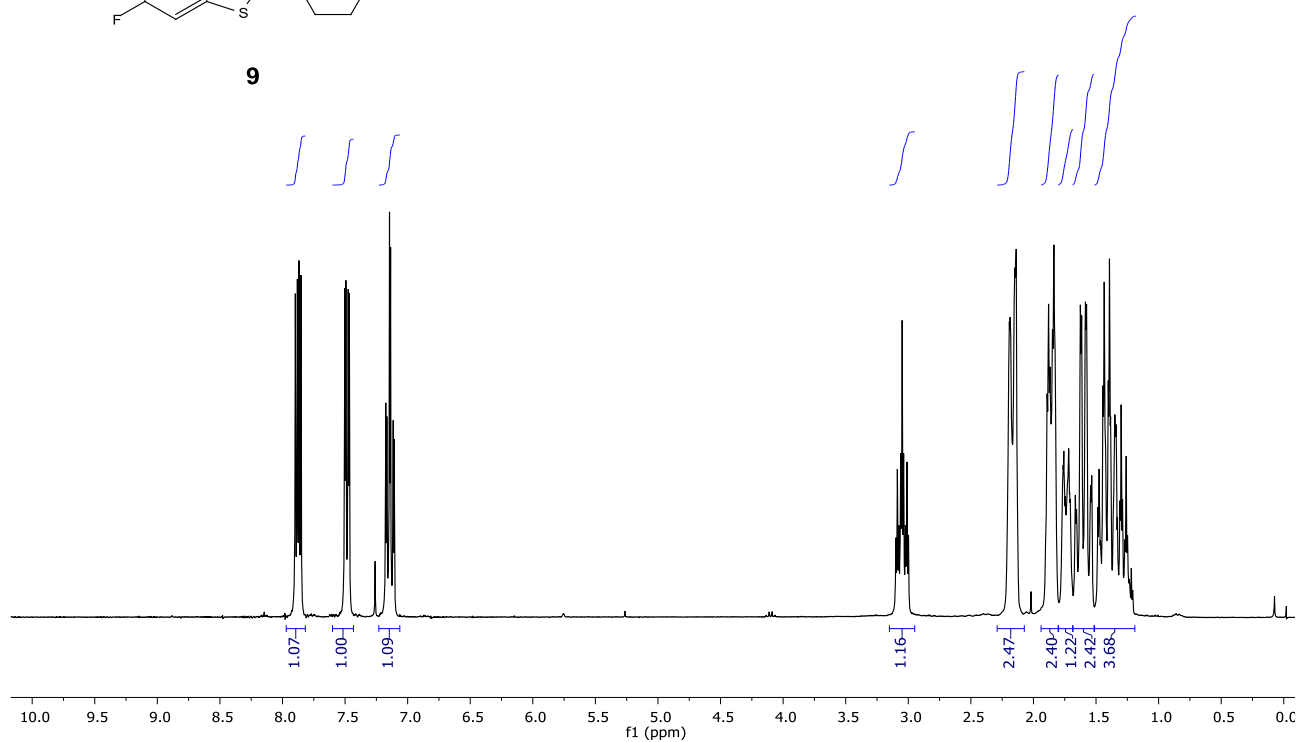


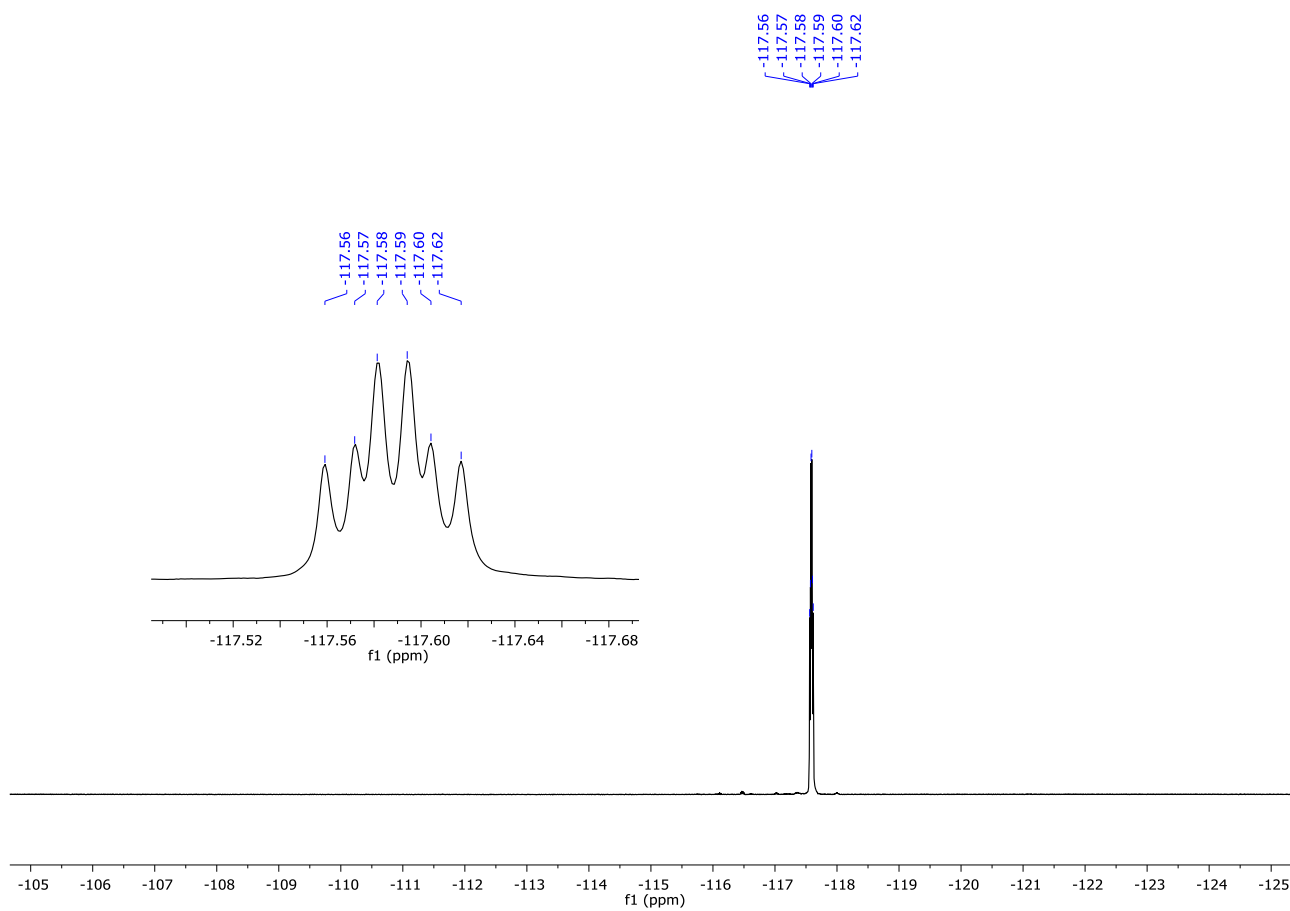
8

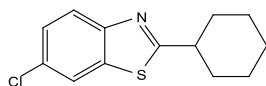




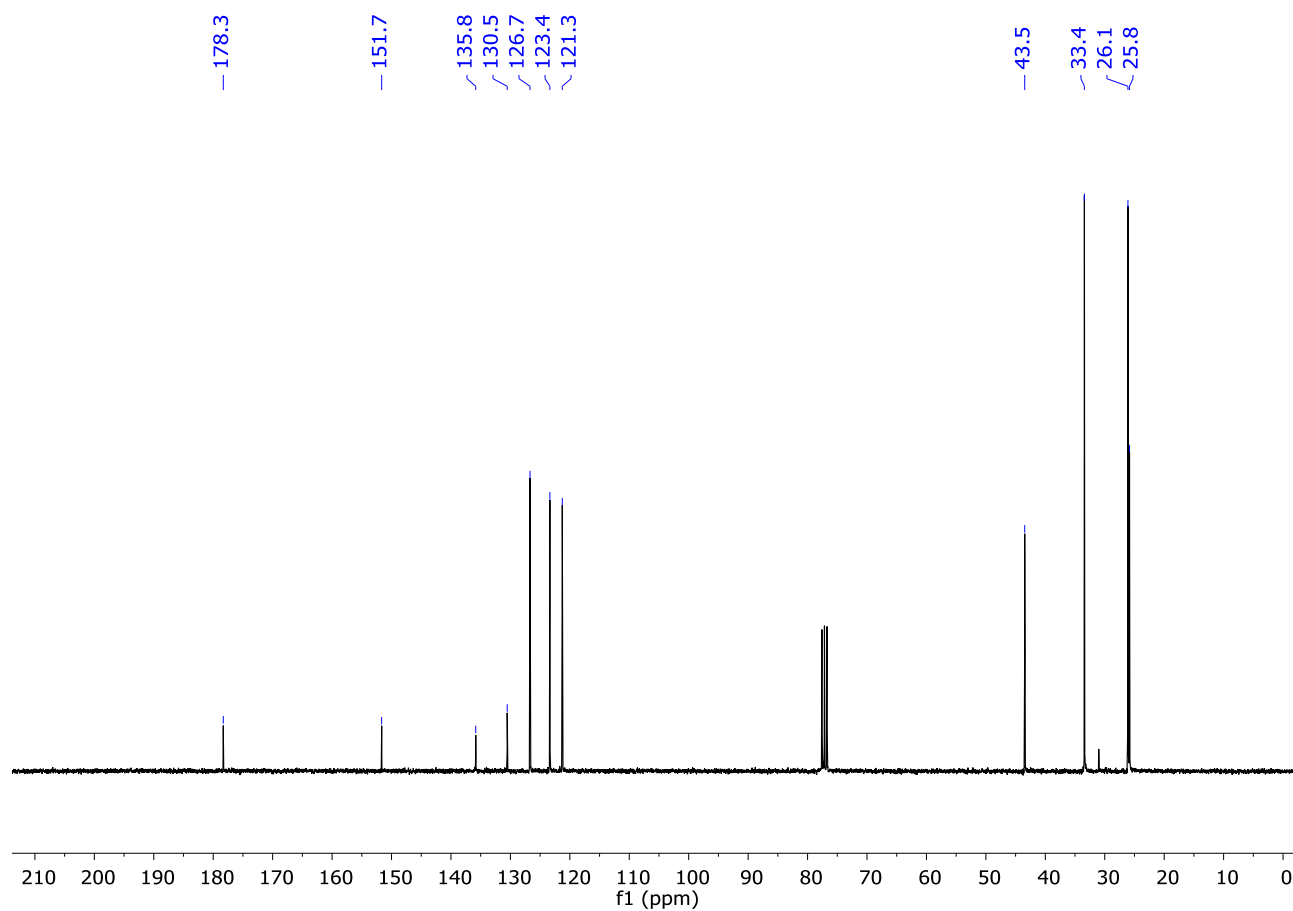
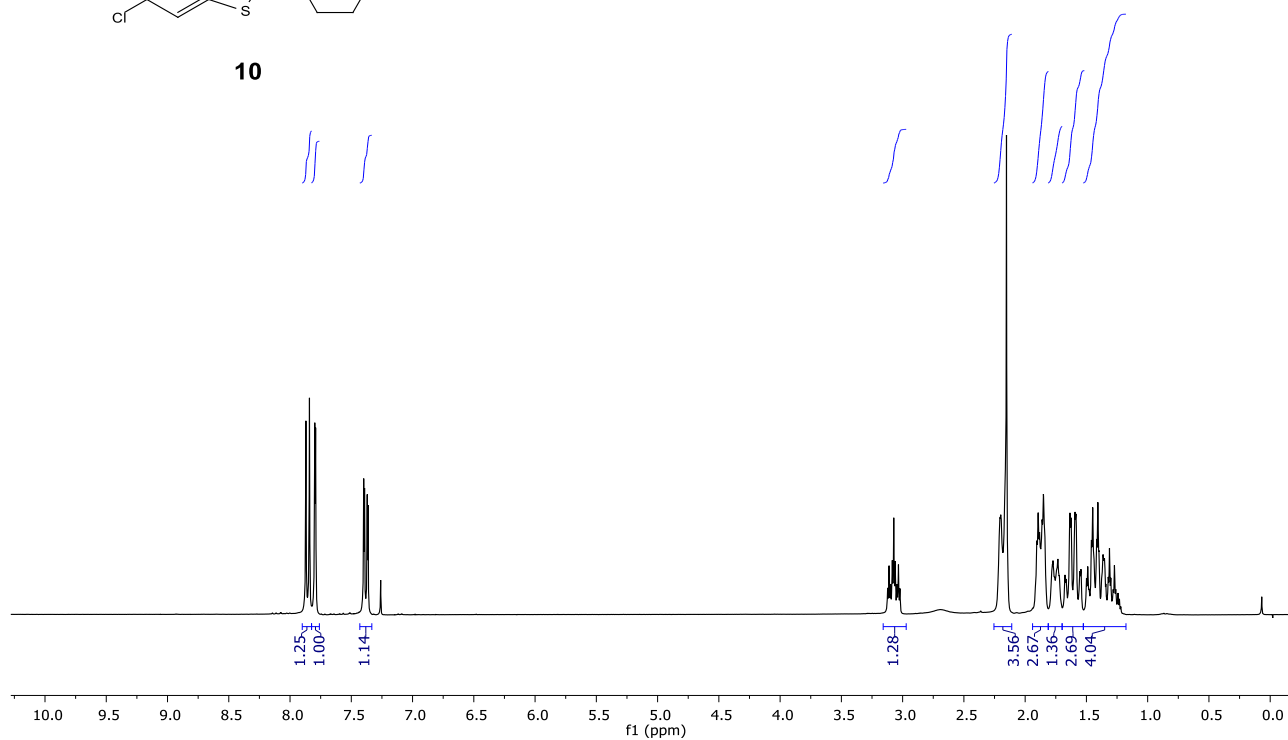
9

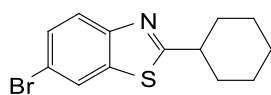




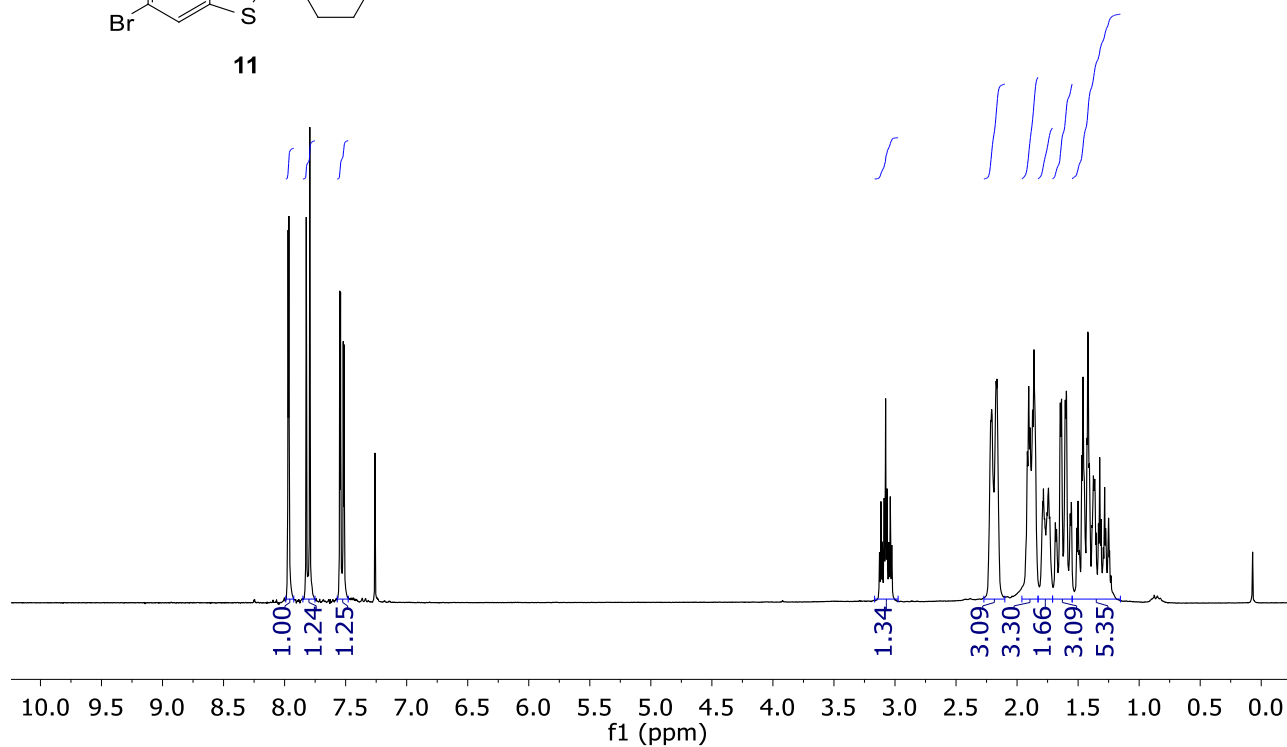


10





11



— 178.3

— 152.1

— 136.4

— 129.4

— 124.2

— 123.8

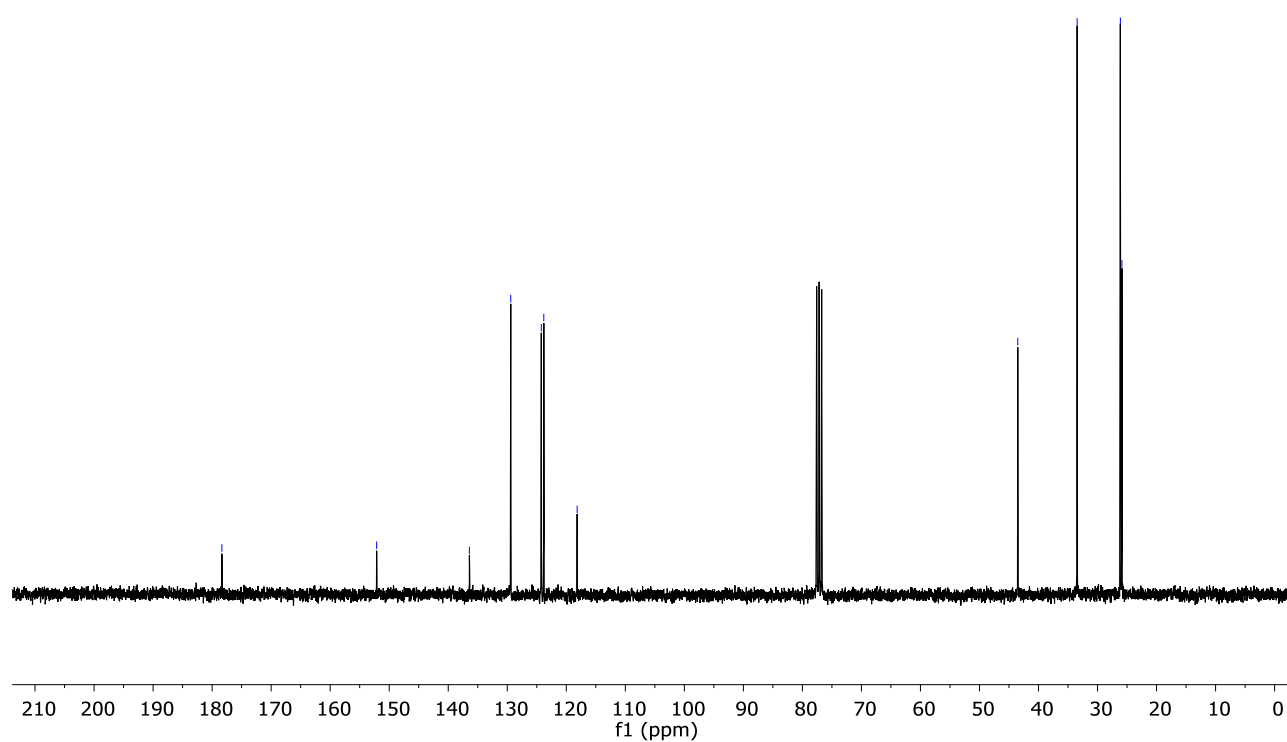
— 118.2

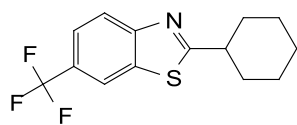
— 43.5

— 33.5

— 26.1

— 25.9

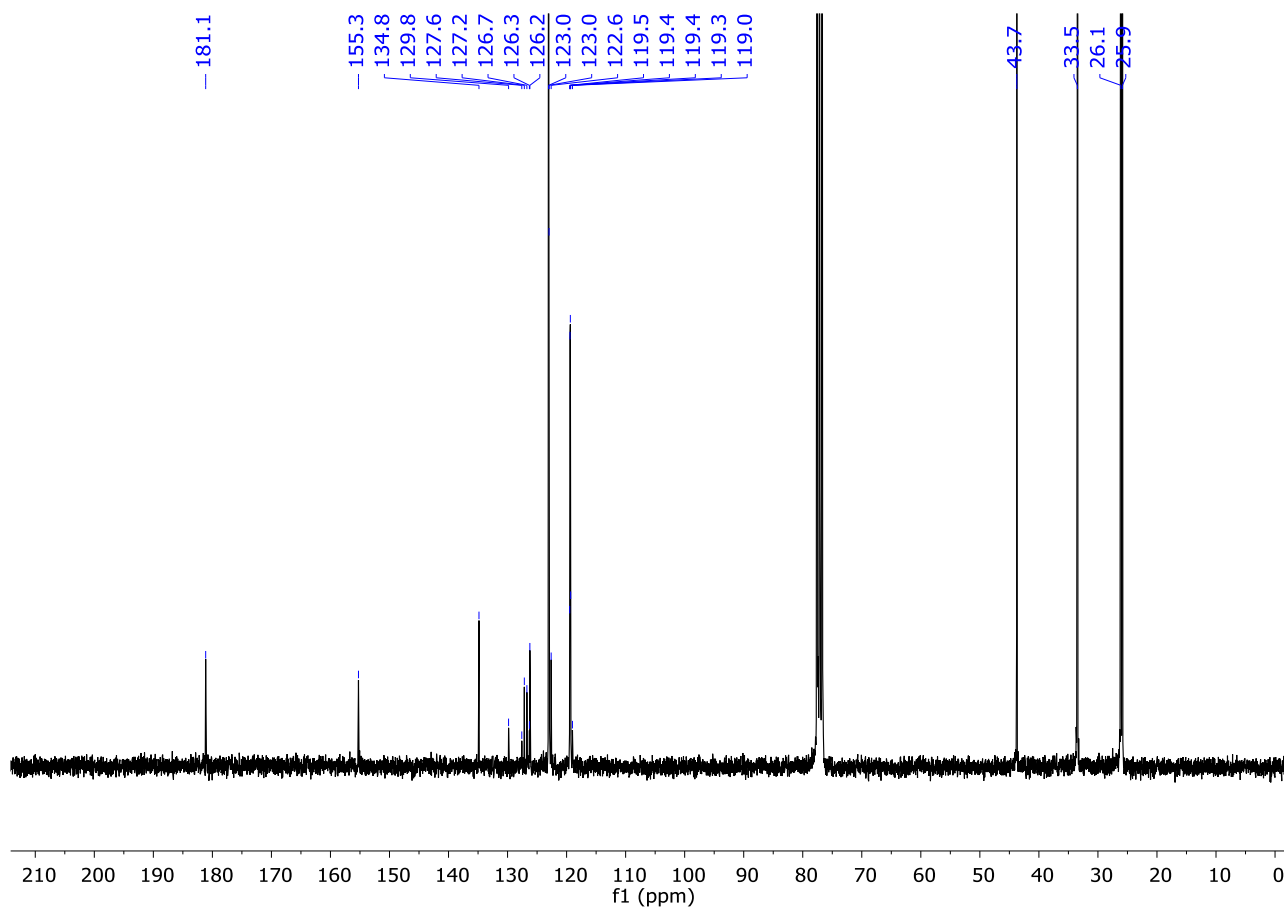
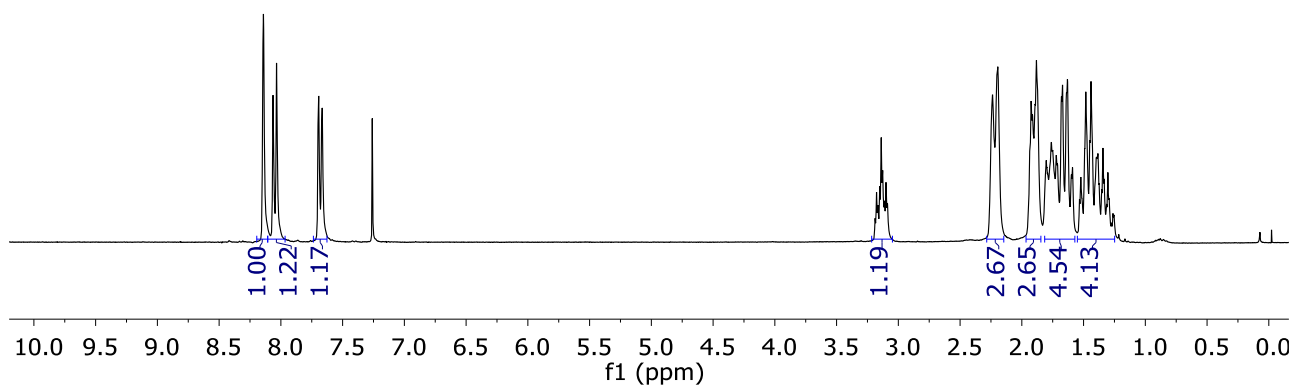


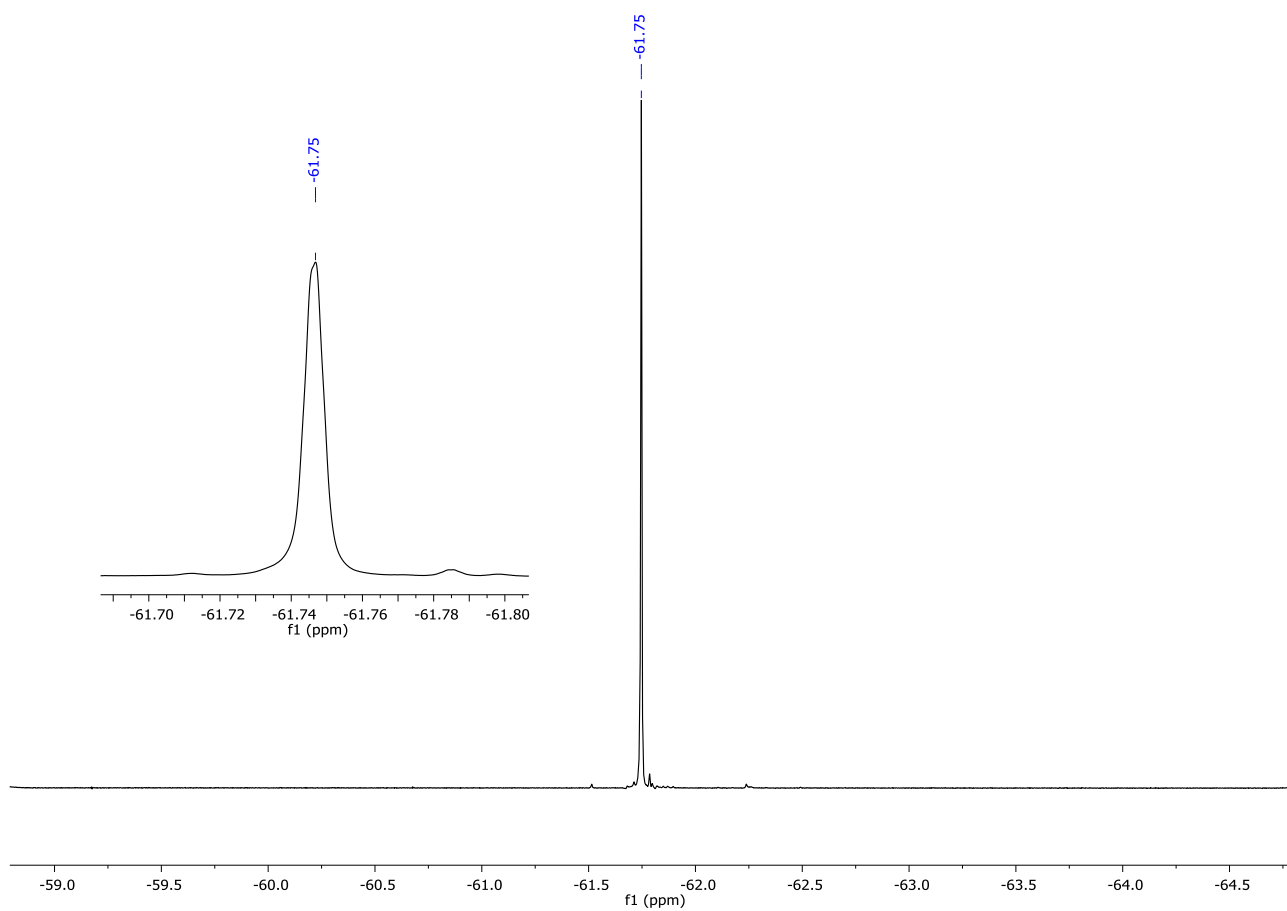


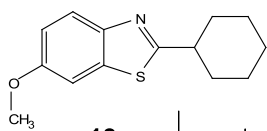
12

1.00 1.22 1.17

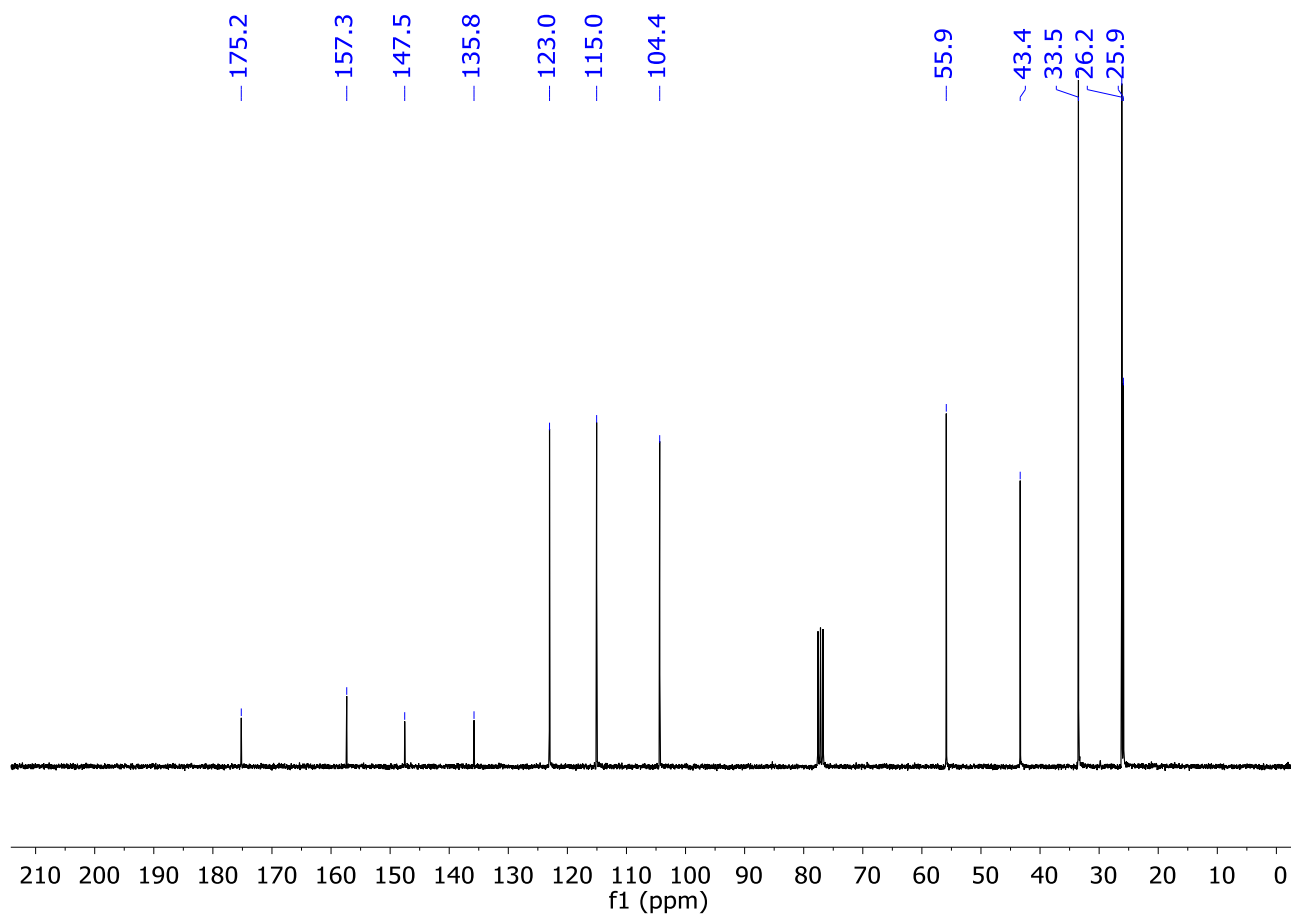
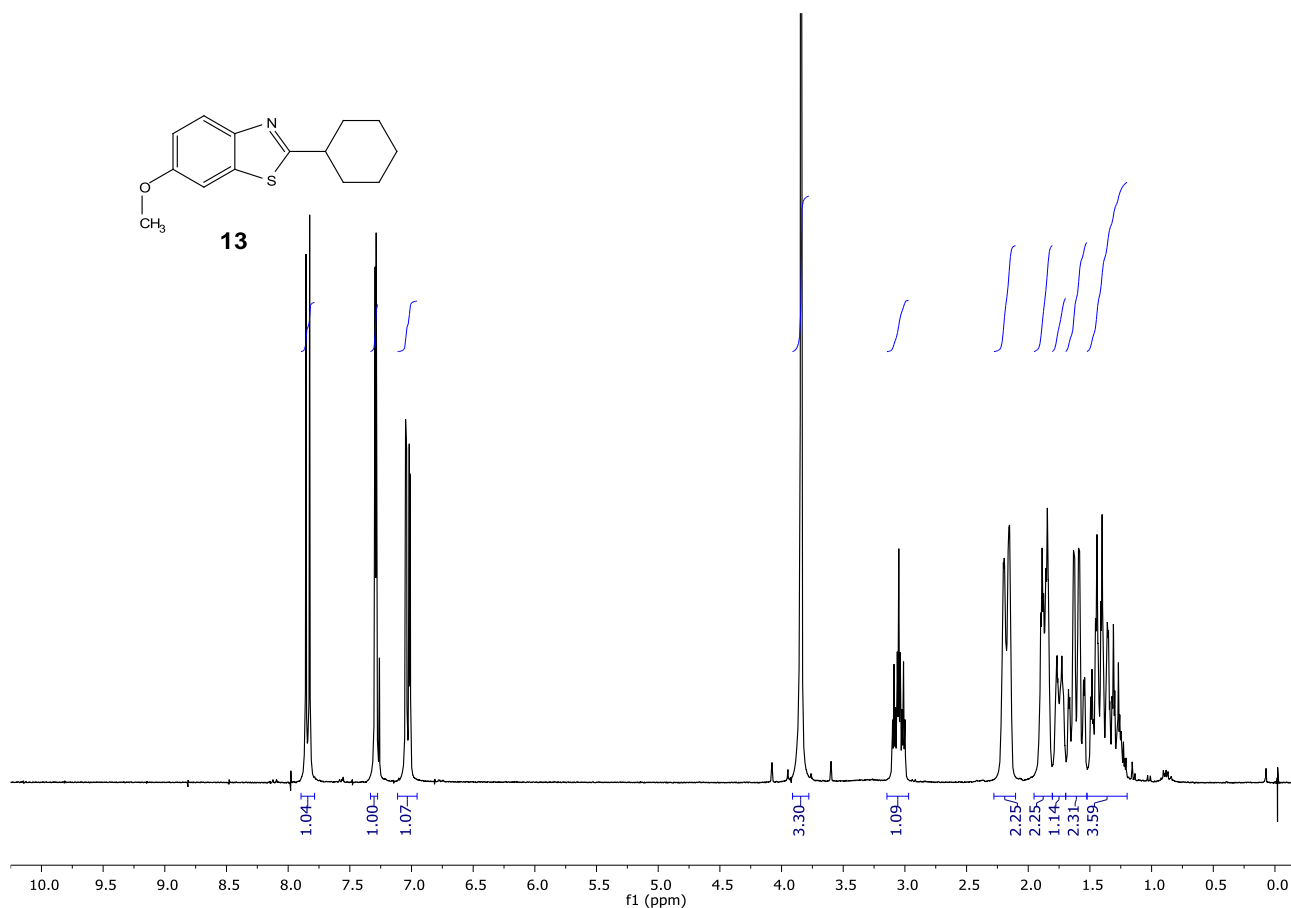
1.19 2.67 2.65 4.54 4.13

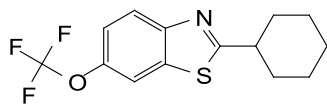




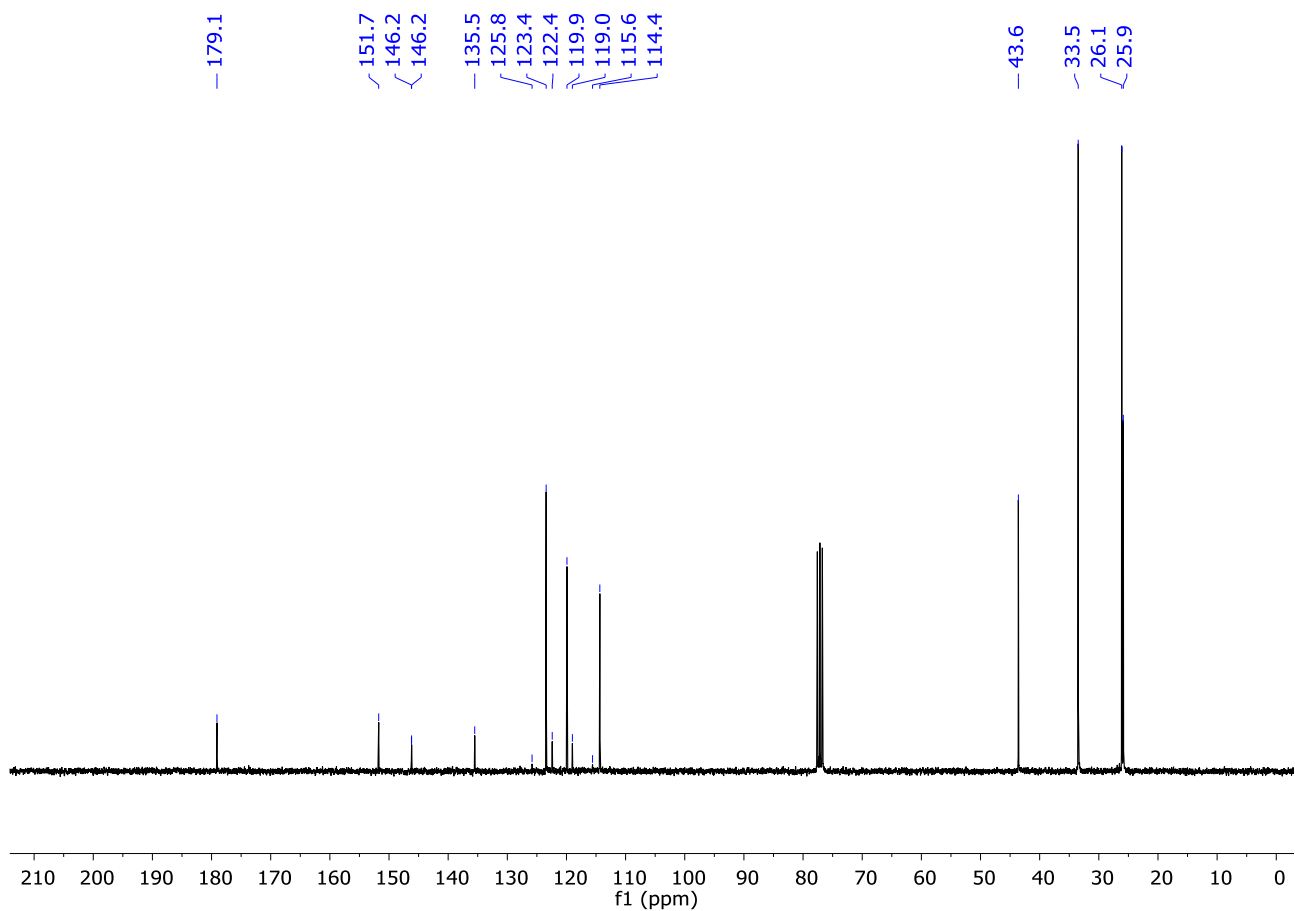
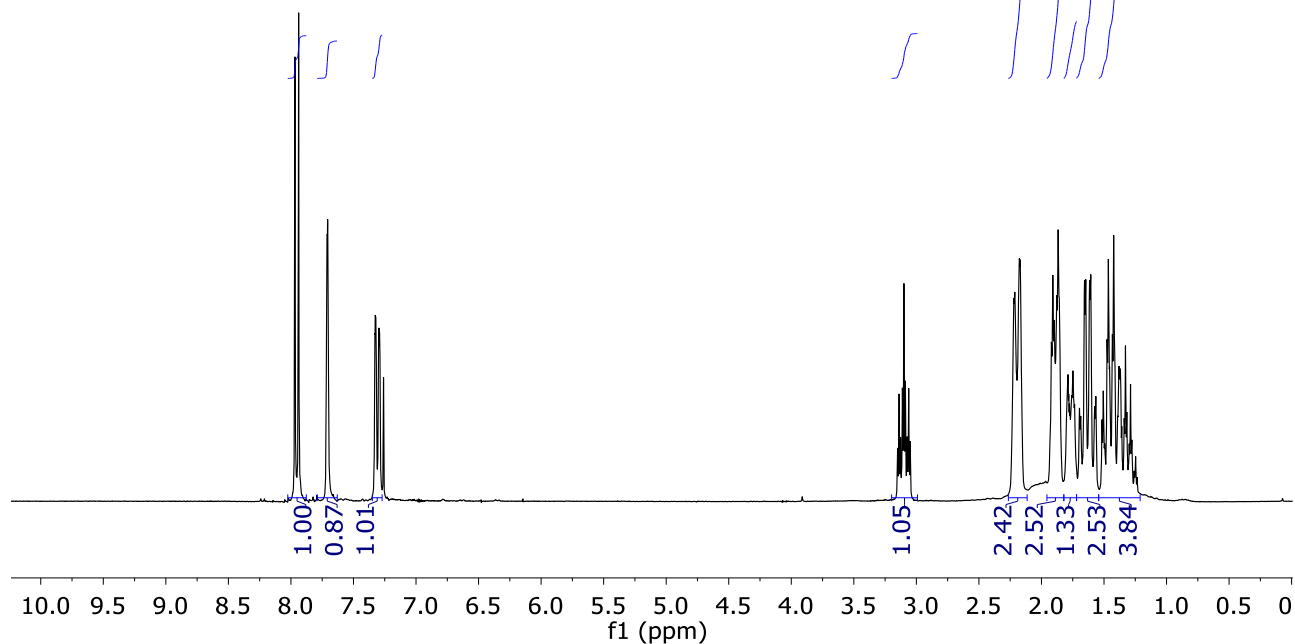


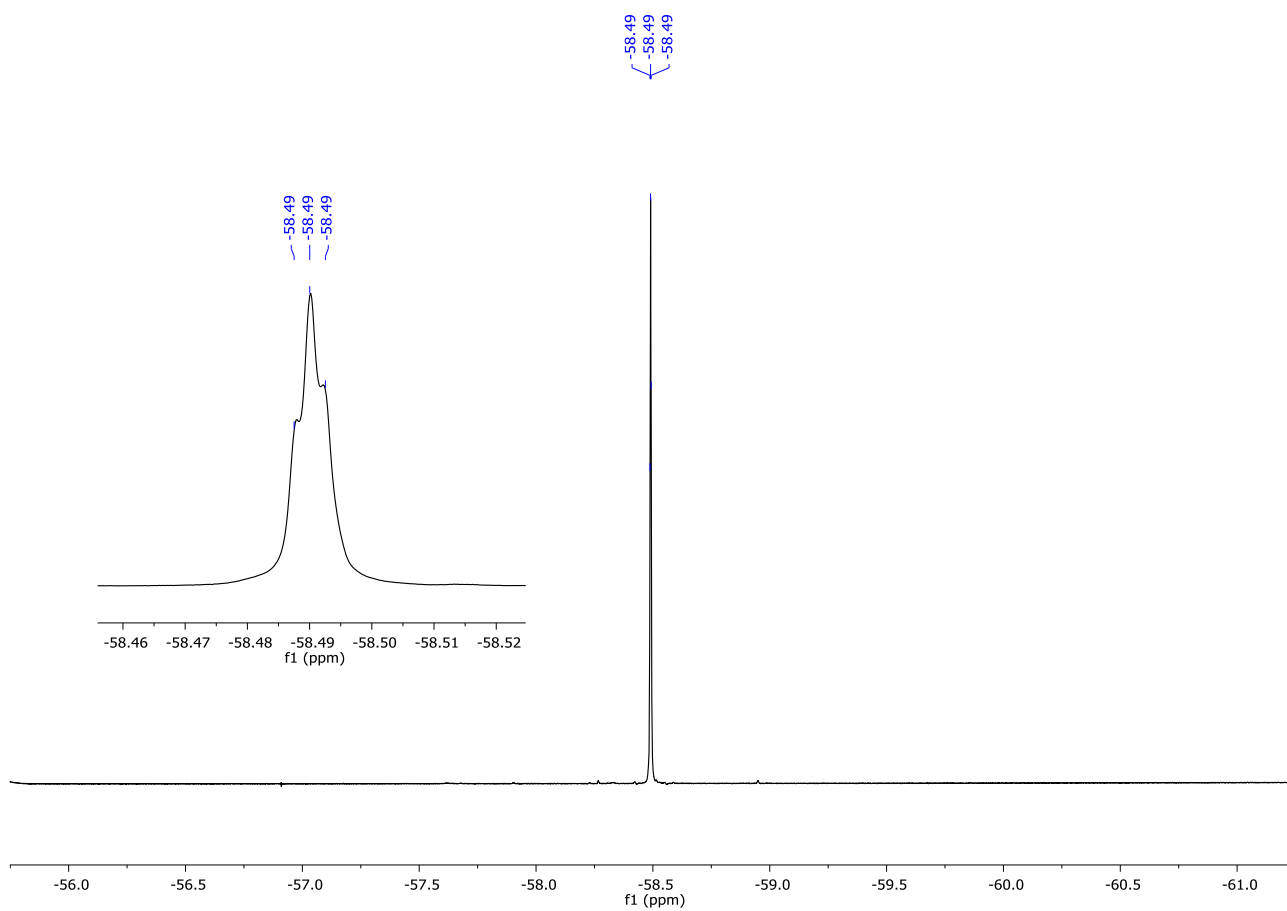
13

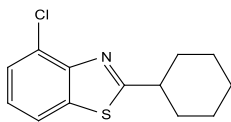




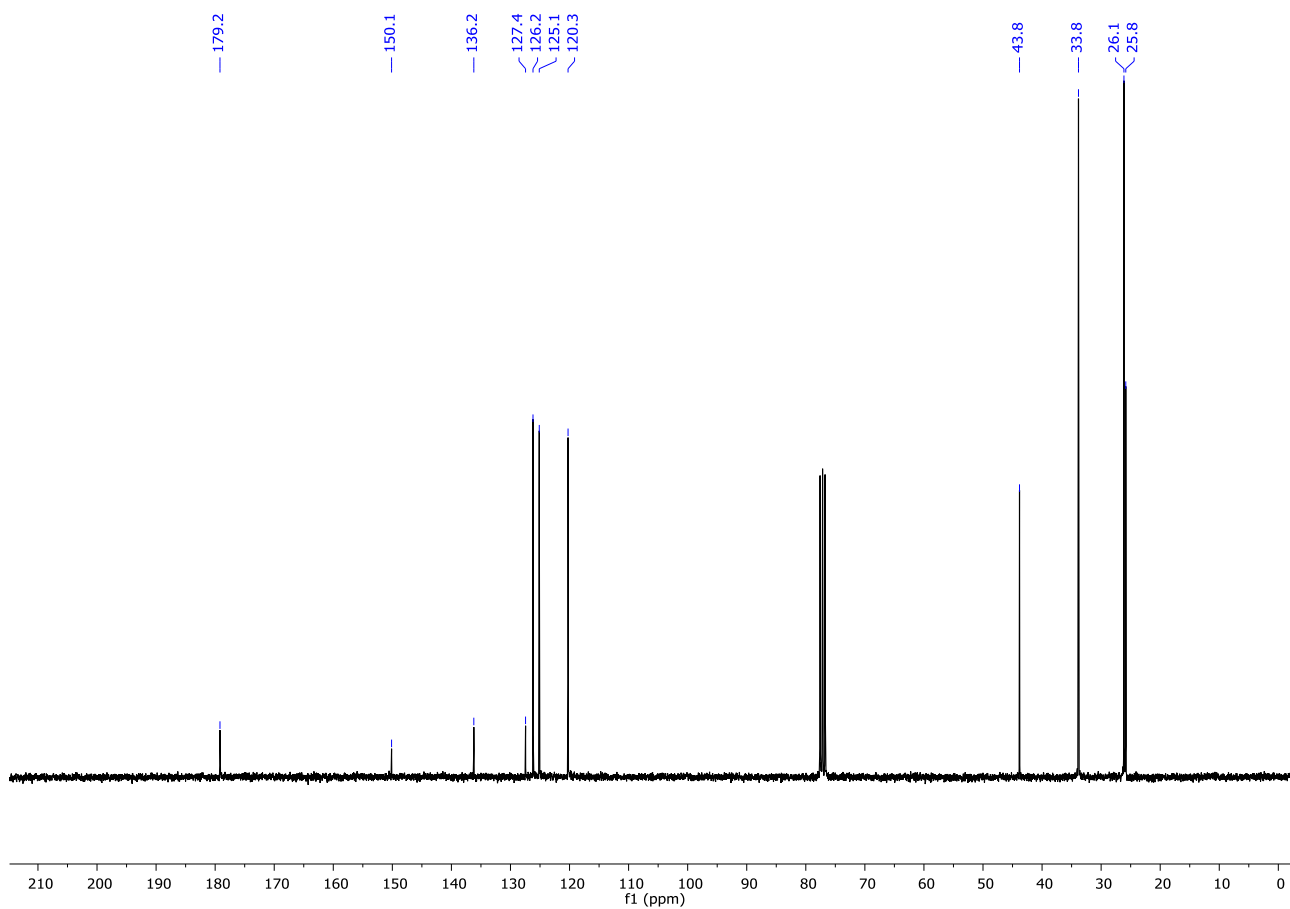
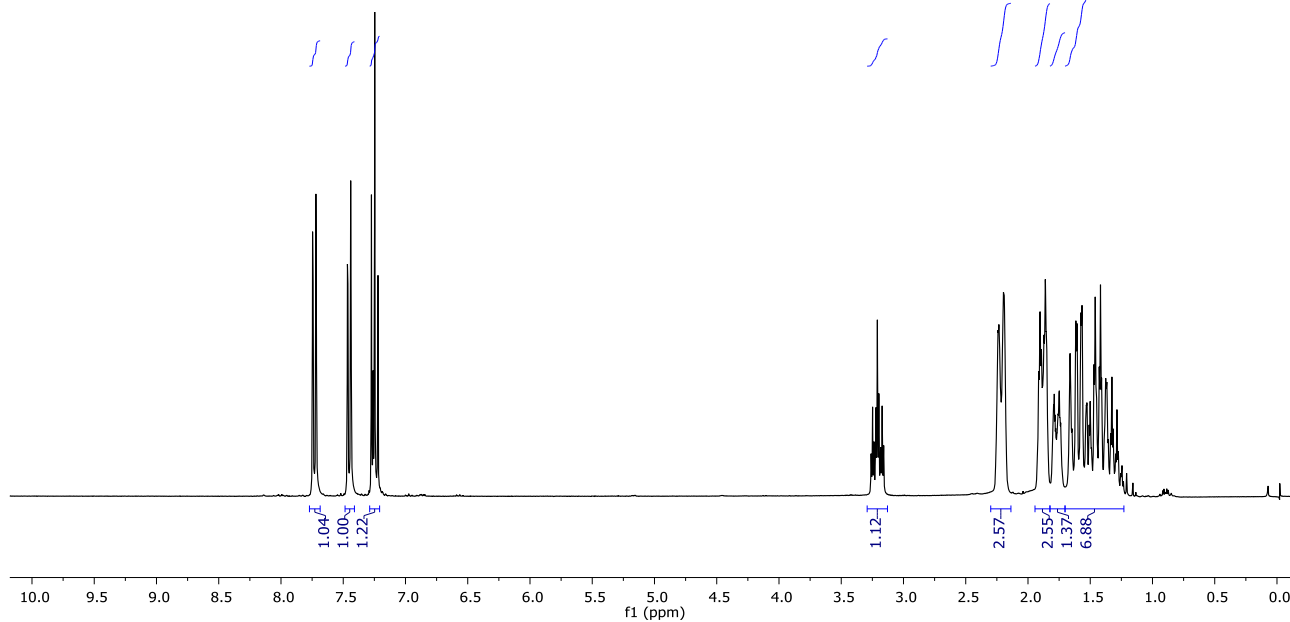
14

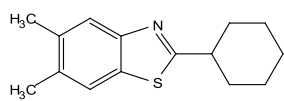






15





16

